Dual Cannabinoid Receptor Agonist, CB13, Modulates Signaling in Ventricular Hypertrophy and Atrial Remodeling

By

Danielle I. Lee

A thesis submitted to the Faculty of Graduate Studies of

The University of Manitoba

in partial fulfilment of the requirements of the degree of

DOCTOR OF PHILOSOPHY

College of Pharmacy

Rady Faculty of Health Sciences

University of Manitoba

Winnipeg, Manitoba, Canada

Abstract

Background: Structural, electrical, and metabolic remodeling contribute to cardiovascular disease, including atrial fibrillation (AF) and left ventricular hypertrophy (LVH). AF is the most common sustained cardiac arrhythmia, and LVH is the leading cause of heart failure. However, the molecular mechanisms to promote LVH, heart failure, and AF are poorly understood, giving rise to the possibility of novel therapeutic approaches. The endocannabinoid system (ECS) consists of endocannabinoids, cannabinoid receptors (CBR) and enzymes for synthesis and degradation. CBR agonists exert cardioprotective effects. By utilizing a dual CBR agonist, CB13 (1-naphthalenyl[4-(pentyloxy)-1-naphthalenyl]methanone), that has limited blood-brain barrier permeability, I aim to separate the potential advantageous peripheral cardioprotective effect from unwanted central effects.

Hypothesis: CB13 prevents hypertrophy and mitochondrial dysfunction in ventricular cardiomyocytes, and this will extend into the stressed atria, and the hallmarks of AF therein.

Results: Neonatal ventricular rat cardiomyocytes (NRVM) were used to determine the effect of CB13 on ventricular hypertrophy. CB13 prevented hypertrophy, restored mitochondrial membrane potential ($\Delta\Psi_m$) and prevented depression of fatty acid oxidation (FAO)-related bioenergetics when NRVM were exposed to the pro-hypertrophic compound, endothelin-1. CB13 activated AMPK and upregulated key signaling regulators of FAO. The effects of ECS activation were further investigated in the stressed myocardium by applying novel tachypacing techniques. CB13 did not alter chronotropic, dromotropic, or hemodynamic properties in non-paced hearts, preserved atrial effective refractory period in tachypaced hearts and activated AMPK. Lastly, neonatal rat atrial cardiomyocytes (NRAM) were used to determine underlying mechanisms in AF-related tachypaced remodeling. The anti-hypertrophic effect of CB13 and ability to preserve $\Delta\Psi_m$ was demonstrated in NRAM. Additionally, AMPK and possibly Cx43 are major mediators for CB13-dependent cardioprotection.

Conclusion: These findings demonstrate the protective effect of CB13 during hypertrophy, mitochondrial dysfunction and electrophysiological changes *in vitro* using NRAM and NRVM, and *ex vivo* using tachypaced SD rat hearts. Moreover, CB13 activates AMPK and may alter Cx43 expression. Due to the beneficial effects of CB13 in pathological hypertrophy and AF-related remodeling, these findings provide further insight into CBR agonists as a potential cardiovascular therapeutic strategy.

Acknowledgements

This thesis would not be complete without thanking everyone who has made an impact on my life; mentors, colleagues, family and friends. Thank you all.

I would like to begin by thanking my advisor, Dr. Hope Anderson. It has been an amazing 8 years working with you. I could not have asked for a better mentor. I remember our first meeting vividly, as you asked me to present some of my undergraduate research on a whiteboard. You challenged me from day one and I could not be more appreciative of your guidance on writing, on research, and on life.

I am grateful for the advice and guidance of my committee members Dr. Larry Hryshko and Dr. Michael Czubryt, thank you. I am also appreciative of our amazing collaborators at Ben Gurion University in Dr. Yoram Etzion's lab. My time in Israel was a pivotal experience during my PhD. Dr. Etzion taught me so much, and he has always provided insightful and helpful research advice. My term in Israel will always be remembered fondly.

My family and friends have always been there for me. I would like to thank my siblings and all my parents for their unwavering support. I extend my gratitude to all my friends who listened to me talk about science and school for 8 years, thanks for sticking by me. I would also like to thank the whole CCARM group, I will miss our pre-COVID lunchtime crew.

Last but not least, I am extremely thankful to my fiancé, Anthony. We started graduate school together and now we are finishing together. I couldn't have done it without you (and Louie) by my side. Looking forward to all of our new adventures ahead!

Table of Contents

Abstract ..... **i**
Acknowledgements ..... **ii**
List of Figures ..... **vii**
List of Tables ..... **ix**
List of Abbreviations ..... **x**
List of Thesis-related Manuscripts ..... **xiv**
Chapter 1 1
1.1. Cardiac Physiology **2**
1.1.1. Cardiomyocytes 2
1.1.2. Cardiac Metabolism 6
1.1.2.1. Mitochondrial Electron Transport Chain 7
1.1.2.2. Mitochondrial Membrane Channels 10
1.1.2.3. Signaling Mediators 11
1.1.3. Cardiac Electrophysiology 13
1.1.3.1. Action Potential Formation 15
1.1.3.2. Conduction Velocity 20
1.2. Pathological Cardiac Remodeling **20**
1.2.1. Atrial Fibrillation 21
1.2.1.1. AF Maintenance and Mechanisms 23
1.2.1.2. Atrial Remodeling 25
1.2.2. Left Ventricular Hypertrophy and Heart Failure 29
1.2.2.1. Hypertrophy Maintenance and Mechanisms 30
1.2.2.2. Ventricular Remodeling 30
1.3.Therapeutic Interventions **35**
1.3.1. Atrial Fibrillation 35
1.3.1.1. Risk Factors 35
1.3.1.2. Antiarrhythmic Therapies 35
1.3.1.3. Cardioversion Therapies 37
1.3.1.4. Rate Control vs. Rhythm Control 37
1.3.1.5. New AF Therapeutic Options 38
1.3.2. Left Ventricular Hypertrophy and Heart Failure 38
1.3.2.1. Risk Factors 39
1.3.2.2. Heart Failure Treatment 40
1.3.2.3. Pitfalls of Hypertrophy Therapeutic Options 42

1.3.2.4. New Hypertrophy Therapeutic Options....42
1.4 Animal Models....43
1.4.1 Small Animal Models....44
1.4.2. Large Animal Models....45
1.5. Cannabinoids....47
1.5.1. The Endocannabinoid System....47
1.5.1.1. Cannabinoid Ligands....47
1.5.1.2. Endocannabinoid Synthesis....48
1.5.1.3. Endocannabinoid Degradation....49
1.5.1.4. Cannabinoid Receptors....49
1.5.2. Cannabinoid Therapeutics....51
1.5.3. Cannabinoid Receptor Signaling in the Heart....54
Chapter 2....56
2.1. Rationale....57
2.2. Hypothesis....57
2.3. Aims....58
2.4. Significance....59
Chapter 3....60
3. Activation of Cannabinoid Receptors Attenuates Mitochondrial Dysfunction in Rat Ventricular Myocytes....61
3.1. Abstract....62
3.2. Introduction....63
3.3. Materials and Methods....64
3.3.1. Materials....64
3.3.2. Neonatal rat ventricular myocytes....65
3.3.3. Treatments....65
3.3.4. shRNA knockdown of AMPKα....66
3.3.5. Measurement of mitochondrial respiration....66
3.3.6. Measurement of Mitochondrial Membrane Permeability Transition....68
3.3.7. Measurement of changes in mitochondrial membrane potential....69
3.3.8. Western blotting....70
3.3.9. RNA extraction and real-time PCR....70
3.3.10. Statistics....70
3.4. Results....71
3.4.1. CB13 attenuates ET1-induced aberrations of fatty acid oxidation-related mitochondrial bioenergetics....71

3.4.2. AMPK contributes to CB13-dependent correction of FAO-related mitochondrial bioenergetics in hypertrophied myocytes. 71
3.4.3. ET1-induced mPT is prevented by CB13. 74
3.4.4. CB13 prevents ET1-induced mitochondrial membrane depolarization in an AMPK-independent manner. 76
3.4.5. CB13 attenuates ET1-reduced expression of PGC-1α and CPT-1β through AMPK 78
3.5. Discussion 80
3.5.1. Acute exposure to ET1 impairs FAO-dependent mitochondrial bioenergetics. 80
3.5.2. Mitochondrial membrane integrity in ET1-treated cardiac myocytes in the presence of palmitate 81
3.5.3. Effects of liganded CB receptor activation on mitochondrial signaling cascades 82
3.6. Conclusion 84
3.7. Connecting Text 85
Chapter 4 86
4. Cannabinoid Receptor Agonist Inhibits Atrial Electrical Remodeling in a Tachypaced *Ex Vivo* Rat Model 87
4.1. Abstract 88
4.2. Introduction 89
4.3. Materials and Methods 91
4.3.1. Animals 91
4.3.2. Isolated perfused heart preparation and basic physiological measurements 91
4.3.3. Atrial electrophysiology and atrial tachypacing experiments 92
4.3.4. Pharmacological treatments 93
4.3.5. Western blotting 94
4.3.6. Statistical analysis 94
4.4. Results 97
4.4.1. Absence of chronotropic, dromotropic or hemodynamic effects of CB13 in the non-paced rat heart 97
4.4.2. CB13-treatment inhibited tachypacing-induced atrial electrical remodeling. 99
4.4.3. Biochemical effects of CB13 in the tachypaced atria 101
4.5. Discussion 106
4.6. Conclusion 111
4.7. Limitations 111
4.8. Connecting Text 112
Chapter 5 113
5. Cannabinoid Receptor Agonist Attenuates Angiotensin II–Induced Hypertrophy and Mitochondrial Dysfunction in Rat Atrial Cardiomyocytes 114
5.1. Abstract 115
5.2. Introduction 116

5.3. Materials and Methods....118
5.3.1. Materials....118
5.3.2. Neonatal rat atrial cardiomyocytes....118
5.3.3. Treatments....119
5.3.4. Cell surface area measurements....119
5.3.5. Mitochondrial membrane potential ($\Delta\Psi_m$) imaging....120
5.3.6. Mitochondrial Permeability Transition (mPT) imaging....120
5.3.7. Western blotting....121
5.3.8. Statistical analysis....122
5.4. Results....122
5.4.1. CB13 suppresses AngII-induced hypertrophy in an AMPK-dependent manner....122
5.4.2. CB13 prevents AngII-induced mitochondrial membrane depolarization in an AMPK-dependent manner. .124
5.4.3. Mitochondrial permeability transition pore (mPTP) is not altered by AngII....126
5.4.4. Biochemical effects of CB13 in atrial cardiomyocytes exposed to AngII....127
5.5. Discussion....131
Chapter 6 136
6.1. Discussion and Future Directions 137
6.1.1. CB13 is anti-hypertrophic....137
6.1.2. CB13 alters mitochondrial dysfunction and metabolic signaling....139
6.1.3. CB13 affects electrical signaling via AERP and Cx43....141
6.2. Overall Conclusion 146
Chapter 7 147
Appendix.... 148
7.1. Supplemental Data File for Chapter 3 - Activation of Cannabinoid Receptors Attenuates Endothelin-1-induced Mitochondrial Dysfunction in Neonatal Rat Ventricular Myocytes..... 148
S7.1. Optimization of working conditions for mitochondrial bioenergetics assays. 148
S7.2. Determination of fatty acid oxidation-associated OCR in cultured neonatal rat cardiac myocytes. ..152
S7.3. Determination of AMPKα1/2 knockdown in cultured neonatal rat cardiac myocytes....154
S7.4. Quantification of cannabinoid receptor protein concentration in neonatal rat cardiomyocytes 155
S7.5. Schematic of events as elucidated from experimental NRVM's results....156
7.2. References: 157

List of Figures

Figure 1.1. Structure of a cardiomyocyte. 5

Figure 1.2. The tricarboxylic acid (TCA) cycle and the electron transport chain (ETC). 9

Figure 1.3. Action potential conduction pathway in the heart. 14

Figure 1.4. Action potential duration and shape within the myocardium. 18

Figure 1.5. G-protein coupled receptor signaling in cardiomyocytes. 34

Figure 1.6. Cannabinoid subtypes. 53

Figure 3.1. CB13 attenuates ET1-depression of fatty acid oxidation-related respiration. 73

Figure 3.2. CB13 ameliorates ET1-induced mPT. 75

Figure 3.3. In the presence of palmitate as energy substrate, CB13 prevents ET1-induced mitochondrial membrane depolarization in an AMPK-independent manner 77

Figure 3.4. ET1-induced down-regulation of PGC-1α and CPT-1β is attenuated by CB13 in an AMPK-dependent manner. 79

Figure 4.1. Example recordings from the ex vivo experimental setup. 96

Figure 4.2. Absence of chronotropic, dromotropic or hemodynamic effects of CB13 in the non-paced rat heart. 98

Figure 4.3. CB13-treatment inhibited tachypacing-induced atrial electrical remodeling. 100

Figure 4.4. Cannabinoid receptor protein levels remain unaltered in atrial tissue 102

Figure 4.5. Tachypacing induced reduction of phosphorylated AMPK, while CB13 treatment abrogated tachypacing effects and increased PGC1α signaling 103

Figure 4.6. Total AMPK and total LKB1 were not altered in atrial tissue. 104

Figure 4.7. Tachypacing-induced reduction of connexin 43 is diminished by CB13 105

Figure 5.1. CB13 suppressed AngII-induced hypertrophy in an AMPK-dependent manner. 123

Figure 5.2. CB13 prevented AngII-induced mitochondrial membrane depolarization in an AMPK-dependent manner. 125
Figure 5.3. Mitochondrial permeability transition pore (mPTP) was not altered by AngII treatment. 126
Figure 5.4. CB13 rescued AngII-induced reduction of phosphorylated AMPK. 128
Figure 5.5. CB13 increased the gap junction, Cx43, compared to AngII controls. 129
Figure 5.6. Cannabinoid receptor 2 expression was downregulated in NRAM by AngII. 130
Figure 6.1. Summary Schematic. 145
Supplemental Figure 7.1. 149
Supplemental Figure 7.2. 150
Supplemental Figure 7.3. 151
Supplemental Figure 7.4. 153
Supplemental Figure 7.5. 154
Supplemental Figure 7.6. 155
Supplemental Figure 7.7. 156

List of Tables

Table 1. Differences in Cardiomyocyte Action Potentials 19

List of Abbreviations

$\Delta\Psi_m$ – membrane potential
2-AG – 2-arachidonoyl glycerol
ACE – angiotensin converting enzyme
ADP – adenosine diphosphate
AEA – anandamide
AERP – atrial effective refractory period
AF – atrial fibrillation
AMP – adenosine monophosphate
AMPK – AMP-activated protein kinase
Ang – angiotensin
AngII – angiotensin II
ANP – atrial natriuretic peptide
AP – action potential
APD – action potential duration
ARB – angiotensin receptor blocker
AT1R – angiotensin type 1 receptor
AT2R – angiotensin type 2 receptor
ATP – adenosine triphosphate
AV node – atrioventricular node
BCS – bovine calf serum
BNP – B-type natriuretic peptide
BSA – bovine serum albumin
CAD – coronary artery disease
CAMKII – calcium calmodulin-dependent kinase II
CAMKK2 – calcium calmodulin-dependent kinase kinase 2
CAVB – chronic AV block
CB13 – 1-naphthalenyl[4-(pentyloxy)-1-naphthalenyl]methanone)
CB1R – cannabinoid receptor 1
CB2R – cannabinoid receptor 2
CBD – cannabidiol
CBFHH – calcium and bicarbonate free Hanks HEPES
CBR – cannabinoid receptor
CCS – cosmic calf serum
CHF – coronary heart failure
CICR – calcium-induced calcium-release
CNR1 – human central cannabinoid receptor gene 1
CNR2 – human central cannabinoid receptor gene 2
CNS – central nervous system
COX-2 – cyclooxygenase-2

CPT-1 – carnitine palmitoyl transferase 1
Cx40 – connexin 40
Cx43 – connexin 43
DAD – delayed afterdepolarization
DAGL – diacylglycerol lipase
DMEM – Dulbecco's Modified Eagle Medium
DMSO – dimethyl sulfoxide
EAD – early afterdepolarization
eCB – endocannabinoid
EC-coupling - electrical contraction coupling
ECM – extracellular matrix
ECS – endocannabinoid system
eNOS – endothelial nitric oxide synthase
EP – electrophysiology
ERK – extracellular signal related kinase
ERR – estrogen receptor-related receptor
ET1 – endothelin 1
ETC – electron transport chain
FAAH – fatty acid amide hydrolase
FADH2 – flavin adenine dinucleotide
FAO – fatty acid oxidation
FCCP – carbonyl cyanide-p-trifluoromethoxyphenylhydrazone
GPCR – G-protein-coupled receptor
GPR – G-protein receptor
GTPase – guanosine triphosphatase
HFpEF – heart failure with preserved ejection fraction
HFrEF – heart failure with reduced ejection fraction
I_{Ach} – acetylcholine-induced current
$I_{Ca(L)}$ – long-type calcium current
$I_{Ca(T)}$ – transient-type calcium current
I_f – funny current
I_{K1} – inward rectifier potassium current
I_{KR} – rapid delayed rectifier potassium current
I_{KS} – slow delayed rectifier potassium current
I_{KUR} – ultrarapid delayed rectifier potassium current
IMAC – inner membrane anion channel
I_{Na} – sodium current
I_{NCX} – sodium/calcium exchange current
I_{to} – transient outward potassium current
JC-1 – tetraethylbenzimidazolylcarbocyanine iodide
JNK – c-Jun N-terminal kinase

Kir – inward rectifier potassium channel
LA – left atrium
LKB1 – liver kinase b1
LVEF – left ventricular ejection fraction
LVH – left ventricular hypertrophy
MI – myocardial infarction
MAGL – monoacylglycerol lipase
MAPK – mitogen-activated protein kinase
MBHE – miniature bipolar hook electrode
MCU – mitochondrial calcium uniporter
MHC – myosin heavy chain
MI – myocardial infarction
mitoK_{ATP} – mitochondrial ATP-sensitive potassium channel
mPT – mitochondrial permeability transition
mPTP – mitochondrial Permeability Transition Pore
mRNA – messenger RNA
mTOR – mechanistic target of rapamycin
NAAA – N-acylethanolamine acid amide hydrolase
NADH – nicotinamide adenine dinucleotide
NAPE – N-acyl phosphatidylethanolamine
NCX – sodium calcium exchanger
NFAT – nuclear factor of activated T-cells
NRAM – neonatal rat atrial cardiomyocytes
NRVM – neonatal rat ventricular cardiomyocytes
OCR – oxygen consumption rate
P/S – penicillin/streptomycin
PBS – phosphate buffered saline
PCR – polymerase chain reaction
PGC1α – peroxisome proliferator-activated receptor gamma coactivator 1-alpha
PIP2 – phosphatidylinositol 4,5-bisphosphate
PKA – protein kinase A
PKC – protein kinase C
PLB – phospholipase B
PLC – phospholipase C
PLD – phospholipase D
PPAR – peroxisome proliferator-activated receptor
PPM1A – protein phosphatase Mg^{2+}/Mn^{2+} 1A
PVDF – polyvinylidene fluoride
RAS – renin-angiotensin system
ROS – reactive oxygen species
RyR – ryanodine receptors

SA node – sinoatrial node
SD – Sprague-Dawley
SEM – standard error of mean
SHR – spontaneously hypertensive rat
SIRT1 – sirtuin 1
TAC – transverse aortic constriction
TCA cycle – tricarboxylic acid cycle
TGFB1 – transforming growth factor beta 1
THC – Δ9-tetrahydrocannabinol
Thr172 – threonine 172
TRPV1 – transient receptor potential vanilloid 1
T-tubules – transverse tubules

List of Thesis-related Manuscripts

- **Lee DI**, Etzion Y, and Anderson HD. Cannabinoid Receptor Agonist Attenuates Angiotensin II–Induced Atrial Hypertrophy and Mitochondrial Dysfunction in Rat Atrial Cardiomyocytes. 2022. *Manuscript complete.*

- **Lee DI**, Murninkas M, Elyagon S, Etzion Y, and Anderson HD. Cannabinoid Receptor Agonist Inhibits Atrial Electrical Remodeling in a Tachypaced Ex Vivo Rat Model. Frontiers in Pharmacology. 2021. 12:642398. doi:10.3389/fphar.2021.642398.

- Murninkas M, Gillis R, **Lee DI**, Elyagon S, Bhandarkar N, Levi O, Polak R, Klapper-Goldstein H, Mulla W, and Etzion Y. A New Implantable Tool for Repeated Assessment of Supraventricular Electrophysiology and Atrial Fibrillation Susceptibility in Freely Moving Rats. American Journal of Physiology - Heart and Circulatory Physiology. 2021. 320: H713–H724. doi:10.1152/ajpheart.00676.2020.

- **Lee DI***, Lu Y*, Chowdhury SR, Kamboj A, Anderson CM, Fernyhough P, Anderson HD. Activation of Cannabinoid Receptors Attenuates Endothelin-1-Induced Mitochondrial Dysfunction in Neonatal Rat Ventricular Myocytes. Journal of Cardiovascular Pharmacology. 2020. 75:54–63. doi:10.1097/FJC.0000000000000758.

Chapter 1

Introduction

1.1. Cardiac Physiology

The heart consists of four synchronized chambers and contains cardiomyocytes, fibroblasts, endothelial cells and vascular cells.(1) Cardiomyocytes are the major cell type of the heart, totaling 70-85% of the heart volume.(2) Although the other cell types are not as abundant in terms of total heart volume, they are instrumental for normal homeostasis of the heart.(1) Non-cardiomyocytes provide structure for the extracellular matrix, cell-to-cell communication, and efficient cardiomyocyte contraction.(1) The heart chambers also have distinct physical and functional properties. Variations between the atria and ventricles include differences in myocardial mass, wall thickness, functional pressure, contractile properties, ion channel composition, and electrophysiological characteristics.(3)

1.1.1. Cardiomyocytes

Myofibrils are the contractile structures of cardiomyocytes, and sarcomeres are formed by repeating myofibril subunits (Figure 1.1). Cardiomyocytes are surrounded by a cell membrane, the sarcolemma, and contain large amounts of mitochondria to supply the cells with enough adenosine triphosphate (ATP) to meet the high energy demand of cardiac contraction.(4) Myofilaments, actin (thin filament) and myosin (thick filament) along with regulatory proteins; such as troponin and tropomyosin, are surrounded by lengths of sarcoplasmic reticulum (Figure 1.1). In ventricular cardiomyocytes transverse tubules (T-tubules) cross the cell and traverse across the myofilaments.(4)

Cardiomyocytes are responsible for contraction via action potentials (AP) that originate at the sinoatrial (SA) node in the right atrium. As the AP flows through the heart, it causes widespread depolarization and subsequent cardiomyocyte contraction via excitation-contraction (EC)

coupling. Contraction occurs due to changes in cytoplasmic calcium (Ca^{2+}) concentrations.(5) In brief, Ca^{2+} enters the cell via voltage-gated Ca^{2+} ion channels that trigger ryanodine receptors (RyR) on the sarcoplasmic reticulum to release stored Ca^{2+} into the cell, termed *Ca^{2+}-induced Ca^{2+}-release* (CICR), resulting in a *Ca^{2+} spark*.(6, 7) Ca^{2+} then binds to troponin resulting in the removal of tropomyosin from myosin binding sites on actin filaments. These conformational changes result in a myosin-actin crossbridge and the initiation of contraction. Simultaneous contraction within the myocardium generates sufficient force to eject blood into the body and the lungs. After myofilament contraction, adenosine diphosphate (ADP) is released, myosin detaches from actin, the cell relaxes, and a new contraction cycle is initiated.

Cardiomyocytes can be generally categorized by conduction potential into pacemaker and non-pacemaker cells.(2) Pacemaker cells are centralized to the SA and atrioventricular (AV) nodes which spontaneously depolarize. The majority of cardiomyocytes are non-pacemaker working cells and do not fire spontaneously.(2) Pacemaker cells are responsible for the autorhythmic nature of the heart. They initiate cardiac AP within the atria and tend to have a shorter action potential duration (APD). Working cardiomyocytes, in comparison, have a more prolonged AP.(2) Additionally, atrial and ventricular cardiomyocytes differ physiologically. Morphologically, atrial cardiomyocytes, in comparison to ventricular cardiomyocytes, have increased mitochondrial mass, generally do not contain T-tubules, contain prominent Golgi complexes, and usually have only one nucleus.(8) Developmental origin, contractile force-generating sarcomere proteins, and specialized functions at the transcriptional level, such as differing electrophysiological processes, have also been demonstrated to vary between atrial and ventricular cardiomyocytes.(9) These differences occur due to significantly different molecular profiles that underlie the varied physiological response required from cardiomyocytes depending on their location in the heart. For

example, atrial cardiomyocytes are thinner and elongated in comparison to ventricular cardiomyocytes, due to lack of T-tubules which account for approximately 50% of the sarcolemma membrane.(7, 10) This results in differential expression of L-type Ca^{2+} channels as well as other ion channels that are present within T-tubules.(11) Only the outer edge of an atrial cardiomyocyte can initiate CICR, while ventricular cardiomyocytes initiate CICR through RyR organized within T-tubules.(11, 12) Furthermore, the ventricular myocardium is thicker and stronger than the atria in order to pump blood further distances, such as into the body and lungs.(7) However, atrial contraction augments the amount of blood that is pumped into the ventricles prior to systole.(7) During periods of rest blood flows passively from the atrium to ventricle, and the majority of ventricular filling is due to venous return. However, during periods of hemodynamic demand (e.g. stress, exercise), the atria can improve cardiac performance by providing 20-30% of the blood volume entering the ventricles, referred to as *atrial kick*.(7) Remodeling of atrial and ventricular cardiomyocytes in conditions such as atrial fibrillation (AF) and heart failure result in pathologic changes, such as reduced contraction and altered protein expression.(7)

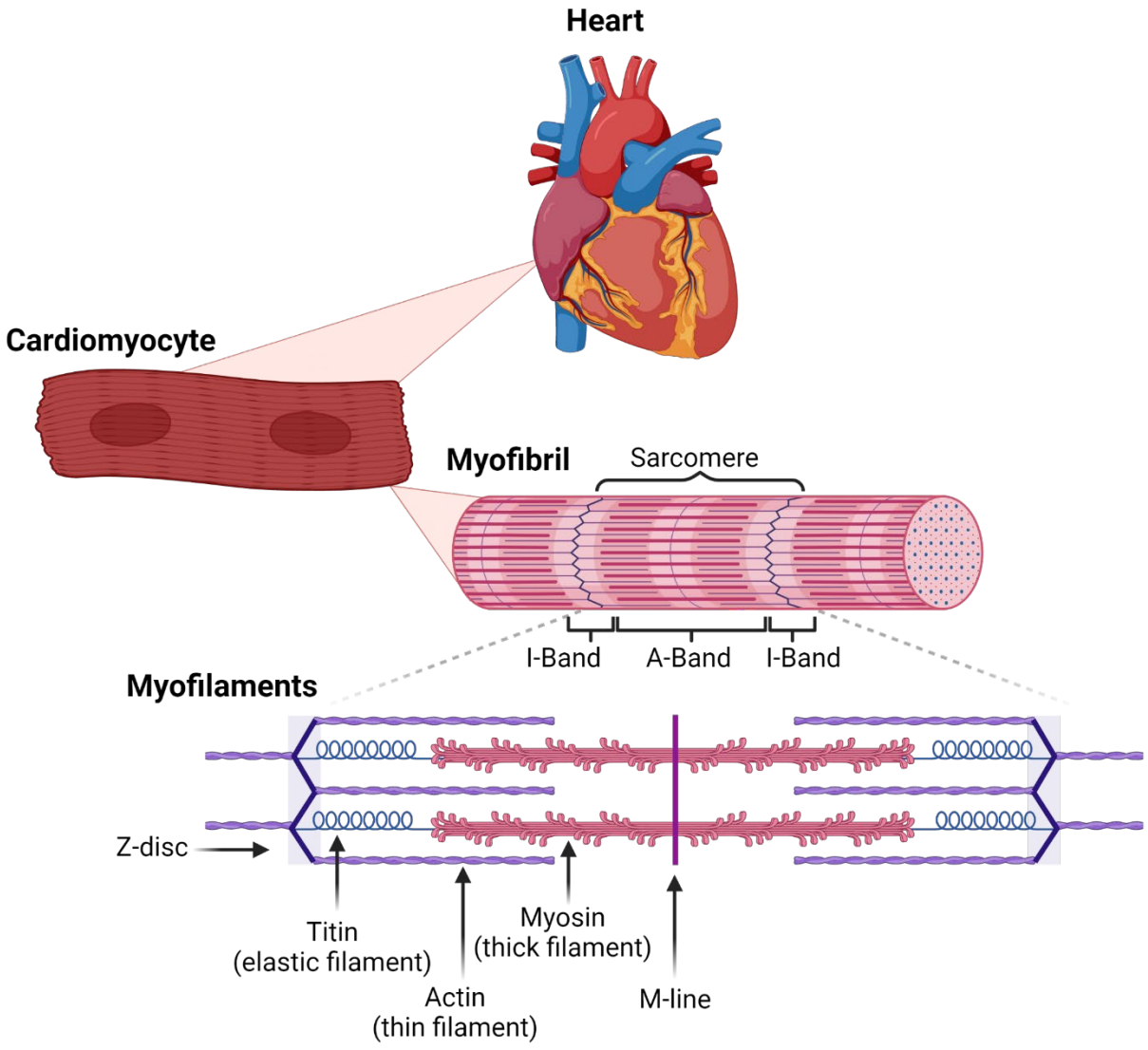

Figure 1.1. Structure of a cardiomyocyte. The heart consists of several different cell types, including cardiomyocytes. Cardiomyocytes are a major structural component of the heart and consist of myofibrils which contain myofilaments, such as actin (thin filament) and myosin (thick filament). *Adapted from "Myofibril Structure" template by Biorender.com (2022). Retrieved from https://app.biorender.com/biorender-templates.*

1.1.2. Cardiac Metabolism

The human heart beats approximately 100,000 times a day.(13) Due to the steady activity of the heart, a consistent supply of energy is required. Approximately 95% of the ATP required by the heart is generated by the mitochondria.(14) Mitochondria also regulate signaling, Ca^{2+} homeostasis, apoptosis, and necrosis.(13) Thus, cardiac metabolism plays a key role in myocardial overall function and energy supply.

Cardiac metabolism involves several substrates, including fatty acids, glucose, ketones, and amino acids. These energy-yielding compounds undergo catabolism prior to converging upon acetyl-CoA production and entry into the tricarboxylic acid (TCA) cycle (i.e. Krebs cycle or Citric Acid Cycle). These catabolized substrates undergo a series of oxidative phosphorylation reactions along the inner mitochondrial membrane (Figure 1.2).(15) A proton gradient, known as the mitochondrial membrane potential ($\Delta\Psi_m$), is generated from this oxidation. This gradient allows protons to enter the mitochondrial matrix through complex V of the electron transport chain (ETC), releasing energy and phosphorylating ADP into ATP (See Section 1.1.2.1. Mitochondrial ETC). Newly formed ATP is quickly shuffled out of the mitochondria and distributed throughout the cell.(15) While fatty acids are the predominant substrate in the healthy adult myocardium, other substrates are used when in abundance or when the myocardium is stressed due to underlying disease.(14) Thus, mitochondria are easily susceptible to stress due to myocardial reliance on ATP. Mitochondrial dysfunction is associated with pathophysiologic consequences and leads to disease development, including AF and heart failure.

Cardiac metabolism is reprogrammed in hypertrophy and AF and increases glucose utilization while shifting away from fatty acid oxidation.(16-18) This shift in substrate is considered a compensatory mechanism, as glucose is more oxygen-efficient compared to fatty

acids with regard to ATP production. However, this compensatory mechanism becomes inadequate over time as hypertrophy and AF progress. This alteration is a reversal of the metabolic maturation that occurs from fetal to adult hearts. While fetal reprogramming is an adaptive mechanism associated with a decrease in energy reserve and oxidative metabolism, the fetal metabolic profile is unable to sustain myocardial energetics and function.(19) In fact, hypertrophied and failing hearts have lower total ATP levels.(20) This is due to increased glycolysis, since glycolytic ATP synthesis provides less than 5% of the ATP energy required by the heart.(19) Glycolytic ATP insufficiency is found in several animal models, such as pressure overloaded mice, where enhancing ATP production and sustaining FAO preserves cardiac function in failing rodent hearts.(21, 22) Whether through β-oxidation or glycolysis, byproducts of the TCA cycle enter the ETC and undergo oxidative phosphorylation to produce cardiac energy.

1.1.2.1. Mitochondrial Electron Transport Chain

The ETC allows the passage of electrons through five different protein complexes located on the inner mitochondrial membrane in close proximity to the TCA cycle (Figure 1.2).(23) These complexes create a proton gradient, or $\Delta\Psi_m$, by pumping protons into the intermembrane space of the mitochondria. ATP is generated at complex V, known as ATP synthase.

The high energy molecules, nicotinamide adenine dinucleotide (NADH) and flavin adenine dinucleotide ($FADH_2$), generated from the TCA cycle donate electrons to the ETC at Complex I (i.e. ubiquinone reductase) or Complex II (i.e. succinate dehydrogenase), respectively (Figure 1.2). Complex I receives two electrons from NADH, passing them to coenzyme Q (also known as ubiquinone) via a series of cofactors from low to high potential. Electron transfer from NADH to Complex I induces the pumping of four protons from the mitochondrial matrix to the

intermembrane space.(23) Similarly, Complex II, a component of both the TCA cycle and ETC, also accepts two electrons from $FADH_2$. Electrons from Complex II are transferred by coenzyme Q (Figure 1.2). However, no proton translocation occurs at Complex II. At Complex III electrons are transferred one at a time to cytochrome C. Complex III pumps four protons from the inner mitochondrial matrix into the mitochondrial intermembrane space for every electron pair (Figure 1.2). Cytochrome C then carries single electrons to Complex IV (i.e. cytochrome C oxidase). Complex IV consists of three subunits, and binds molecular oxygen. Oxygen is then reduced to H_2O, in a process called mitochondrial respiration (Figure 1.2).(23) Oxygen reduction consumes eight electrons and four protons, forming two H_2O molecules; thus a net of four protons is translocated into the intermembrane space at Complex IV.

Overall, there is net translocation of ten protons into the intermembrane space. This movement of protons creates an electrochemical proton gradient, $\Delta\Psi_m$. The proton concentration in the intermembrane space and the $\Delta\Psi_m$ generates a proton motive force which couples electron transport from Complex I-IV with Complex V. $\Delta\Psi_m$ is reduced at Complex V when protons return from the intermembrane space back into the matrix. Movement of protons through Complex V results in phosphorylation of ADP, finally regenerating ATP (Figure 1.2).(15) However, the ETC does not always function ideally, and electron leak leads to reactive oxygen species (ROS) such as superoxide anion. Thus, ETC dysfunction has been implicated in cardiovascular disease due to elevated ROS.(23)

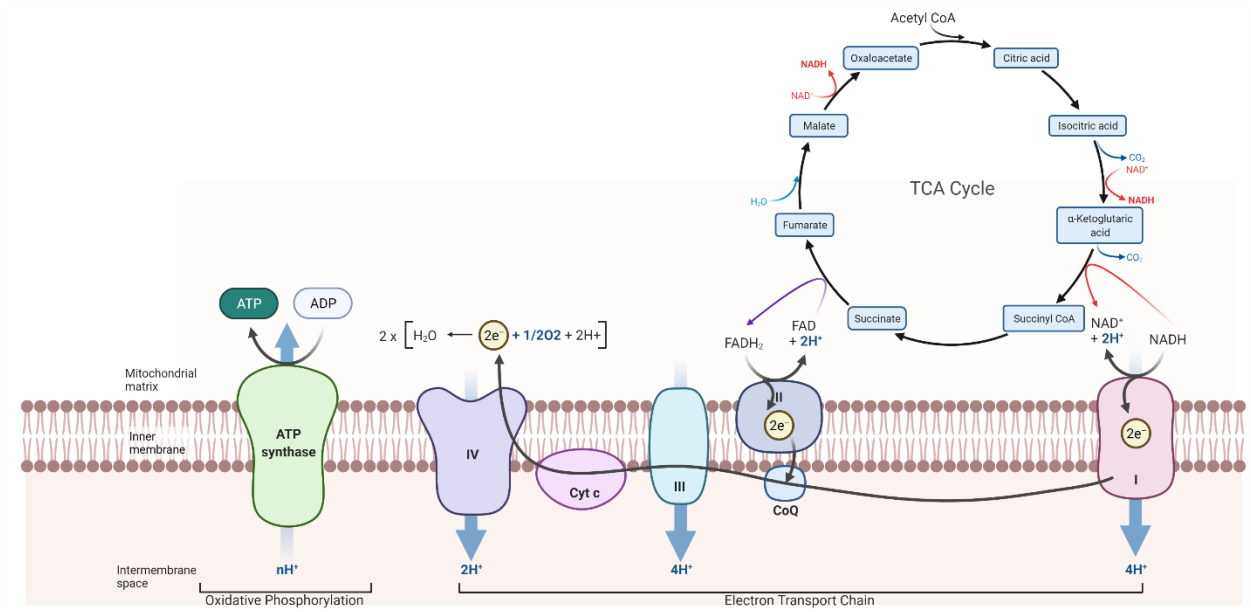

Figure 1.2. The tricarboxylic acid (TCA) cycle and the electron transport chain (ETC). High energy molecules, NADH and $FADH_2$, donate 2 electrons to the ETC at Complex I or Complex II, respectively. Electron transfer from NADH to Complex I pumps 4 protons (H^+) from the mitochondrial matrix to the intermembrane space. At Complex III electrons are transferred to cytochrome C. Cytochrome C then carries single electrons to Complex IV, which binds oxygen (O_2). O_2 is reduced to H_2O. Mitochondrial respiration consumes 8 electrons and 4 H^+, creating two H_2O molecules. There is net translocation of 10 H^+ into the intermembrane space which creates an electrochemical proton gradient. Movement of protons through Complex V results in phosphorylation of ADP and generates ATP. *Adapted from "Krebs Cycle" and "Electron Transport Chain", by BioRender.com (2022). Retrieved from https://app.biorender.com/biorender-templates.*

1.1.2.2. Mitochondrial Membrane Channels

ROS produced by the ETC causes $\Delta\Psi_m$ collapse and cell wide depolarization within the myocardium.(24) Disruption to the mitochondrial membrane causes permeability transition due to loss of volume homeostasis, i.e. swelling. Damage to the outer membrane of the mitochondria occurs when the cell undergoes stress, causing mitochondrial permeability transition (mPT) via opening and closing of pores. Opening of mPT pores (mPTP) increases permeability of ions into the mitochondrial intermembrane space resulting in collapse of $\Delta\Psi_m$ and depolarization.(25) Depolarization halts ATP synthesis and may lead to cell death.

However, mPT is a reversible process that is tightly linked to matrix Ca^{2+} levels and opening of mPTP. In fact, limiting mPT was protective against cardiac stress during diabetic cardiomyopathy and ischemia/reperfusion injury in rodents.(26-28) mPTP opening is a controlled process that is regulated by cyclophilin D binding, free fatty acids, matrix Ca^{2+} levels, ROS byproducts, and low transmembrane potential.(25) Prolonged opening of the mPTP has pathological consequences, especially for the heart.(25) Blocking mPTP opening with cyclosporin A attenuated cardiomyocyte death and mitochondrial dysfunction, but did not affect incidence of arrhythmia.(24, 29) Thus, preventing membrane depolarization and mPTP opening may be protective in stressed cardiomyocytes. Oxidative stress, membrane depolarization and mPTP opening all contribute to mitochondrial dysfunction and have been observed in cardiomyocytes in response to hypertrophic stimuli such as ET1.(30, 31)

In addition to mPTP, the Ca^{2+} uniport (MCU) complex, mitochondrial ATP-sensitive potassium (mitoK_{ATP}) channels, and inner membrane anion channels (IMAC) are located on the inner mitochondrial membrane.(24) Of note, IMAC mediates transport of various anions across the inner membrane and is an important contributor to mitochondrial volume homeostasis.

Blockade of IMAC attenuates ROS-induced collapse of $\Delta\Psi_m$.(32) Targeting IMAC also prevented fluctuations in APD, suggesting that IMAC blockade may protect against the development of arrhythmia.(24) Overall, cardiac mitochondrial membrane complexes play a key role in regulating mitochondrial energy production by maintaining $\Delta\Psi_m$. Dysfunction of mitochondrial membrane complexes during metabolic stress promotes severe cardiovascular outcomes such as arrhythmia and heart failure.(15, 24)

1.1.2.3. Signaling Mediators

AMP-activated protein kinase (AMPK) is an energy sensor of the cell that consists of three protein subunits: α, β and γ. Activation of AMPK occurs when AMP and ADP bind to the γ subunit of the protein and conformational change and phosphorylation at threonine 172 (Thr172) of the α subunit.(33) Upstream signaling mediators that activate AMPK at Thr172 are liver kinase b1 (LKB1) and Ca^{2+} calmodulin-dependent kinase kinase 2 (CAMKK2).(34) AMPK regulates multiple physiological pathways including fatty acid oxidation, glycolysis, and mitochondrial biogenesis. Under stress conditions such as heart failure and AF, AMPK activation is cardioprotective by regulating cellular metabolism.(33, 34)

As mentioned previously, in the stressed heart the major substrate for energy metabolism switches from fatty acids to glucose, and ATP production is reduced. The heart loses its ability to be metabolically flexible, and there is an imbalance between energy production and energy consumption. Mitochondrial dysfunction can occur due to increased ROS, loss of Ca^{2+} homeostasis, impaired mitochondrial dynamics, and transcriptional aberrations.(35) AMPK regulates enzymes related to ATP biosynthesis that enables restoration of the balance between ATP supply and ATP demand within the myocardium. This includes the ability of AMPK to

restore fatty acid uptake and oxidation by rescuing expression of carnitine palmitoyl transferase 1 (CPT-1), which is responsible for fatty acid translocation during β-oxidation. This facilitates increased ATP production and restores energy supply within the heart.

Additionally, during heart failure, transcription factors that are critical for regulating mitochondrial energy production are downregulated. Peroxisome proliferator-activated receptor α (PPARα) is responsible for fatty acid transport into the peroxisome and mitochondria PPAR-γ-coactivator 1α (PGC1α) regulates mitochondrial biogenesis.(15, 33) However, AMPK activation also induces mitochondrial biogenesis via serine phosphorylation of PGC1α, or indirectly by deacetylating PGC1α through sirtuin 1 (SIRT1) activation.(33)

Activation of AMPK induces autophagy, which can assist in restoring both structure and function of a hypertrophic myocardium. In the hypertrophic heart, inhibition of mammalian target of rapamycin (mTOR) using rapamycin promoted autophagy, cell survival, and cardioprotection.(33, 36) In fact, AMPK activation inhibited cardiac hypertrophy by enhancing autophagy via inhibition of the mTOR complex I pathway.(33, 36) However, the AMPK-mTOR signaling pathway is complicated, as excessive upregulation of autophagy leads to cell death and impaired cardiac function.(33, 37) Additionally, both Ozcan *et al.* and Allessie *et al.* demonstrated that LKB1 knockout mice (i.e. decreased level of AMPK activation) develop structural remodeling including bi-atrial enlargement, inflammation, fibrosis, necrosis, and apoptosis.(34, 38, 39) Ozcan *et al.* reported that inhibition of AMPK also impacted electrical parameters through reduction in gap junction proteins, connexin43 (Cx43) and connexin40 (Cx40).(38) Furthermore, AMPK activation in LKB1 knockout mice improved mitochondrial oxygen consumption, atrial myocardium cellular structure, and gap junction proteins.(38) Overall, these data establish AMPK as an effective upstream signaling mediator for prevention of AF.

1.1.3. Cardiac Electrophysiology

The synchronous contraction of the heart is dependent on an intrinsic electrophysiological (EP) system. The SA node generates an electrical AP which propagates throughout the atria via cell-to-cell conduction and the interatrial pathway (Figure 1.3). APs spread from depolarized cardiomyocytes to less depolarized neighbouring cardiomyocytes through intercellular gap junctions and ion channels. EC-coupling results when APs depolarize cardiomyocytes and convert this electrical signal into a contraction signal (i.e. through elevation of cytosolic Ca^{2+} and CICR in the sarcoplasmic reticulum). APs from the SA node travel through the atria to the AV node, and into the ventricles (Figure 1.3). Specialized cardiac conduction cells slow the AP impulse at the AV node. This delay allows complete atrial depolarization and contraction preceding ventricular depolarization. Finally, APs travel through the bundle of His into the left and right bundle branches, and lastly through the Purkinje fibres (Figure 1.3).

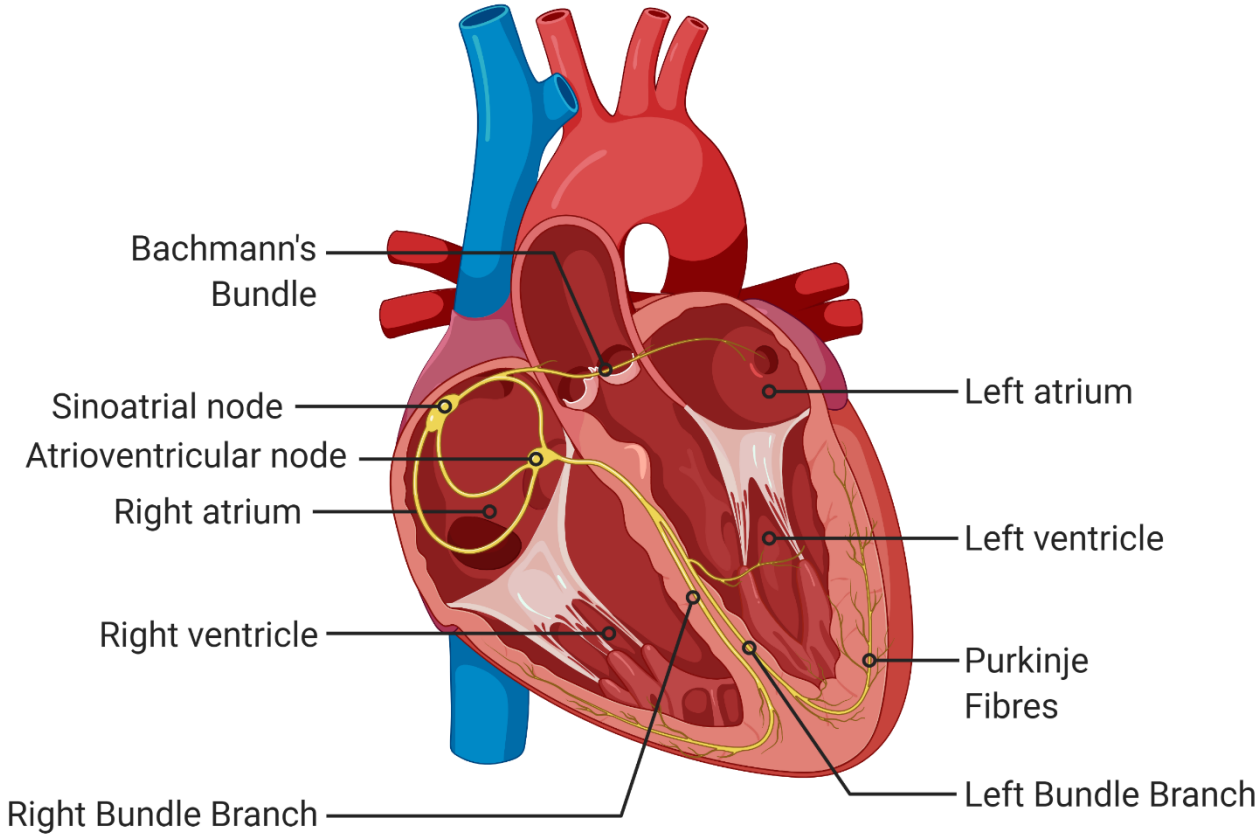

Figure 1.3. Action potential conduction pathway in the heart. The SA node generates an electrical AP which propagates throughout the heart. APs generated at the SA node travel through the atria and Bachmann's bundle. AP travel from SA to the AV node. Specialized cardiac conduction cells slow the AP impulse at the AV node. APs travel from AV node to the bundle of His into the left and right bundle branches, and finally into the Purkinje fibres. *Adapted from "Heart Anatomy", by BioRender.com (2022). Retrieved from https://app.biorender.com/biorender-templates*.

1.1.3.1. Action Potential Formation

Ion channels allow the passage of ions across cell membranes and are essential for ion homeostasis and cellular excitability.(40) Activation of ion channels occurs by changes in cellular voltage, intracellular and extracellular ligands, neurotransmitters, pressure and volume.(41) Many ion channels are highly selective and allow the passage of a single type of ion.(40) However, some ion channels remain less discriminating than others such that ions of similar charge flow through them. Augmentation of ion channel activity can lead to arrhythmias through a process termed enhanced automaticity.(42) The AP of cardiomyocytes is regulated by complex interaction between ion channels and gap junctions on the cell membrane. However, it should be noted that not all cardiomyocytes have the same AP shape, duration, resting membrane potential, and threshold potential (Figure 1.4 & Table 1).

1.1.3.1.a. Pacemaker Cardiomyocytes

Pacemaker cells of the SA node and AV node do not have a resting membrane potential, as they are in constant flux of repolarization and depolarization. The Purkinje fibres have slightly altered APD and formation compared to the other regions of automaticity. Thus, for the purpose of this review pacemaker cells of the AV and SA node will be of focus. Pacemaker APs are separated into only three phases; Phase 0, 3, and 4 (Figure 1.4). During Phase 4 the cell undergoes spontaneous depolarization that will trigger initiation of AP once a threshold potential between -30 to -40 mV is reached. Phase 0 is the depolarization phase and lacks fast Na^+ currents (I_{Na}). Lastly, Phase 3 repolarizes the cell to approximately -60 mV where the AP cycle will spontaneously repeat. When the AP is at the end of repolarization in Phase 3, the ion channels that control the slow inward Na^+ currents sequentially open; these are termed funny currents (I_f). These

currents depolarize the cell and trigger Phase 4, opening transient T-type Ca^{2+} currents ($I_{Ca(T)}$). Eventually this inward Ca^{2+} current depolarizes the cell enough to initiate long lasting L-type Ca^{2+} currents ($I_{Ca(L)}$) and the threshold potential is reached. Fundamental to pacemaker automaticity is the release of Ca^{2+} from the sarcoplasmic reticulum and activation of Na^{+}/Ca^{2+} exchange current (I_{NCX}).(43) Chronotropy of pacemaker cells is modified if any of the aforementioned currents are altered. For example, the sympathetic system can activate I_f, and vagal stimulation can block I_f, leading to increase and decrease in heart rate, respectively. Pacemaker cells utilize several currents to control rate of diastolic depolarization including, but not limited to, I_f, $I_{Ca(T)}$, $I_{Ca(L)}$, I_{NCX} and through reduction of repolarizing potassium (K^{+}) currents (I_K).(43)

1.1.3.1.b. Ventricular and Atrial Non-pacemaker Cardiomyocytes

A fully initiated AP for non-pacemaker cardiomyocytes is described through 5 phases (Figure 1.4). In non-pacemaker cardiomyocytes the major depolarization phase (Phase 0) begins with the sequential opening of voltage-gated sodium (Na^{+}) channels. As Na^{+} flows into the cell, it becomes more positive, increasing from the resting membrane potential (approx. -90 mV) to the threshold potential (approx. -70 mV) (Table 1).(40, 44) Once at threshold potential, the potential rises rapidly, to approximately 40 mV. During Phase 1 there is partial repolarization caused by sequential inactivation of Na^{+} channels and K^{+} channels, resulting in a slight negative charge, or "notch" in the AP.(44) A characteristic of the atrial AP is that the "notch" formation is significant due to increased voltage gated transient outward K^{+} current (I_{to}).

The plateau (Phase 2) consists of concomitant movement of Ca^{2+} into the cell via $I_{Ca(L)}$ and I_{NCX} currents and K^{+} out of the cell through ultra-rapid, rapid, and slow delayed rectified K^{+} currents (I_{KUR}, I_{KR}, I_{KS}). L-type Ca^{2+} channels open and produce a major current (i.e. $I_{Ca(L)}$) that

regulates the duration of the action potential.(44) Briefly, during Phase 2 Ca^{2+} binds to RyR in the sarcoplasmic reticulum which induces CICR and cardiomyocyte contraction.(40) To maintain ionic equilibrium, Ca^{2+} exits the cell during diastole through the NCX.(45)

Following the plateau phase, Phase 3 begins where rapid repolarization of the cell is initiated. L-type Ca^{2+} channels begin to close while slow delayed rectifier K^+ channels remain open resulting in a net outward positive charge, and an inward negative membrane potential.(44) Finally, Phase 4, or the relaxation and rest phase, is initiated by an increase in K^+ outward currents (I_{K1}) restoring the resting membrane potential, which is typically -90 mV for ventricular cardiomyocytes and -80 mV for atrial cardiomyocytes (see Table 1).(43, 44) The resting potential is primarily determined by I_K, and is close to the equilibrium potential of K^+ ions. Lastly, the AP profile for atrial and ventricular cardiomyocytes differs (Figure 1.4). Atrial AP have a shorter duration, elevated I_{to} leading to more defined "notch", increased I_{KUR} resulting in shorter and more inclined "plateau" and decreased I_{K1} resulting in a more positive resting membrane potential. Overall, initiation and conduction of an AP relies on ion channels.

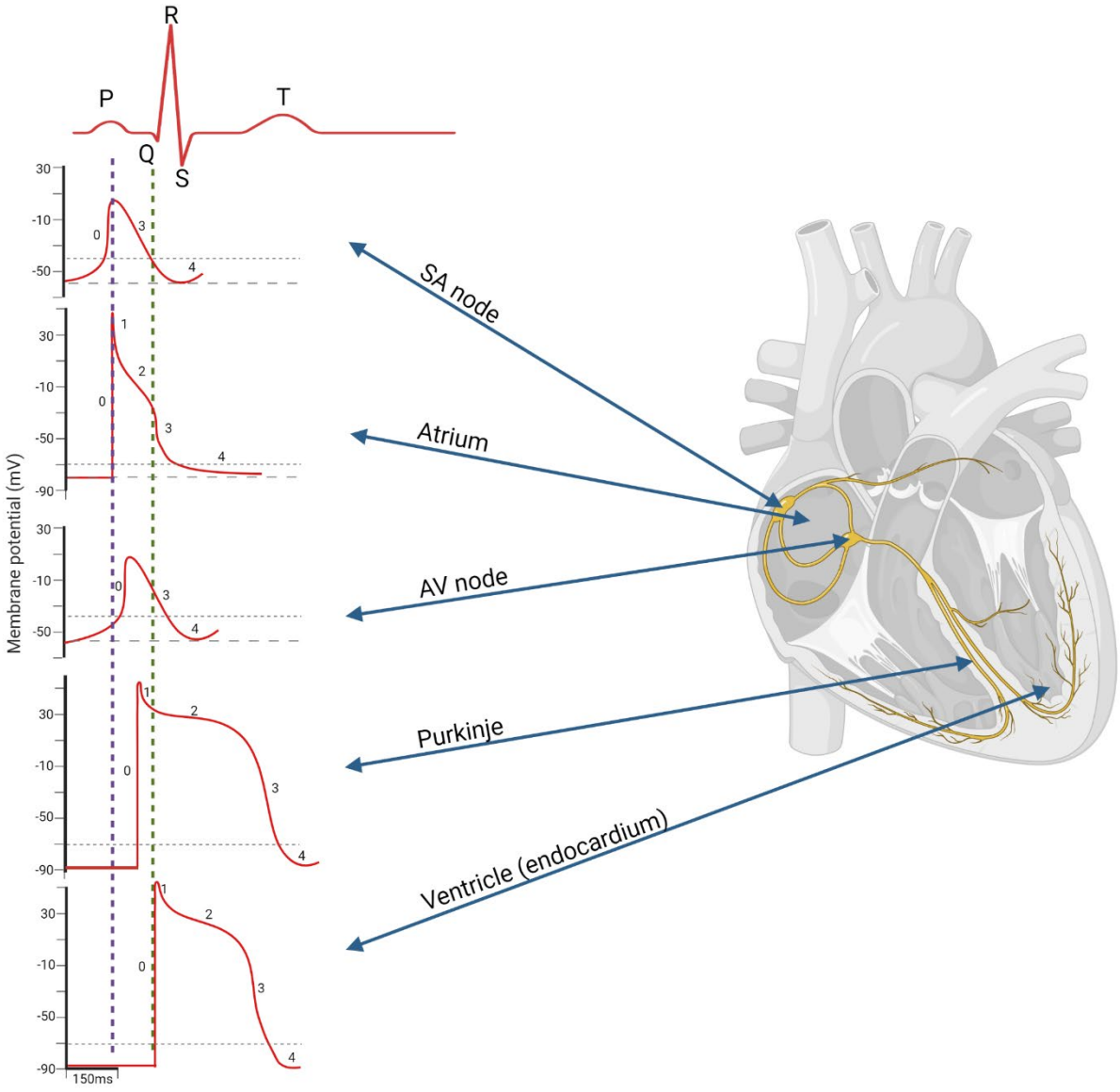

Figure 1.4. Action potential duration and shape within the myocardium. Electrical activity of pacing, and non-pacing atrial and ventricular cardiomyocytes. Pacemaker AV and SA node AP are separated into three phases; Phase 0, 3, and 4. Non-pacemaker AP are separated into 5 phases; Phase 0 to 4. This figure is adapted from ref(41): *Nerbonne, and Kass (2005). Physiol Rev 85(4): 1205-1253. Created with BioRender.com (2022).*

Table 1. Differences in Cardiomyocyte Action Potentials

	Atrial Cardiomyocyte	Ventricular Cardiomyocyte	Pacemaker cardiomyocyte (SA/AV node)
Phases	5 (Phase 0 – 4)	5 (Phase 0 – 4)	3 (Phase 0, 3, 4)
Threshold potential (mV)	-70	-70	-30 to -50
Resting membrane potential	-80	-90	n/a
Major currents (I)	I_{Na}, $I_{Ca(L)}$, $I_{Ca(T)}$, I_{NCX}, $I_{to(fast)}$, $I_{to(slow)}$, I_{Kur}, I_{Ks}, I_{K1}	I_{Na}, $I_{Ca(L)}$, $I_{Ca(T)}$, I_{NCX}, $I_{to(fast)}$, $I_{to(slow)}$, I_{Kur}, I_{Ks}, I_{K1}	I_f, I_{NCX}, $I_{Ca(L)}$, $I_{Ca(T)}$, I_K
Differences in AP	$\uparrow I_{to}$, $\uparrow I_{Kur}$, $\downarrow I_{K1}$ - More positive resting potential compared to ventricular - Abbreviated plateau phase - Slow terminal repolarization	- Large plateau phase - Fast response cells - Fast terminal repolarization	- Lacks fast Na^+ current - Primarily slow Ca^{2+} current at Phase 0 - Slow response cells - Mainly Ca^{2+} and K^+ currents

1.1.3.2. Conduction Velocity

Conduction velocity is the speed at which depolarization waves move throughout the myocardium. Within the atria the maximum upstroke velocity (V_{max}) of phase 0 is 150-300 V/s, compared to 300-400 V/s in the ventricles due to the higher resting potential of the atrium.(46) The depolarization wave travels from the SA node, through both atria via the interatrial pathway (i.e. Bachmann's bundle), to the AV node, Bundle of His, Purkinje fibres, and to the ventricles. This all occurs in approximately 200ms. Conduction velocity is dependent on the rate of depolarization of the AP through neighboring cells. This wave moves cell-to-cell via the transport of ions through ion channels and gap junctions that allow Na^+ and Ca^{2+} to enter the cell and initiate a sequential AP. Alterations in conduction velocity occur through mechanisms affecting Phase 0 such as changing membrane potential or inhibiting I_{Na} currents.(47) Both of these mechanisms decrease the amplitude of the AP and the speed in which it is conducted. Alterations in membrane potential occur during myocardial ischemia and in response to certain antiarrhythmic drugs that alter Na^+ channel function.(47) Alterations to the conduction system in both the atria and ventricles lead to complex arrhythmia and fibrillation events.(3)

1.2. Pathological Cardiac Remodeling

Cardiac remodeling results in pathological complications including AF, ventricular hypertrophy, and heart failure.(48-50) Structural, electrical and metabolic changes contribute to the remodeling process by developing substrate to initiate and progress cardiac complications. Highlighted below are two cardiovascular diseases, AF and ventricular hypertrophy; these diseases target either atrial or ventricular chambers, respectively. Regional cardiac remodeling involved in disease progression is discussed below.

It should be noted there are forms of physiological remodeling as seen in athletes and pregnant women.(51) However, for the purpose of this thesis any reference to cardiac remodeling should be presumed to be under pathological conditions.

1.2.1. Atrial Fibrillation

Atrial fibrillation is the most common sustained cardiac arrhythmia.(52) It is an endpoint of atrial remodeling that occurs during several cardiovascular diseases.(53) AF results from concomitant interactions of morbidities such as high blood pressure, congestive heart failure, coronary artery disease (CAD), genetic predisposition, sleep apnea, and other environmental factors.(54-57) However, it should be noted that AF can occur without pre-existing cardiovascular conditions and is defined as *lone-AF*. Initiation of AF involves sources of electrical activity, termed drivers, that trigger arrhythmic episodes. (45) As cardiovascular complications progress within a patient, atrial substrate development occurs. AF is a disease that results in further remodeling over time which contributes to progressive and sustained arrhythmias. (52, 58) Persistent arrhythmias lead to reduced cardiac performance, quality of life, and survival.(52, 58) Thus, AF is an important contributor to the morbidity and mortality of the human population.(59, 60) Currently, AF affects approximately 200,000 Canadians, and is becoming more prevalent with the aging population.(59, 61, 62)

AF is a multifactorial disease, and there are multiple mechanisms for initiation and continuation of arrhythmias. Untreated AF leads to a higher risk of stroke and heart failure.(63, 64) In persons above the age of 60, one in three strokes is a result of AF.(65) AF is categorized into three subtypes; paroxysmal, persistent, and permanent. Paroxysmal AF is short-lived and patients return to normal heart rate within 7 days, while persistent AF lasts more than 7 days, and

will likely not return to spontaneous heart rate without treatment intervention.(54) Paroxysmal AF has been shown to develop into persistent AF in the clinic.(45) Lastly, permanent AF does not respond to treatment or medication.

Sustained electrical activity within the atrial tissue triggers arrhythmic episodes that result in AF initiation. Changing the structural and electrical properties of the atria, termed atrial remodeling, increases "AF substrate", resulting in vulnerability to arrhythmia development. Due to the heterogenous nature of AF, underlying cardiac disease increases susceptibility of the atria to arrhythmias. Thus, the onset and promotion of AF is likely a convergence of several molecular mechanisms. Maintenance of AF occurs through two major sources, re-entry or rapid ectopic firing.(66) Patients with cardiovascular disease have an increased risk of AF through disruption of atrial EP. Electrical remodeling creates an environment for re-entry to begin and AF to be maintained, and structural remodeling of the atria results in internal propagation of AF within the atria.(67)

Gap junction modifications can lead to conduction irregularities. Gap junctions are altered by interstitial fibrosis, dilation and enlargement of left atrium (LA), aging, hypertension, and congestive heart failure (CHF).(68, 69) Fibrosis development from *de novo* collagen accumulation and apoptosis contributes to random excitation of the atria, and subsequently AF initiation.(70, 71) Dilation and stretch enhance atrial substrate through myocyte hypertrophy, apoptosis, fibrosis, and change mitochondrial bioenergetic parameters.(72-75) In fact, atrial dilation alters electrical parameters and increases AF susceptibility in animal models.(76) Furthermore, congestive heart failure, a common cause and consequence of AF, is associated with increased number of sustained AF events in canine models.(56)

1.2.1.1. AF Maintenance and Mechanisms

As discussed in the previous section, AF is a multifactorial disease that has several mechanisms for initiation and self-perpetuation. Structural remodeling of the atria can lead to changes in electrical and anatomical parameters which internally propagate AF within the atria.(67) Electrical modification in the atria ranges from altering atrial effective refractory period (AERP) and APD, ion channel activity and expression, and increased fibrosis.(71, 77, 78) The culmination of atrial remodeling creates an environment for re-entry to begin and AF to be maintained.

1.2.1.1.a. Re-entry

Although AF appears to have a random and chaotic nature, the driver behind AF, *re-entry*, is highly organized. Atrial structural changes slow conduction and create barriers for electrical wave propagation, inducing initiation and maintenance of re-entry circuits.(53) Re-entry occurs when there is a reduction in AERP and a decrease in conduction velocity, causing cells to be re-excitable when a slowed impulse wave arrives.(79) Reduction of these parameters can lead to multiple circuit re-entry in the atrial tissue and further AF substrate development.(50)

First described in 1977, re-entry can be explained simplistically through the *leading circle model*.(80) In this model a wavefront moving in a circular pattern is continuously propagated. Refractoriness of the wave front occurs due to continuous centripetal activation at the centre of the circle, at the refractory tissue.(80) Unidirectional block in the tissue forms an impulse that can then propagate out to the surrounding myocardium and inwards to the refractory tissue. However, if there is a decrease in the wavelength (a product of the conduction velocity and the refractory period)(45, 80) re-entrant waves become smaller and AF has enhanced sustainability.(45) Despite the fact that the leading circle model was first described, the current major mechanistic model

describing sustained re-entry in AF is the *spiral wave model*. This model is dependent on functional properties of the atrial tissue.(81, 82) Fibrillation results from multiple spirals around core tissue, where each spiral produces additional spirals that propagate throughout the atrial tissue.(82)

Stabilization of re-entry occurs through conduction disturbances, sustaining AF without wavelength decreases.(45, 83) Ectopic activity originating in the atrial myocardium surrounding the pulmonary vein is fundamental in the instigation and persistence of AF.(84, 85) Arora *et al.* and Kalifa *et al.* showed in canine and sheep models, respectively, that pulmonary veins are a source for re-entry and rapid activity.(86) The cardiomyocyte sleeve surrounding the pulmonary vein contributes to conduction slowing and wavelength reduction, making this an ideal area for re-entry to occur. Consequently, AF maintains itself through wavelength decreases resulting in AF-related remodeling, which contributes to self-perpetuating arrhythmic activity.(71, 87)

Tachycardia remodels atrial tissue similar to AF,(66) and promotes re-entry through altering atrial substrate.(88-91) Despite the fact that electrical remodeling from atrial tachycardia is reversible after cessation of tachypacing, remodeling of structural properties likely does not reverse.(92) Perhaps this form of remodeling is responsible for inducing the transition from paroxysmal AF to persistent AF. As the duration of persistent AF increases the likelihood that sinus rhythm cannot be restored after catheter ablation also increases.(45, 92) Overall, AF modifies both electrical and structural properties to sustain AF.(91)

1.2.1.1.b. Afterdepolarizations

Afterdepolarizations are abnormal impulses that are triggered by a preceding AP and may cause certain types of ventricular and atrial arrhythmias. There are two types of afterdepolarizations, delayed afterdepolarizations (DAD) and early afterdepolarizations (EAD). DADs arise from

resting potential following a full repolarization of an AP at the end of phase 3 or early phase 4 of an AP.(93) Ca^{2+} overload and rapid activation rates can result in DADs and may lead to a series of rapid depolarizations, such as tachyarrhythmias.(93) EADs arise at the end of a AP before it reaches resting potential during late phase 2 or phase 3.(93) Slow preceding activation rates and prolonged APD result in EADs.(93) Therefore, drugs that decrease APD are effective in treating EAD initiation and resulting tachyarrhythmia.

1.2.1.1.c. Triggers

Triggers are considered the instigators of AF, whereas severity and sustainability of the arrhythmia are a result of atrial substrate. Tachycardia, bradycardia, cardiac hypertrophy, sympathetic and parasympathetic stimulation are all possible triggers.(39, 79) Furthermore, ectopic beats, primarily in proximity to the pulmonary veins, trigger paroxysmal AF.(84, 85, 94) Alterations in electric properties of pulmonary vein cardiomyocytes result in DADs and EADs.(95) In cardiac hypertrophy, prolonged APD can trigger DADs, resulting from reduction of K^+ currents.(79) Experimental models initiating triggers, such as atrial tachypacing models and thyroid hormone exposure, increase arrhythmia susceptibility.(96, 97) Triggers propagate into the atrial myocardium and instigate re-entery wavelets and shortened wavelengths.

1.2.1.2. Atrial Remodeling

Atrial remodeling involves a wide range of growth factors, cytokines, hormones, and stress signals.(70, 71) AF substrate, or the susceptibility of atrial tissue to fibrillation or arrhythmia, is developed through structural, electrical, and metabolic remodeling.(50, 98) A major consequence of remodeling is shortened refractoriness and AERP. AERP is the time interval during which a

new AP cannot be initiated within the atria. Shortening of AERP enhances AF by increasing atrial vulnerability and susceptibility to DADs.(99) Atrial refractoriness in humans is shortened after several minutes of AF induction and atrial tachycardia, indicating that AF perpetuates itself by shortening atrial wavelength.(89-91, 99) Changes in AERP may be a result of rapid changes in intracellular ion concentrations, ion pump activity and phosphorylation events.(45) The mechanisms and signals that induce AERP shortening remain to be elucidated.

Structural changes of atrial tissue result from fibrosis, hypertrophy, and dilation.(100) As AF becomes more persistent, fibrosis and atrial dilation increase in severity. Thus, as atrial substrate develops, atrial regions become suitable to initiate and sustain re-entry circuits. Dilation and hypertrophy increase atrial surface providing more circuits and longer wavelengths to be maintained. Interstitial fibrosis also contributes to AF substrate development; elevated levels of secreted profibrotic molecules such as angiotensin II (AngII) and transforming growth factor-β1 (TGF-β1) mediate signaling pathways that lead to initiation of fibrosis.(50) AngII mediates cardiac fibrosis in several cardiovascular diseases, such as hypertension and heart failure.(50) Binding of AngII to angiotensin type 1 receptors (AT_1R) begins a signaling cascade that stimulates fibroblast proliferation, cardiomyocyte hypertrophy and apoptosis.(101) However, AT_1R and angiotensin type 2 receptors (AT_2R) signaling cascades tend to be distinct and somewhat opposing. AT_1R triggers remodeling through cascades initiated from activation of guanosine triphosphatase (GTPase) protein Ras (e.g. extracellular signal related kinase (ERK) and c-Jun N-terminal kinase (JNK) signaling).(102) AT_1R also stimulates phospholipase C (PLC) prompting downstream Ca^{2+} release, and thus, promoting remodeling.(102) However, AT_2R activation inhibits mitogen-activated protein kinases (MAPK) (e.g. ERK and JNK) via dephosphorylation. Underlying

conditions such as heart failure, promote fibrosis and hypertrophy, which slows conduction velocity within the atria promoting atrial remodeling and incidence of AF.(50, 83, 103)

Electrical remodeling, including changes to gap junctions and ion currents, leads to shortening of APD and AERP.(38, 71, 77, 78) These modifications cause AF initiation through DADs and EADs.(100) Furthermore, the development of atrial substrate potentially leads to non-distinct ion channel remodeling.(3) AF-related remodeling is provoked by rapid electrical activity and subsequent Ca^{2+}-overload within cardiomyocytes, predominantly during Phase 2 of an AP.(71, 87) Upregulation of $I_{Ca(L)}$ and upregulation of I_K mediated by inward rectifying potassium channel (Kir2.1) overload Ca^{2+} into the cardiomyocyte.(53) Furthermore, AF induced by atrial tachycardia suppresses contractility through Ca^{2+} homeostasis, resulting in contractile remodeling.(104, 105) Overloading of Ca^{2+} is cytotoxic to cardiomyocytes; therefore cellular mechanisms protect cardiomyocytes from excessive influx.(45) To reduce Ca^{2+} loading cardiomyocytes downregulate or inactivate L-type Ca^{2+} channel mRNA, as long-term and short-term mechanisms, respectively.(45, 106) Sustained modification of $I_{Ca(L)}$ results in atrial contractile dysfunction that causes APD and AERP reduction.(45, 107) It is speculated that decreasing the concentration of extracellular Ca^{2+} could inhibit tachycardia-remodeling.(105)

Downregulation of I_{Na} also contributes to slowed conduction rate within the atria.(45, 108) As a result of slower conduction rate, wavelength and AERP are reduced, facilitating re-entry.(109) Reductions in tachycardia-induced conduction may also be a result of I_{Na} as shown by Gaspo *et al.* and Yagi *et al*.(108, 110) Notably, however, I_{Na} changes have only been demonstrated in canine atria and I_{Na} reduction has not been described in cardiomyocytes from AF patients.(108) Less is known about the relationship between K^+ channels and AF, and there are inconsistent results. Evidence of downregulation of transient outward K^+ current in AF has been shown;

however the functional importance of this reduction is still unresolved.(106, 107) Furthermore, Yue *et al.* demonstrated that Kir channels did not change during atrial tachycardia remodeling in a canine model.(106, 107) However, more recent studies by Cha *et al.* and Ehrlich *et al.* demonstrated upregulation of Kir channels, and background I_K and acetylcholine activated K^+ currents (I_{Ach}) are augmented.(111, 112)

Gap junctions are altered in AF. Gap junctions, such as Cx40 and Cx43, are formed from transmembrane ion channels called connexins and transfer ions between cardiomyocytes. Cx40 and Cx43 are essential for cell-to-cell coupling and cardiac conduction. Decreased connexin expression results in changes to cell coupling, altered refractoriness, and increased susceptibility for re-entry.(113) Several groups have demonstrated reduction in Cx43 expression in AF pacing models and LKB1 knockout models.(114-117) In fact, Igarashi *et al.* reported that gene transfer of Cx40 and Cx43 into an atrial pacing model (i.e. increasing gap junction levels) resulted in significantly higher probability of sinus rhythm and improved atrial conduction compared to sham pacing.(118)

Additionally, metabolic dysregulation consisting of AMPK downregulation, increased ROS activation of CAMKK2, and calcineurin–nuclear factor of activated T lymphocytes (NFAT) signaling promote AF.(34, 119) Furthermore, inhibiting AMPK by deleting its upstream activator, LKB1, leads to atrial enlargement, fibrosis, and fibrillation as well as reduced Cx40 and Cx43.(117, 120) As previously mentioned, AMPK plays an important functional role to conserve ATP levels in the mitochondria, and when disrupted influences atrial remodeling. By increasing fatty acid uptake and oxidation, AMPK maintains energy homeostasis in the heart, while decreasing high energy expenditure pathways. Activation of AMPK through phosphorylation is likely increased in paroxysmal AF as a compensatory mechanism to address metabolic stress.(121)

Additionally, AMPK phosphorylation is reduced by aldosterone via protein phosphatase 1A (PPM1A) (122) and during chronic AF.(123, 124) Furthermore, our lab reported that the synthetic cannabinoid, CB13, increased the phosphorylation of AMPK$\alpha_{1/2}$ in hypertrophic ventricular cardiomyocytes.(125) Additionally, Kola *et al.* showed that endocannabinoid, 2-arachidonyl glycerol (2-AG), activates AMPK in the heart.(126) Overall, AF is a multifactorial disease that can be initiated and maintained through triggers, re-entry, ectopic beats, and is further propagated by multiple remodeling mechanisms.

1.2.2. Left Ventricular Hypertrophy and Heart Failure

Left ventricular hypertrophy (LVH) is an increase in ventricular mass which occurs due to an increase in wall thickness or dilation and in response to pressure and volume overload, respectively. Heart failure is the end result of underlying conditions such as LVH, hypertension, congestive heart disease, and myocardial infarction.

Morphological, electrical and metabolic changes that occur to myocardial tissue resulting from ventricular hypertrophy lead to further cardiac dysfunction. In fact, hypertrophy significantly increases the risk of heart failure and is the leading cause for heart failure and sudden death.(127) LVH is thus a predictor of more severe cardiovascular complications and an important research target. Currently, over 650,000 Canadians over the age of 40 are diagnosed and living with heart failure.(128) However, LVH is not just an increase in cardiomyocyte size, and is a result of several remodeling events, including alterations to signaling, EP, and metabolism.(48)

1.2.2.1. Hypertrophy Maintenance and Mechanisms

Cardiac hypertrophy is a result of chronic stress and work overload in the heart, and can be categorized into two forms: concentric and eccentric hypertrophy. Concentric hypertrophy develops due to sustained pressure overload, while eccentric hypertrophy develops due to volume overload.(129) Pressure overload results in thickening of the myocardium without change to the chamber volume, whereas volume overload results in the opposite (increased chamber volume, no wall thickening).(129) Compensatory mechanisms resulting from increased cardiac stress, such as hypertrophy, support the additional workload, resulting in changes to Ca^{2+} handling, structural and metabolic functionality.(129) However, compensatory mechanisms become decompensatory over time and heart failure develops as chronic stress and remodeling result in ventricular dilation and diminished contractile function.

1.2.2.2. Ventricular Remodeling

Hypertension, obesity, aortic valve stenosis, and diabetes myelitis contribute to increased stress on the heart, leading to LVH and eventually to heart failure.(129-131) Hypertension leads to concentric or eccentric damage of the left ventricle.(129) Intracellular signaling pathways induced by mechanical stretch lead to changes in gene expression and synthesis of sarcomere proteins, such as actin and myosin.(129) Wall stress resulting from pressure overload is reduced by increasing the size of cardiomyocytes in parallel within sarcomeres, while in volume overload cardiomyocytes are reorganized in series.(129) This compensatory response is linked to increased activation of the sympathetic response, specifically RAS and neurohormones such as catecholamines.(48, 129, 132, 133)

Adaptive and innate immune responses are also altered in hypertension, resulting in increased inflammatory cytokines and dysfunction of macrophages, B cells and T cells.(48) Mechanical stretch of cardiomyocytes and upregulation of pro-inflammatory markers contribute to perpetuation of cardiac fibrosis by converting fibroblasts to myofibroblasts and increasing collagen production.(129, 134) Increased myocardial fibrosis results in induction of heart failure, reduced coronary flow and arrhythmia development.(129, 134-136) Fibroblasts maintain the extracellular matrix (ECM) and facilitate the synthesis and degradation of ECM proteins (e.g. collagen and fibronectin).(132) Additionally, fibroblasts support EC coupling through interactions with cardiomyocytes and propagation of electrical signals.(132, 137) During fibrosis ECM proteins are elevated through increased production and simultaneous downregulation of degradation proteins (e.g. matrix metalloproteinases).(132) However, elevated levels of fibroblasts interfere with EC coupling through disruption to gap junctions and improper propagation of AP. Fibrotic regions are therefore ideal for initiation of arrhythmias.(138, 139) Overall, LVH is simultaneously a compensatory response to hemodynamic changes and a risk factor for downstream pathological cardiovascular outcomes.

In addition to morphological changes, cardiac hypertrophy is associated with fetal gene reprogramming and loss of cardiomyocytes. Conversion to fetal reprogramming includes mRNA gene expression of atrial and B-type natriuretic peptide (ANP and BNP, respectively), shifting from fast contractile α-myosin heavy chain (α-MHC) to slow MHC isoform (β-MHC), and downregulation of sarco(endo)plasmic reticulum Ca^{2+}-ATPase 2a (SERCA2a).(48, 130, 140). Cardiomyocyte loss is due to increased necrosis and apoptosis caused by elevated oxidative stress. Furthermore, autophagy, the removal of dysfunctional cellular components by lysosomes, has both deleterious and adaptive roles.(48) Alterations to signaling pathways mediate stress-induced

alterations to protein homeostasis which can lead to accumulation of dysfunctional proteins and therefore, increased autophagy.(48)

Augmentation to downstream signaling pathways in LVH leads to alterations in protein synthesis and results in cardiac remodeling. Select signaling pathways altered in hypertrophy are AMPK, PGC1α, endothelial nitric oxide synthase (eNOS), and G-protein coupled receptor (GPCR) alterations (Ang and ET1 receptors included).(130) (It should be noted there are many signaling pathways that are altered in hypertrophy and those listed are selected for this thesis.) Metabolic remodeling occurs due to AMPK and PGC1α modulation, eNOS is elevated due to increased oxidative stress, and GPCR changes occur due to neurohormonal and RAS elevation in the stressed heart.(130)

The switch in energy metabolism, from fatty acid to glucose oxidation can result in lipotoxicity, increased ROS, and mitochondrial atrophy as energy demands are not met.(48) Mitochondrial dysfunction has been demonstrated in several cardiovascular diseases, and specifically in heart failure.(141). Mitochondrial aberrations lead to altered biogenesis via PGC1α, alterations to energy signaling from AMPK reduction, and loss of Ca^{2+} homeostasis.(130) In fact, AMPK activation is initially an adaptive response to cardiac injury, and is associated with enhanced glucose uptake. However, aberrations of AMPK signalling develop with elevated ROS and changing [Ca^{2+}]. Inhibiting AMPK in mice resulted in increased LVH severity and adverse remodeling, while AMPK activation via resveratrol or AICAR attenuated cardiomyocyte hypertrophy.(142-144) Overall, AMPK controls energy metabolism and activation may reduce LVH.

Prominent remodeling in hypertrophy also occurs due to increased oxidative stress produced by increased electron leakage at the mitochondrial ETC.(130) While ROS can be an

adaptive response, damage to mitochondria during cardiac stress can result in excessive ROS and mitophagy. However, increased mitophagy, which is considered an initial compensatory response to stress, develops to apoptosis over time leading to cell death and loss of cardiomyocytes.(130) Increased oxidative stress can also be a result of uncoupled eNOS.(130) Lu *et al.* have demonstrated that targeted signaling through AMPK-eNOS had an antihypertrophic effect in cardiomyocytes.(125)

As previously mentioned, both the sympathetic system and RAS are involved in cardiac remodeling. Hypertrophic stimuli such as AngII and ET1 increase ROS production in cardiomyocytes. Receptors for AngII (i.e. AT1R/AT2R) and ET1 (i.e. ET_A/ET_B) are GPCRs. GPCRs are transmembrane proteins consisting of three subunits (Gα, Gβ, Gγ). G-protein isoforms are determined primarily by α subunit, of which there are 3 major subtypes; $G\alpha_q$, $G\alpha_i$, and $G\alpha_s$. Ligands for AT_1R/AT_2R and ET_A/ET_B activate $G\alpha_q$ and the downstream signaling proteins, PLC and phosphokinase C (PKC) (Figure 1.5).(140) Elevated CAMKII signaling is also associated with $G\alpha_q$ and an increase in intracellular Ca^{2+}.(145) Overall, major mechanisms for cardiac remodeling that are involved in LVH include cardiomyocyte loss, increase in cardiomyocyte size, fibrosis, metabolic dysfunction, neurohormonal changes and alterations to contractile proteins.

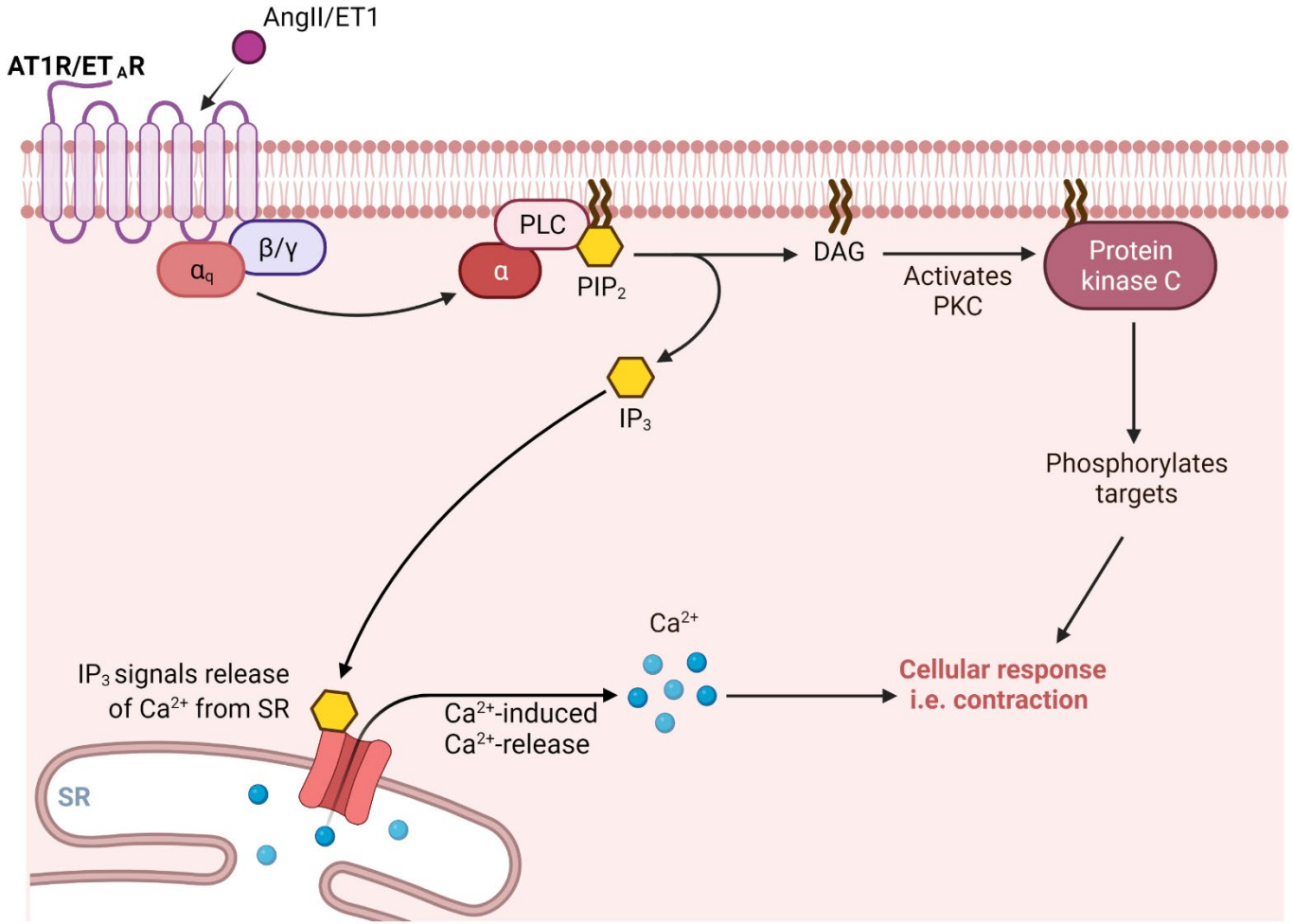

Figure 1.5. G-protein coupled receptor signaling in cardiomyocytes. GPCRs are transmembrane proteins consisting of three subunits (Gα, Gβ, Gγ). Ligands for AT_1R and ET_A activate $G\alpha_q$ and downstream signaling proteins, PLC and PKC. *Adapted from "Activation of Protein Kinase C", by BioRender.com (2022). Retrieved from https://app.biorender.com/biorender-templates*.

1.3.Therapeutic Interventions

1.3.1. Atrial Fibrillation

AF-related atrial remodeling is a major determinant in patient response to antiarrhythmic pharmacotherapies.(45) By investigating the underlying structural, electrical and functional modifications that initiate and sustain AF, highly targeted and, ideally, more effective AF therapeutics can be developed and designed. Improving the efficacy of AF pharmacotherapies is currently being studied.(146, 147)

1.3.1.1. Risk Factors

AF may develop due to underlying morbidities including hypertension, heart disease (CHF and CAD), age, genetics, sleep apnea, obesity, diabetes and other environmental factors.(54-57, 148) There is also evidence that abnormalities in myocardial metabolism play a key role in the development of AF substrate.(149) However, it should be noted that AF can occur without pre-existing cardiovascular conditions, as found in lone-AF.(45)

Lifestyle and risk factor modification for patients susceptible to AF development is a focus for primary AF prevention. By targeting modifiable risk factors, the prevalence and presentation of AF may decrease.(150) Multiple studies have demonstrated that these strategies reduce AF-burden and ideally increase arrhythmia-free survival.(150, 151)

1.3.1.2. Antiarrhythmic Therapies

Antiarrhythmic drugs restore rhythm and normal conduction, and are categorized into four classes: Class 1: Na^+ channel blockers, Class 2: beta-blockers, Class 3: K^+ channel blockers, and Class 4:

Ca^{2+} channel blockers. However, a major side effect of antiarrhythmic therapies is the possibility of provoking new arrhythmias while concealing others by altering APs.(152)

Class 1 antiarrhythmics are further categorized into three subcategories for moderate, weak, and strong Na^{+} channel blockers.(153) Moderate Na^{+} channel blockers tend to increase AERP, while weak Na^{+} channel blockers decrease AERP, leading to increasing chance of developing arrhythmia. Increasing APD may be beneficial when tachycardias are caused by re-entry. However, prolongation of AP may result in EADs. Inhibiting sympathetic response by β-blockers, with regard to cardiac electrical activity, is also beneficial for arrhythmias. Class 2 β-blockers decrease sinus rate, prolong repolarization at the AV node and decrease conduction velocity.(153) Class 2 drugs prevent re-entry mechanisms. Class 3 therapies prolong repolarization, and increase AERP and APD through inhibiting the opening of K^{+} channels in Phase 3 of the AP. Similar to Class 1 drugs, Class 3 are also contradictorily proarrhythmic.(153) The likelihood of EADs increases with APD, leading to the major consequence of Torsades de Pointes, a life-threatening ventricular tachyarrhythmia.(153) Lastly, Class 4 therapies decrease heart rate, inhibit Ca^{2+} channel opening at Phase 2 of the AP and increase AERP. Class 4 therapies targeting Ca^{2+} channels show potential in patients with paroxysmal and persistent AF.(154, 155) L-type Ca^{2+} channel blockers are beneficial in patients who have experienced less than 24 hours of atrial tachycardia.(154) Therapies targeting Ca^{2+} channels have shown some potential in patients with paroxysmal and persistent AF.(154, 155) Overall, current therapies for AF and arrhythmias treat symptoms and not the underlying mechanism or cause.(152)

1.3.1.3. Cardioversion Therapies

Electrical cardioversion or ablation is also an effective therapy for treating ectopic AF. Electrical cardioversion can restore sinus rhythm by targeting the tissue source of ectopic firing.(150) Long-term complications from atrial remodeling include AF returning after cardioversion, and AF becoming unmanageable after pharmacological treatments.(104) Success rates range from 65-90% dependent on AF duration and pre-treatment with antiarrhythmic drugs.(156)

1.3.1.4. Rate Control vs. Rhythm Control

Attempts to tailor AF treatment and management to individuals is complicated. The first step is to determine the type (i.e. paroxysmal, persistent, permanent). Following diagnosis, AF treatment plans aim to control ventricular response rate, convert patient to sinus rhythm and prevent stroke.(156) Management of the disease is varied, as AF induction is caused by several comorbidities.(157) While some underlying triggers can be managed directly to prevent AF reoccurrence (e.g. hyperthyroidism, sleep apnea, alcohol and obesity), other underlying conditions cannot be managed as easily (e.g. CAD, hypertension and heart failure).(157)

Treatment of AF symptoms can be controlled via rate or rhythm. Rate control therapy strategies set a target heart rate to less than 100 bpm. Pharmacotherapy is decided through algorithms based on risk factor assessment. Patients with AF and no history of heart disease, CAD and/or hypertension are given a β-blocker, and/or a Ca^{2+} channel blocker, with accompanying Class 3 antiarrhythmic (i.e. dronedarone) to manage rate, while patients with AF and heart failure are given digoxin along with a β-blocker for rate control management.(158)

Rhythm control pharmacotherapy is categorized by left ventricular function (LVF). Furthermore, rhythm control treatments can be separated into pharmacological and electrical

cardioversion. While certain patient factors may favor rhythm or rate control, there is currently no data suggesting increased survival rates for either control strategy.(65) Patients with normal LVF are given Class 1 or Class 3 antiarrhythmics, and patients with abnormal LVF with impaired ejection fraction are prescribed Class 3 antiarrhythmics.(158) In patients with persistent AF, rate control is viewed as favorable due to lower embolic and adverse events,(157) whereas rhythm control is favored in patients who show magnified symptoms and have new initiation of paroxysmal AF.(157) Ang-converting enzyme (ACE) inhibitors and AngII receptor blockers (ARBs) are also used alongside rhythm control therapies. ACE inhibitors used in clinical AF studies prevented AF initiation in patients with left ventricular dysfunction.(45) If rhythm control is unsuccessful, patients will undergo catheter ablation.

1.3.1.5. New AF Therapeutic Options

Failure of AF treatment is due to adaptive changes in atrial substrate. The longevity of AF symptoms is very important as atrial remodeling due to AF duration is a key issue.(45) New therapeutics that address inflammatory and oxidative stress mechanisms of AF have shown promise.(45, 159) C-reactive protein is elevated in humans with paroxysmal and persistent AF.(45, 159) The steroid, prednisone, and antioxidants probucol and oxypurinol appear to reduce AF-related remodeling. Furthermore, vitamin C and polyunsaturated fatty acids antioxidant properties reduce AF symptoms and recurrence.(159)

1.3.2. Left Ventricular Hypertrophy and Heart Failure

There are several conditions that lead to the development of LVH including, but not limited to, hypertension, hypertrophic cardiomyopathy, aortic stenosis, dilated cardiomyopathy and septal

defects.(129, 160-163) Furthermore, heart failure is the end stage consequence of various heart diseases, and is the leading cause of mortality worldwide.(164) Thus, treatment and regression of underlying cardiovascular disease is a therapeutic target to prevent heart failure development. Heart failure was initially thought to be a consequence of progressive left ventricular systolic dysfunction, diagnosed through the measurement of the fraction of the left ventricular volume pumped per beat, or left ventricular ejection fraction (LVEF). Patients with heart disease demonstrated a lower proportion of volume ejected with every contraction. Thus, LVEF become a predominant characteristic of heart failure due to its convenience and non-invasive assessment criteria. However, patients suffering from heart failure were not always observed to have systolic dysfunction and LVEF reduction. (165) In fact, up to one half of patients suffering from heart failure have preserved or only mildly impaired systolic function.(165) These patients were termed to have diastolic heart failure and characteristic hypertrophied left ventricles with increased mass to volume ratios.(166) Diastolic heart failure is, more recently, categorized as heart failure with preserved ejection fraction (HFpEF), while patients with reduced LVEF are categorized as heart failure with reduced ejection fraction (HFrEF).

1.3.2.1. Risk Factors

The pathophysiological progression from LVH to heart failure is complex and involves several concomitant risk factors for cardiovascular disease, such as hypertension, low-density lipoprotein (LDL) cholesterol plasma levels, diabetes mellitus, obesity, and smoking.(165, 167) However, there are also non-modifiable factors that contribute to disease progression such as age, sex, and racial and ethnic variations. In fact, population-based studies have demonstrated that women have a higher incidence for HFpEF compared to HFrEF, and the incidence of women with HFrEF has

decreased dramatically over time.(165, 168) In addition, patients who develop HFpEF tend to be approximately 6 years older than those diagnosed with HFrEF.(168) Furthermore, black individuals have approximately 50% higher prevalence of heart failure, in general, when compared to white individuals.(169) LVH increases the risk of cardiac arrhythmias; more specifically it is associated with increased risk of progression from paroxysmal to persistent/permanent AF.(170, 171) In fact, anti-hypertensive treatment decreased left ventricular mass but importantly also leads to a decrease in the prevalence of AF.(172)

1.3.2.2. Heart Failure Treatment

Current treatments for patients with heart failure include a combination of pharmacological therapies, lifestyle modifications, and in severe cases, implantable devices and surgery. The goal behind these treatment regimens is to improve symptom progression and patient quality of life by reversing pathological remodeling and prolonging heart function.

There are several drug therapies currently utilized to treat heart failure that target different underlying mechanisms; these include ACE inhibitors, ARBs, aldosterone antagonists/mineralocorticoid receptor antagonists (MRAs), β-blockers, and diuretics. ACE inhibitors and ARBs exhibit similar efficacy for treatment. However, ARBs are used in patients who have developed ACE inhibitor intolerance and a recognizable dry cough. These two therapies act on the same pathway; ACE inhibitors inhibit the conversion of AngI to AngII, while ARBs block the AngII receptor, AT_1R, directly. (130) ACE inhibitors and ARBs relax blood vessels, assist with reduction of fluid retention through salt and water excretion, and lower blood pressure. Furthermore, the interaction of ACE inhibitors and ARBs with AT1R may have a direct effect on

myocardial growth by altering downstream signaling.(130) Therefore, these pharmacotherapies are regularly prescribed for hypertension and heart failure as first-line treatments.

Diuretics, β-blockers and MRAs are usually administered in conjunction with ACE inhibitors and ARBs to control heart failure symptoms. Diuretics reduce symptoms of edema, including shortness of breath. However, they do not necessarily contribute to improved morbidity and mortality.(173) β-blockers also relieve shortness of breath, slow heart rate and decrease blood pressure, allowing improved chamber filling, dilation of blood vessels and improved heart function. MRAs are prescribed in addition to ACE/ARBs and β-blockers as activation of mineralocorticoid receptors promotes fibrosis and inflammation.(174) MRAs reduce hospitalization and total mortality by altering ECM remodeling and renal K^+ and Na^+ levels.(174)

In addition to pharmacological treatments, lifestyle modifications are an important element of treatment regimens. As mentioned previously, some risk factors for LVH development are modifiable. For example, cessation of smoking, low sodium diet, Mediterranean diet, and exercise all contribute to improved cardiac prognosis.(130, 175-177) One of the greatest challenges facing lifestyle modification is patient adherence.(178)

Lastly, implantable devices, such as defibrillators, and surgeries, such as transplantation, are available. However, these therapeutic options have increased barriers and risks associated with them. For example, cardiac transplantation does prolong survival in patients with heart failure, however, donors are limited, there are socioeconomic barriers, and risk of contraindications are high.(130) Implantable devices, such as defibrillators and LV assist devices, are available for decreasing risk of sudden death in patients and are successful.(130) Overall, pharmacological treatments are the most widely available and adopted options for heart failure patients.(130)

1.3.2.3. Pitfalls of Hypertrophy Therapeutic Options

Side effects from heart failure treatments do occur; as previously mentioned some patients are intolerant to ACE inhibitors and develop a cough. Additionally, diuretics cause light headedness, hypotension and electrolyte depletion.(130) As patients with heart failure tend to be elderly, issues associated with treatment strategies include complex drug profiles, comorbidities and non-adherence.(179) Furthermore, there are also differing treatment guidelines for patients with HFrEF and HFpEF. For HFrEF, a large subset of data and trials supports the use of ACE inhibitors, MRAs, ARBs, and β-blockers. However, sufficient data supporting the notion that drug therapy reduces mortality in HFpEF patients is lacking; thus first-line treatment is to improve symptoms of edema and dyspnea.(180) Research is required to determine more effective treatment strategies for HFpEF patients. Current pharmacological strategies to treat heart failure and its underlying conditions primarily target symptom relief and to a lesser extent remodeling. However, as previously discussed there are many remodeling mechanisms contributing to hypertrophy and heart failure development.

1.3.2.4. New Hypertrophy Therapeutic Options

Cardiac hypertrophy and heart failure are diseases that result from several underlying pathological conditions and during prolonged periods of cardiac stress. Current pharmacotherapies target disease progression, but the mortality rate remains high. New therapeutic options are therefore under investigation. Altered Ca^{2+} handling is a major mechanism that underlies hypertrophy and heart failure development. Thus, SERCA2a overexpression is being investigated as a potential therapy to normalize activity. Clinical trials for SERCA2a gene therapy in HF patients have been shown to be safe and improve cardiac function.(181, 182) LCZ696 combines an AngII receptor

antagonist, valsartan, with an inhibitor of neprilysin, sacubitril. The clinical trial PARADIGM-HF showed lower cardiovascular mortality and fewer hospitalizations with LCZ696 compared to enalapril, an ACE inhibitor.(183) In fact, LCZ696 was approved by the US Food and Drug Administration, and is sold under the brand name, Entresto™.

Furthermore, there are also promising therapeutics that target mitochondrial function and simultaneously alleviate hypertrophy.(184) For example, AMPK activation has been demonstrated to be cardioprotective. Metformin, a therapy used to treat diabetes, reduces cardiac hypertrophy, fibrosis and collagen synthesis in hypertrophied mice hearts.(185) Resveratrol, a stilbenoid polyphenol found in grapes, also attenuates cardiomyocyte hypertrophy in an AMPK-dependent manner via LKB1.(142) Overall, cardiac hypertrophy is a promising target to prevent heart failure progression. Thus, as there are numerous pathophysiological mechanisms that underlie cardiomyocyte hypertrophy, there is potential for new and effective therapeutic targets.

1.4 Animal Models

The pathophysiology of arrhythmias and AF is complex, and is dependent on a patients cardiac status, genetics and environmental factors (stress, drugs, diet). Thus, symptomatic therapy is regularly used in contrast to therapeutics targeting the pathophysiological mechanisms.(79) However, animal models are improving the clinical understanding of AF, and allowing the development of novel therapeutic approaches. The animal model chosen to study arrhythmia development demonstrates only a limited component of the pathophysiological spectrum of AF.

1.4.1 Small Animal Models

Small animal models utilized in arrhythmia research commonly include, mice, rats, guinea pigs, and rabbits.(79) While the cardiovascular anatomy, heart rate, and action potential duration vary compared to humans; the low cost, high accessibility, and availability of genetic manipulation make these small animals excellent base models for drug targets and genetic variations leading to arrhythmias.(79, 186)

Cardiac anatomy parameters of rats and guinea pig models, such as heart:body mass ratio, are similar to humans.(79) Rats advantageously have balanced coronary circulation, unlike guinea pigs, mice, and rabbits where coronary circulation is left-dominant.(79) However, the overall action potential shape of rats and mice do not demonstrate a plateau phase, whereas guinea pigs and rabbits resemble a more similar human action potential profile comprising of a plateau region.(79)

Small animal models are commonly used in several pathophysiological arrhythmia models, such as transverse aortic constriction (TAC) to induce cardiac hypertrophy, a trigger of AF.(81) Rat, guinea pig, and rabbit TAC models induce ventricular arrhythmias and tachycardic events.(79) Mice subjected to TAC have demonstrated vulnerability to AF and ventricular tachycardia.(79) Furthermore, while mice do not show increased susceptibility to arrhythmias in a model of left atrial volume overload, rats had increased fibrillation and tachycardic episodes.(79)

Cardiac hypertrophy induction by pulmonary artery constriction, hyperthyroidism, and exercise are all models predominantly established in mice and rats.(79) Endurance rat models have demonstrated increased vagal tone, atrial dilatation and fibrosis, and AF susceptibility and inducibility.(79) Furthermore, pulmonary hypertension models have high incidence of

arrhythmias, mainly AF and atrial flutter.(79, 186) Rat models of pulmonary hypertension result in L-type Ca^{2+} channel downregulation causing AV node dysfunction and conduction block.(79) Furthermore, ischemia rat models demonstrate elevated vulnerability to AF, and greater inducible AF events compared to mice.(79)

Major advancements in molecular mechanisms of AF are a product of genetically modified mice.(187) Due to the success of these genetic strains, and the partiality of rabbits for repolarization models; genetically modified rabbits are currently being developed. Additionally, *ex vivo* Langendorff-perfused heart preparations in rats, guinea pigs, and rabbits have been used to complement *in vivo* studies.(188) *Ex vivo* preparations allow specific investigation of heart regions, monophasic action potential measurements, and AERP characteristics, through precise rapid and burst pacing.(188) A major limitation of small animals is AF inducibility. Lee *et al.* demonstrated limited arrythmia induction in tachypaced rat hearts.(189) However, these models remain ideal for both molecular (e.g. Cx43, AMPK) and electrophysiological (e.g. AERP) studies and are useful for studying atrial remodelling induced through rapid atrial rate. Additionally, there are some reports in the literature which indicate an ability to induce AF in the isolated heart of normal rats.(190) This might reflect difference in the strain (Wister vs SD rats), the physiological solution (Kreb's vs. Tyrode's buffer) and more.

1.4.2. Large Animal Models

The first animal model to show sustained AF was reported in goats.(81) Presently, large animal models for arrhythmia research have been popularized and expanded into pigs and dogs. A major advantage of large animal models is physiologically relevant heart size compared to humans. However, there are still dissimilarities within these models. Pig models are the only

large-animal to demonstrate balanced coronary perfusion and similar heart:body mass ratios similar to humans. Although, goat and dog models have comparable conduction systems and ion currents to that of humans.(79)

Electrical remodeling and structural changes resultant from atrial burst pacing are common findings in both dog and goat models. Alterations in AERP, gap junction formation, fibrosis, and cardiomyocyte hypertrophy after atrial burst pacing assist with antiarrhythmic drug research, and ion channel function interactions.(81) Hypertrophy models including TAC and chronic AV block (CAVB) models, first described in dogs, induce volume overload and downstream compensatory mechanisms.(79) Goat CAVB models show atrial dilatation and conduction delay, AERP shortening, and increased AF susceptibility.

Traditionally, dogs were a common animal model for arrhythmia research due to their cardiac anatomy and electrophysiology similarities to that of humans. However, with increasing cost, unavailability of housing, and social stigma, alternatives are becoming more common. Pig and goat models are even being used to investigate genetic modifications. Transgenic goat models, with cardiac-overexpression of TGFB1, leads to fibrosis and increased AF inducibility.(79) Genetically engineered pigs with SCN5A-mutatations used to study Brugada syndrome have developed ventricular fibrillation during stimulation.(79)

When interpreting findings between animal models it is important note there are caveats, and that human AF is a disease stemming from various disease states, remodeling, and genetics and not all animal models will encompass these characteristics in their entirety. However, common observations found between research models, such as abnormal repolarization and reduced conduction velocity can lead to potential targets for AF therapeutics.(79)

1.5. Cannabinoids

The endocannabinoid system (ECS) is composed of cannabinoid receptors (CBR), endocannabinoid (eCB) ligands, and enzymes for biosynthesis, degradation and transport of eCBs.(191) During the 1990s with the increasing prevalence of *Cannabis sativa* (*C. sativa*) use, research interest around Δ9-tetrahydrocannabinol (THC) amplified and the major target for THC was discovered.(192) THC is a major constituent of *C. sativa* and is partly responsible for eliciting psychoactive properties.(193, 194) Thus, discovery research into the ECS followed and only recently has the ECS been described in detail. The ECS is implicated in controlling key processes such as inflammation, pain, and maintaining homeostasis.(193)

1.5.1. The Endocannabinoid System

Cannabinoids are chemical compounds that can be synthetically derived, produced by plants, or produced by the body. Thus the 3 major groups of cannabinoids are synthetic cannabinoids, phytocannabinoids, and endocannabinoids. There are two G protein-coupled receptors known to interact with cannabinoids. Cannabinoid type 1 receptors (CB1R) are expressed in the brain, where they mediate psychoactive effects, and are also expressed less abundantly in the heart, and vasculature. (194-197) Cannabinoid type 2 receptors (CB2R) are not expressed in the brain, but are expressed in heart at levels comparable to CB1R.(198)

1.5.1.1. Cannabinoid Ligands

eCBs are derivatives of polyunsaturated fatty acids and exert regulatory roles for maintenance of internal homeostasis. (193) The two major orthosteric ligands in the ECS are anandamide (AEA) and 2-AG.(199) 2-AG and AEA are derivatives of ω-6 arachidonic acid, which is an essential

polyunsaturated fatty acid.(200, 201) The effects of eCBs are limited to the cellular site in which they are synthesized and released.(202)

Exogenous cannabinoids, i.e. phytocannabinoids and synthetic cannabinoids, have a wide range of physiological effects. Exogenous cannabinoid administration typically results in excess compound concentration. Thus, their effects are prolonged compared to eCBs.(193) Phytocannabinoids originate from the *C. sativa* plant, and there are over 100 different chemical compounds found within this plant. The major constituents of *C. sativa* are THC and cannabidiol (CBD). These two compounds have varied physiological effects. While THC has psychoactive properties through CB1R-mediated action in the brain, CBD does not appear to elicit this side-effect.

Synthetic cannabinoids were originally developed as pharmacological probes of the ECS and are derivatives of natural exogenous cannabinoids and eCBs.(203) Several hundred varieties of new and novel synthetic cannabinoids exist, as minor modifications to the chemical structure alter the affinity and selectivity to CBRs.(203)

1.5.1.2. Endocannabinoid Synthesis

As previously mentioned, the two major eCBs are 2-AG and AEA. However, biosynthesis and degradation of 2-AG and AEA varies. AEA is synthesized by N-arachidonoyl phosphatidyl ethanol (NAPE) through multiple pathways.(204) Currently, there are four pathways for AEA synthesis: NAPE-PLC, NAPE-phospholipase D (PLD), hydrolysis of both acyl groups by phospholipase B (PLB), or hydrolysis of only one acyl group.(204) Reportedly, certain physiological or pathophysiological functions may favour a specific AEA synthesis pathway.(204)

The biosynthesis of 2-AG is simpler than AEA. 2-AG is produced from phosphatidylinositol bis-phosphate (PIP_2) in a Ca^{2+}-dependent manner involving PLC and diacylglycerol lipase (DAGL).(204) However, there is a secondary synthesis pathway for 2-AG in the brain, involving PIP_2 and phospholipase A (PLA) followed by hydrolysis by lyso-PLC.(204) The function of this secondary pathway remains to be elucidated.

1.5.1.3. Endocannabinoid Degradation

AEA degradation occurs via fatty acyl amide hydrolase (FAAH) on the post-synaptic neuron.(205-207) FAAH degrades multiple fatty acid amides besides AEA, such as palmitoyl and oleoyl ethanolamide.(208) Alternatively, hydrolysis of AEA may occur by cyclooxygenase-2 (COX-2) or via N-acylethanolamine-hydrolyzing acid amidase (NAAA). Degradation of 2-AG occurs by monoacylglycerol lipase (MAGL), which is primarily located in presynaptic terminals.(205-207)

1.5.1.4. Cannabinoid Receptors

Currently, there are two major cannabinoid receptors known to be part of the ECS; CB1R and CB2R. Both 2-AG and AEA have affinities for CB1R and CB2R.(193) However, 2-AG has a higher affinity for CB1R, while AEA only has a slight affinity for CB1R.(193) CB1R and CB2R are GPCRs that interact with a variety of signaling molecules and mediators.(193) CBRs are coupled to $G_{i/o}$ inhibitory proteins, and inhibit adenylyl cyclase and decrease intracellular cyclic-AMP levels. (199, 209) However, CBRs can undergo "*biased signaling"* and may also signal through G_s proteins, depending on the bound cannabinoid.(210)

Of the five different GPCR classes, CBRs are part of Class A: rhodopsin. The orthosteric site may be in the transmembrane bundle or the extracellular pocket and varies between GPCR

classes. Hurst *et al.* reported that 2-AG binds with CB2R between transmembrane 6 and transmembrane 7 helices and passes through the lipid bilayer.(211) Additionally, CB1R has one or more allosteric sites that are targeted by ligands.(199, 209) However, the therapeutic potential of allosteric ligands is still emerging.(199, 209)

Both eCBs and exogenous cannabinoids interact with the binding site of CBRs. While the structure of exogenous cannabinoids is different in both size or shape compared to eCBs, all processes regulated by eCBs are susceptible to activation or obstruction by exogenous cannabinoids.(204) Once a ligand binds to a CBR, the structural conformation changes and results in activation of downstream signaling mediators. Activation of CBRs, depending on the cell type, may inhibit or activate certain physiological mechanisms. For example, CB1R agonism may promote obesity and diabetes through impaired lipid metabolism, or mitigate hypertensive outcomes by limiting adrenoreceptor responsiveness.(212)

The first described receptor of the ECS is CB1R, which is predominant in the central nervous system (CNS) at the terminals of both central and peripheral neurons.(194, 209) The gene encoding CB1R, human central cannabinoid receptor gene 1 (CNR1), is located on chromosome 6.(193, 194) CNR1 encodes three 60kDa isoforms of CBR1 that are located within areas of the CNS that control motor behaviour, memory, learning, endocrine functions, and peripheral nerves.(209) CB1R activation mediates inhibition of the release of excitatory and inhibitory neurotransmitters at their pre-synaptic location.(194, 209) Thus, CB1Rs are ideal pharmacological agents for targeting neurotransmission.

The gene encoding CB2R, human central cannabinoid receptor gene 2 (CNR2) is located on chromosome 1 and encodes multiple 40kDa isoforms.(193) The expression level of CB2Rs is lower in the CNS compared to CB1Rs.(204) However, CB2Rs are prevalent in the immune

system.(213) Ligand activation of CB2Rs typically results in immunomodulatory effects, such as immune cell migration and cytokine release.(213) These findings incited research on the non-psychoactive effects and properties of the ECS, as agonists that bind to CB2R lack the psychoactive effects seen with CB1R agonism.(209, 213) Thus, CB2R-selective targeting may have therapeutic potential. Furthermore, CB2R expression appears to be inducible.(204) Maresz *et al.* have shown that CB2R expression can increase up to 100-fold following tissue injury or inflammation.(214)

Polymorphisms that occur in CNR1 and CNR2 have been linked to schizophrenia and Parkinson's disease, and to postmenopausal osteoporosis, respectively.(209) CB1R and CB2R are both found in the periphery and regulate processes in the gastrointestinal tract, lungs, skin, bone, heart, liver, etc.(195-198) Several factors of the ECS are present in the heart, including CB1R, CB2R, AEA, 2-AG, and FAAH. (195, 215-218) Although CB1R and CB2R are the predominant receptors in current ECS research, other receptors are also targets for cannabinoids. Transient potential receptors (i.e. TRPV1), peroxisome proliferator activated receptors (i.e. PPARα) as well as orphan G-protein receptors (i.e. GPR55) all bind cannabinoid ligands.(193, 199, 204) For example, AEA interacts with TRP channels, specifically TRPV1, and also alters gene transcription through PPARα and PPARγ. (204)

1.5.2. Cannabinoid Therapeutics

As of 2022, there are two approved cannabinoid prescription medications available in Canada, nabilone (Cesamet®) and nabiximols (Sativex®). Both medications derive from phytocannabinoids, THC and CBD, and are only approved for specific disease-states. Nabilone is a synthetic THC analogue approved for use for nausea related to cancer therapy. Nabiximols is a

botanical extract of 1:1 THC to CBD and is only prescribed for treatment of pain during advanced cancer and multiple sclerosis neuropathy. Furthermore, CBD (Epidiolox®) is available in the United States and is approved for the treatment of two childhood epileptic disorders.

Manipulating the ECS can have a plethora of downstream effects. Preventing eCB degradation has been explored as a possible target for therapeutics. Inhibition of MAGL, responsible for the degradation of 2-AG, prevented inflammation and oxidative stress in murine liver.(212) Inhibition of FAAH is a potential therapy for pain and CNS disorders.(219)

Targeting CB2R vs. CB1R may also yield therapeutic potential. This approach would avoid the adverse psychoactivity associated with CB1Rs in the brain and downstream repercussions demonstrated by inhibiting ECS enzymes. For example, the heart has comparable levels of CB1Rs and CB2Rs.(198) In fact, the ECS is activated in the heart under stress conditions, such as myocardial infarction.(220) Therefore, exogenous cannabinoid interactions with the cardiovascular ECS may elicit beneficial effects. Understanding the mechanisms by which cannabinoids modify structural, metabolic, and electrical parameters is key for generating targeted therapeutics.

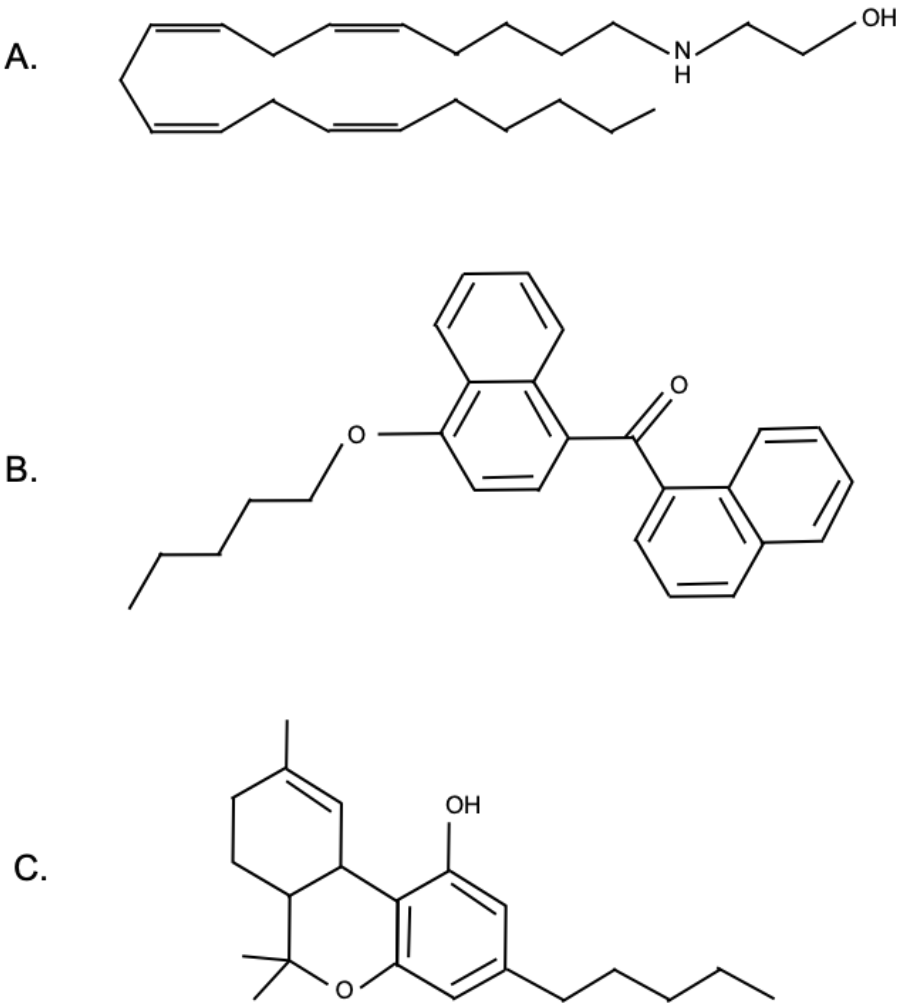

Figure 1.6. Cannabinoid subtypes. There are 3 subtypes of cannabinoids (A) endocannabinoids, e.g. anandamide (AEA; (5Z,8Z,11Z,14Z)-N-(2-hydroxyethyl)icosa-5,8,11,14-tetraenamide), (B) synthetic cannabinoids, e.g. CB13 (1-naphthalenyl[4-(pentyloxy)-1-naphthalenyl]methanone), and (C) phytocannabinoids, e.g. 9-tetrahydrocannabinol (THC; (−)-(6aR,10aR)-6,6,9-trimethyl-3-pentyl-6a,7,8,10a-tetrahydro- 6H-benzo[c]chromen-1-ol).

1.5.3. Cannabinoid Receptor Signaling in the Heart

The endocannabinoid system is activated in the cardiovascular system.(125) Neonatal rat cardiomyocytes treated with a dual agonist CB1/CB2 receptor agonist blocked ET-1-induced hypertrophy via activation of the endocannabinoid system with synthetic cannabinoid, CB13 and endogenous cannabinoid, anandamide.(125) Molecular abnormalities resulting in development of atrial substrate are similar to pathological changes occurring during ventricular hypertrophy and ischemia.(221) Thus, this finding by Lu *et al* supports the notion that CB agonists may be beneficial for AF.(125) Endocannabinoids have been show to decrease the risk of arrhythmia development through CB2 interaction, demonstrating an enhanced role of CB2 receptors over CB1 receptors in regards to antiarrhythmic effects.(222) In fact, activation of cannabinoid receptors with CB13 attenuates hypertrophy in isolated cardiomyocytes through an AMPK-eNOS axis.(125)

CB receptor agonists exert cardioprotective effects, specifically in the context of ischemic insult and through interactions with CB2 receptors.(223-226) JWH-133, a CB2R selective agonist prevents cardiomyocyte hypertrophy, also reduces infarct size in rats before and after ischemia.(125, 227) Furthermore, CB2R agonism results in a reduced inflammatory response, reduces plaque size in atherosclerosis, and inhibits oxidized LDL.(228) Additionally, cannabidiol also reduced infarct size in ischemia and reperfusion models.(229) Cannabinoids additionally exert anti-arrhythmic effects in the context of ischemia(222) and prevent endothelial dysfunction in coronary arteries.(198, 230, 231)

Moreover, cannabinoids have been shown to interact with channels that generate the ultra-rapid delayed rectifier current, Kv1.5 channels.(232) This interaction of cannabinoids at an extracellular site may influence and regulate atrial AP shape.(232) However, cannabinoid effects

on other cardiac channels is unknown, and physiological implications of this interaction on electrical activity cannot be certain. Additionally, CB13 is an ideal potential therapeutic as it is peripherally restricted with limited blood-brain barrier penetration.(233) Furthermore, CB13 has been demonstrated to have good bioavailability and long-lasting effects when synthesized with nano-particles.(233, 234) Understanding the mechanisms by which cannabinoids interact with atrial substrate and electrical parameters are key for generating targeted therapeutics.

Chapter 2

Rationale, Aims and Hypothesis

2.1. Rationale

Structural, electrical, and metabolic tissue remodeling cause AF and LVH development. There is need for improved therapeutics to protect and prevent progression of mechanisms underlying pathophysiological cardiac remodeling. AF is the most common sustained cardiac arrhythmia, and affects approximately 200,000 Canadians.(59, 61, 62) LVH is the leading cause of heart failure, and over 650,000 Canadians over the age of 40 are diagnosed with heart failure.(128)

There is interest in investigating the ECS as a therapeutic target to treat multiple disorders.(235, 236) However, medicinal use of cannabinoids is limited due to unwanted psychoactive side effects mediated by CB1R.(236) Therefore, strategies concentrating on CB2R agonists, or peripherally restricted CB1R agonists are ideal.(235-237) Thus, I will investigate CB13, a peripherally restricted, dual CB1R/CB2R agonist with limited brain penetration.(233, 238)

CB13 was previously found to attenuate NRVM hypertrophy by our laboratory.(125) Building upon this data, the role of AMPK activation by CBR agonists in ventricular hypertrophy was investigated. Additionally, LVH increases the risk of cardiac arrhythmias and AF progression.(170, 171) Thus, cardioprotection exerted by CB13 may extend into the stressed atria. In conclusion, this research was designed to generate knowledge regarding the cardioprotection offered by CB13 during LVH and AF-related remodeling.

2.2. Hypothesis

CB13 prevents hypertrophy and mitochondrial dysfunction in NRVM, and this will extend into the stressed atria, and the hallmarks of AF therein.

2.3. Aims

This thesis addresses three objectives that query possible cardioprotective effects of CB13. Each objective is addressed in a separate chapter.

- **Aim 1**: Define the effects of CB13 on mitochondrial dysfunction and metabolic remodeling *in vitro* using ET-1-treated NRVM. (See *Chapter 3: Activation of Cannabinoid Receptors Attenuates Mitochondrial Dysfunction in Rat Ventricular Myocytes*)
    - **Hypothesis:** ET-1 will cause mitochondrial dysfunction in ventricular cardiomyocytes and CB receptor signaling will rescue mitochondrial function and activate AMPK signaling

- **Aim 2**: Investigate the effects of CB13 on structural and electrical atrial remodeling in tachypaced atria using novel *ex vivo* Langendorff hanging heart methodology in Sprague Dawley (SD) rats. (See *Chapter 4: Cannabinoid Receptor Agonist Inhibits Atrial Electrical Remodeling in a Tachypaced Ex Vivo Rat Model*)
    - **Hypothesis:** CB13 activation of AMPK signaling will be relevant to the stressed tachypaced atria

- **Aim 3**: Extend upon findings in tachypaced-atria (Aim 2); and define the effects of CB13 on structural, mitochondrial, and metabolic remodeling *in vitro* using AngII-treated NRAM. (See C*hapter 5: Cannabinoid Receptor Agonist Attenuates Angiotensin II–Induced Atrial Hypertrophy and Mitochondrial Dysfunction in Rat Atrial Cardiomyocytes)*

- **Hypothesis:** Angiotensin II (AngII) will cause structural and metabolic abnormalities in atrial cardiomyocytes and CB receptor signaling will rescue mitochondrial function through AMPK and Cx43 signaling

2.4. Significance

This thesis identifies CB13 as a potentially viable treatment strategy for ventricular and atrial pathophysiological remodeling. *In vitro* and *ex vivo* techniques were used to investigate the effects of CB13 on structural, electrical, and metabolic changes in hypertrophy and AF-related remodeling.

Chapter 3

Activation of Cannabinoid Receptors Attenuates Mitochondrial Dysfunction in Rat Ventricular Myocytes

3. Activation of Cannabinoid Receptors Attenuates Mitochondrial Dysfunction in Rat Ventricular Myocytes

This section contains collaborative work that has been published as an original research article in the journal;

"Activation of Cannabinoid Receptors Attenuates Endothelin-1–Induced Mitochondrial Dysfunction in Rat Ventricular Myocytes"

Journal of Cardiovascular Pharmacology. 2020 Jan; 75(1): 54–63.

Danielle I. Lee,[*1,2] Yan Lu,[*1,2] Subir Roy Chowdhury,[3] Ping Lu,[4] Amit Kamboj,[4] Christopher M. Anderson,[4,5] Paul Fernyhough,[3,5] and Hope D. Anderson.[1,2,4]

[1]College of Pharmacy, Rady Faculty of Health Sciences, University of Manitoba, Winnipeg, Manitoba, Canada;
[2]Centre for Agri-Food Research in Health and Medicine, St. Boniface Hospital Research Centre, Winnipeg, Manitoba, Canada;
[3]Division of Neurodegenerative Disorders, St. Boniface Hospital Research Centre, Winnipeg, Manitoba, Canada;
[4]Neuroscience Research Program, Kleysen Institute for Advanced Medicine, Winnipeg Health Sciences Centre and Max Rady College of Medicine, University of Manitoba, Winnipeg, Manitoba, Canada; and
[5]Department of Pharmacology and Therapeutics, Max Rady College of Medicine, University of Manitoba, Winnipeg, Manitoba, Canada

[*]co-first authors.

Author contributions:

DIL: Performed experiments, analyzed data, generated figures, assisted in preparing and drafting of the manuscript, and completed submission of the manuscript (e.g. submitted manuscript, responded to reviewers, and made appropriate revisions). DIL completed all experiments in Figure 3.1 with Compound C pre-treatment, Figure 3.4, Figure S7.4 and Figure S7.5 and assisted with experiments for Figure S7.1, S7.2 and S7.3.
YL: Contributed to the conception and design of the study, performed experiments, analyzed data, generated figures, and prepared the first draft of the manuscript. YL completed experiments for Figure 3.1 (no Compound C treatment), Figure 3.2 and Figure 3.3.
SRC, PL, AK, CMA, PF: Provided experimental expertise.
HDA: Conceived and designed the study, guided the data analysis and design of the figures, and led completion of the manuscript. All authors approved the submitted version.

Acknowledgements: We are grateful to Dr. Zongjun Shao for her excellent technical assistance. This work was supported by the Canadian Institutes of Health Research (MOP 130297) and studentships from the Manitoba Health Research Council/St. Boniface Hospital Foundation (Y.L.) and Canadian Institutes of Health Research (D.L.).

3.1. Abstract

Evidence suggests that the activation of the endocannabinoid system offers cardioprotection. Aberrant energy production by impaired mitochondria purportedly contributes to various aspects of cardiovascular disease. We investigated whether cannabinoid receptor (CBR) activation would attenuate mitochondrial dysfunction induced by endothelin-1 (ET1). Acute exposure to ET1 (4 hours) in the presence of palmitate as primary energy substrate induced mitochondrial membrane depolarization and decreased mitochondrial bioenergetics and expression of genes related to fatty acid oxidation (i.e. peroxisome proliferator–activated receptor-gamma coactivator-1α, a driver of mitochondrial biogenesis, and carnitine palmitoyltransferase-1β, facilitator of fatty acid uptake). A CB1R/CB2R dual agonist with limited brain penetration, CB13, corrected these parameters. AMP-activated protein kinase (AMPK), an important regulator of energy homeostasis, mediated the ability of CB13 to rescue mitochondrial function. In fact, the ability of CB13 to rescue fatty acid oxidation–related bioenergetics, as well as expression of proliferator-activated receptor-gamma coactivator-1α and carnitine palmitoyltransferase-1β, was abolished by pharmacological inhibition of AMPK using compound C and shRNA knockdown of AMPKα1/α2, respectively. Interventions that target CBR/AMPK signaling might represent a novel therapeutic approach to address the multifactorial problem of cardiovascular disease.

3.2. Introduction

Endocannabinoids are endogenous polyunsaturated fatty acids that bind to cannabinoid receptors to elicit physiological effects. These G-protein-coupled receptors include CB1R and CB2R subtypes. Both CB1R and CB2R are present in the cardiovascular system (i.e. heart (195) (198) and blood vessels(196, 197)), although CB1R and CB2R are also profusely expressed in the brain (194) and immune cells.(213)

Aside from CBRs other constituents of the endocannabinoid signaling system are present in the heart. These include endocannabinoid ligands such as arachidonoylethanolamide (AEA or anandamide) (200) and 2-arachidonoylglycerol (2-AG),(201) as well as the enzyme, fatty acid amide hydrolase (FAAH),(206, 239) which hydrolyzes anandamide and 2-AG.(206, 240)

Manipulating the endocannabinoid system may be a salutary approach worth pursuing, as endocannabinoid signaling plays a diverse role in modulating central and peripheral physiology.(241) In fact, extant evidence suggests that cannabinoids are protective in the ischemic heart. For example, infarct size is reduced by endogenous and synthetic cannabinoid agonists,(224, 225) reportedly via CB2R (223), and this was associated with recovery of ventricular function.(224, 225) We also previously reported that cannabinoid receptor signaling prevents cardiac myocyte hypertrophy.(125) Here, we extended these findings by determining the effects of CB receptor activation on mitochondrial function.

The heart requires a large amount of ATP, for which mitochondria are the major source. In the healthy heart, cardiac myocytes use predominantly fatty acids as energy substrate, and this accounts for 50% to 70% of total ATP production.(242, 243) The electron transport chain (ETC) embedded within the mitochondrial inner membrane is responsible for oxidative phosphorylation, thereby yielding approximately 95% of the total ATP.(244) Accordingly, mitochondria constitute

a significant 30% of cardiac myocyte volume.(14) Given this key role, mitochondrial dysfunction has been linked to ischemia reperfusion injury,(245) cardiomyopathy,(246) left ventricular hypertrophy,(247) and heart failure.(141)

Here, we determined the early effects of endothelin-1 (ET1) on mitochondrial membrane permeability, membrane polarization, and bioenergetics in cardiac myocytes, in the presence of fatty acids as primary energy substrate. Furthermore, we tested the hypothesis that CB receptor signaling would rescue mitochondrial function and probed the signaling pathway(s) involved.

3.3. Materials and Methods

3.3.1. Materials

Endothelin-1 (ET1), compound C, β-actin antibody, L-carnitine hydrochloride, oligomycin, carbonylcyanide 4-(tri-fluoromethoxy) phenylhydrazone (FCCP), rotenone, antimycin A, and etomoxir were from Sigma Aldrich (St Louis, MO). CB13 and the JC-1 mitochondrial membrane potential assay kit were from Cayman Chemical (Ann Arbor, MI). Calcein-AM (Molecular Probes) and carnitine palmitoyltransferase (CPT)-1β primers were from Life Technologies (Carlsbad, CA). p-AMPKα (Thr172) and AMPKα antibodies were from Cell Signaling (2535S and 2603S, respectively; Whitby, Canada). CB1R and CB2R antibodies were from Abcam (ab23703 and ab45942, respectively; Toronto, Canada). Peroxisome proliferator-activated receptor-gamma coactivator (PGC)-1α antibody was from EMD Millipore (ST1202; Temecula, CA). XF24 FluxPaks were from Agilent (Santa Clara, CA).

3.3.2. Neonatal rat ventricular myocytes

This study was conducted according to recommendations from the Animal Care Committee at the University of Manitoba and the Canadian Council on Animal Care. Neonatal rat pups were produced from a larger Sprague-Dawley rat breeding colony. The pups were born in aspen bedding-enriched polycarbonate rat cages suspended in a racking system that forms the cage lid. Pups were subsequently housed alone with the mother. Animals were maintained at 22-25℃, 55-60% humidity, a 12:12 light:dark cycle, and allowed free access to water and food (PMI RMH-3000 feed). Ventricular myocytes were isolated from 1-3-day-old neonatal Sprague-Dawley rats by digestion with several cycles of 0.1% trypsin and mechanical disruption, as previously described (248). Cells were cultured on gelatin-coated plates in DMEM containing 10% cosmic calf serum (CCS; Hyclone) for 18-24 h prior to experimentation.

3.3.3. Treatments

As applicable, myocytes were subjected to lentiviral infection. Myocytes were rendered quiescent by serum deprivation for 24 h, and then exposed to ET1 (0.1 μM; 4 h) in the presence or absence of vehicle, CB13 (1 μM), and/or a chemical inhibitor of AMPK (compound C; 1 μM; 1 h). The concentration of ET1 (0.1 μM) is predicated on our extensive use of neonatal rat cardiac myocytes treated with ET1 as our experimental paradigm of cardiac myocyte hypertrophy.(249-251) Accordingly, we used this experimental paradigm to generate our finding that ligand activation of cannabinoid receptors attenuates hypertrophy of neonatal rat cardiomyocytes.(125) Here, this concentration of ET1 increased hypertrophic parameters (myocyte cell size and fetal gene activity) in an AMPK-dependent manner.(125) The 4-hour incubation time is based first, on literature precedent in which Sun *et al.* (252) reported disruption of mitochondrial function in pulmonary

arterial endothelial cells after 4 h, and second, time course experiments, in which we found that CB13 significantly activated AMPK at 4 h.(125) Ligands remained in the culture media for the remainder of the experiment. CB13 is a non-selective CB1R/CB2R agonist with limited brain penetration (Ki: CB1=6.1 nM vs. CB2=27.9 nM).(233, 238) The concentration of CB13 was selected based on first, our finding that it attenuates myocyte hypertrophy (125), and second, that micromolar plasma concentrations are achievable following oral administration of CB13 (3 mg/kg).(233) Levels of CB1R and CB2R expression are unaffected by CB13 in the presence or absence of ET1 (see Figure S7.6, Appendix).

3.3.4. shRNA knockdown of AMPKα

Lentiviral vectors expressing shRNA against AMPK α1 and α2 were prepared, as previously described. Myocytes were infected for 24 hours, and then cultured for a further 72 hours to allow knockdown before further experimentation. Degree of knockdown was confirmed by Western blotting (see Figure S7.5, Appendix)

3.3.5. Measurement of mitochondrial respiration

An XF24 Analyzer (Agilent, Santa Clara, CA) was used to measure mitochondrial bioenergetics. The XF24 creates a reversible 7 μL enclosure above cells; this facilitates real-time monitoring of oxygen consumption rate (OCR) before re-equilibration with the unenclosed incubation medium (253, 254). Fatty acid-dependent OCRs, driven by palmitate/BSA conjugate, were measured under basal conditions. Briefly, myocytes were seeded at 100,000 cells/well and exposed to assay media 1 h prior to the assay. Independent experiments were conducted using distinct neonatal myocyte preparations to generate an n-value ≥3 (5 replicates per n-value). Krebs-Henseleit buffer

containing L-carnitine hydrochloride (0.4 mM), glucose (2.5 mM) and for NRVM palmitate/BSA conjugate (200 μM) was used to measure fatty acid-dependent respiration. Following the measurement of *basal OCR*, oligomycin (1 μg/mL), FCCP (palmitate assays – 10 μM), and rotenone+antimycin A (1 μM each) were sequentially injected. Oligomycin is an ATP synthase inhibitor and eliminates OCR associated with ATP synthesis (*ATP-linked OCR*). Remaining OCR represents oxygen consumption attributable to *proton leak*. *Mitochondrial coupling efficiency* is the ratio of ATP-linked OCR-to-basal OCR. FCCP is a protonophore that uncouples the ETC and allows protons to flow back into the mitochondrial matrix to reduce oxygen. Thus, OCR in the presence of FCCP reflects *maximal respiratory capacity*, and the difference between maximal OCR and basal OCR reflects *spare respiratory capacity*. Finally, rotenone+antimycin A abolishes electron flow through complexes I to III, preventing oxygen consumption by cytochrome *c* oxidase. The remaining OCR in this case is due to non-mitochondrial respiration.(254) Non-mitochondrial respiration was subtracted during the calculation of all bioenergetic parameters, as previously described.(253, 254) The CPT1 inhibitor, etomoxir (40 μM), was used to verify that fatty acid-dependent respiration was due to oxidation of exogenous palmitate, and BSA served as negative control. OCR is represented as pmoles/min per 10 μg protein and is expressed as % untreated control. The aforementioned experimental conditions are predicated on optimization experiments (supplemental data, Figures S7.1-S7.4, Appendix) showing that OCR peaked at a seeding density of 75,000-100,000 cells/well, as previously reported,(255) that reduction of OCR by oligomycin is concentration-dependent, and that the maximal effect of FCCP on fatty acid oxidation (FAO) was achieved at 10 μM. Also, etomoxir (40 μM) dramatically inhibited palmitate-related OCR, and BSA only generated negligible OCR, thereby confirming that oxygen consumption was due to oxidation of exogenous palmitate.

3.3.6. Measurement of Mitochondrial Membrane Permeability Transition

Calcein-AM and $CoCl_2$ dual staining is a well-established method used to assess the extent of membrane permeability transition (mPT) in intact cells. Calcein-AM is a membrane-permeant dye that, upon entry into the cell, is converted to green fluorescent calcein by intracellular esterases. $CoCl_2$ selectively quenches cytosolic calcein fluorescence, thereby improving detection of bright fluorescent calcein puncta within mitochondria. Mitotracker-Red (0.1 mM) was also coloaded and overlap between calcein and Mitotracker-Red verified mitochondrial localization of calcein puncta (images not shown). When mPT pores (mPTPs) open, calcein leaks from mitochondria into the cytosol, thereby decreasing the fluorescence contrast between mitochondria and cytosol.

Myocytes were cultured in 48-well plates ($2{,}5x10^5$ cells/well) and pretreated with CB13 (1 μM; 1 hour) or vehicle in Krebs–Henseleit buffer supplemented with palmitate/BSA substrates (200 μM), L-carnitine hydrochloride (0.4 mM), and glucose (2.5 mM). Myocytes were then coloaded with calcein-AM (2 μM), $CoCl_2$ (2 mM), and MitoTracker-Red (0.1 μM) for 15 minutes, followed by a 5-minute wash with phosphate-buffered saline. The excitation/emission wavelengths for calcein and MitoTracker-Red are 494/517 nm and 579/599 nm, respectively. Images were acquired using an Olympus inverted fluorescence microscope before and after treatment (i.e. 0 and 15 minutes) with ET1 (0.1 mM) or vehicle. Fluorescence contrast was determined as the difference in fluorescent calcein intensity between mitochondria (e.g. puncta) and cytosol using Image J. For each replicate, images were captured for 5 myocytes, and within each myocyte, fluorescent calcein intensity was quantified in 3 separate fields within mitochondria. Results are presented as percent values of post-treatment:pre-treatment fluorescence contrast. Cells were incubated with ionomycin (2 μM) for 5 minutes at the end of the experiment; this causes mPT and served as positive control.

3.3.7. Measurement of changes in mitochondrial membrane potential

The lipophilic fluorescent probe JC-1 (Cayman Chemical Company) was used to investigate $\Delta\Psi_m$ in cardiac myocytes, as per the manufacturer's protocol. In healthy mitochondria with relatively high $\Delta\Psi_m$, JC-1 concentrates as J-aggregates and emits red fluorescence. In contrast, in mitochondria with reduced $\Delta\Psi_m$, JC-1 presents mainly as monomeric form because of decreased concentration and emits green fluorescence. The ratio of aggregate to monomer fluorescence serves as an indicator of changes in $\Delta\Psi_m$.

Myocytes were loaded with JC-1 for 60 min at 37ºC in specific working buffers: 1) Krebs-Henseleit buffer containing palmitate/BSA substrates (200 μM), L-carnitine hydrochloride (0.4 mM) and glucose (2.5 mM) was used to measure fatty acid-dependent $\Delta\Psi_m$) or 2) DMEM with glucose (10 mM) and pyruvate (1 mM) was used to measure glucose-dependent $\Delta\Psi_m$. Myocytes were then washed with PBS for 5 min, and images were acquired using an Olympus brightfield fluorescence microscope. Samples were excited at 485 nm for monomer fluorescence and at 560 nm for JC-1 aggregate fluorescence. Emission fluorescence images were recorded at 535 nm for JC-1 monomer and 595 nm for JC-1 aggregates. Fluorescence intensity was also quantified using the SpectraMax Gemini XS fluorescence microplate reader. The ratio of aggregate to monomer fluorescence was measured as an indicator of changes in $\Delta\Psi_m$. Also, as JC-1 may respond to plasma membrane depolarization, the mitochondrial uncoupler p-trifluoro-methoxy carbonyl cyanide phenyl hydrazine (FCCP; 1 μM) was added at the end of each experiment to achieve maximal dissipation of $\Delta\Psi_m$, and therefore served as positive control.

3.3.8. Western blotting

Myocytes were cultured in 6-well plates (2 x 10^6 cells/well). Following treatments, cell lysates were prepared in radioimmune precipitation assay buffer and clarified by centrifugation. Antibodies against p-AMPK (1:1000), AMPK (1:1000), and PGC-1α (1:1000) were used for the detection by conventional Western blotting. Membranes were stripped and reprobed with β-actin antibody to account for loading variations among lanes.

3.3.9. RNA extraction and real-time PCR

Myocytes were cultured in 12-well plates (1.5×10^6 cells/ml) and after 24 h in 10% CCS DMEM were serum deprived in 0.5% CCS DMEM for 24 h. Following treatments, total RNA was extracted from myocytes using the RNeasy mini kit (QIAGEN, Hilden, Germany). Real-time PCR was performed using the iScript^{TM} One-Step RT-PCR SYBR® Green kit (Bio-Rad, Ontario, Canada) in the presence of BNP primers (forward: CAGCTCTCAAAGGACCAAGG; reverse: CGATCCGGTCTATCTTCTGC), and CPT-1β primers (forward: 5'-CTTCTCAGTATGGTTCATCTTCTC-3'; reverse: 5'-CGAACATCCACCCATGATAG-3'). GAPDH was employed as the internal control. (forward: CTCATGACCACAGTCCATGC; reverse: TTCAGCTCTGGGATGACCT).

3.3.10. Statistics

Data are presented as mean±SEM. As applicable, 1-way analysis of variance, followed by a Newman–Keuls or Dunn Multiple Comparison test, was used to detect between-group differences. P value of < 0.05 was considered significant.

3.4. Results

3.4.1. CB13 attenuates ET1-induced aberrations of fatty acid oxidation-related mitochondrial bioenergetics.

As shown in Figure 3.1, ET1 reduced a number of bioenergetic parameters pertaining to FAO using palmitate, including (*vs.* control) basal OCR (82±5%, $p<0.05$), coupling efficiency (86±6%, $p<0.05$), maximal (78±4%, $p<0.01$) and spare (72±5%, $p<0.01$) respiratory capacity, as well as respiratory control ratio (81±5%, $p<0.01$). Basal OCR consists of both ATP-linked and proton leak-linked OCR; Figures 3.2C and D suggest that reduction of basal OCR was solely attributable to a decrease in ATP-linked OCR (74±7%, $p<0.05$ *vs.* control). CB13 pre-treatment partially attenuated the depression of basal OCR (95±3%, not significant (ns) *vs.* control nor ET1) and coupling efficiency (97±2%, ns *vs* control nor ET1), and significantly restored maximal (97±5%, $p<0.05$ *vs.* ET1) and spare respiratory capacity (97±4%, $p<0.01$ *vs.* ET1), as well as respiratory control ratio (94±2%, $p<0.05$ vs. ET1). Proton leak-related OCR was unaffected by either ET1 or CB13.

3.4.2. AMPK contributes to CB13-dependent correction of FAO-related mitochondrial bioenergetics in hypertrophied myocytes.

AMPK maintains or promotes ATP production by improving FAO.(256, 257) Thus, we queried whether AMPK mediates preservation of FAO by CB13. CB13 effects on FAO-dependent bioenergetics in ET1-treated myocytes were abolished by a chemical inhibitor of AMPK, compound C. We first determined that compound C treatment alone (1 μM) did not affect bioenergetic parameters (data not shown). However, in the presence of compound C, CB13 failed to rescue (*vs.* control) basal OCR (66±6%, $p<0.01$), ATP-linked OCR (64±9%, $p<0.01$), as well

as maximal (67±4%, $p<0.01$) and spare (65±6%, $p<0.01$) respiratory capacity (Figure 3.1) in ET1-treated myocytes. Interestingly, fatty acid-related respiration was also impaired in the CB13+compound C group (*vs.* control), as shown by reduced basal OCR (81±3%, $p<0.05$), ATP-linked OCR (77±4%, $p<0.05$), coupling efficiency (92±2%, $p<0.05$), maximal (78±4%, $p<0.01$) and spare (71±7%, $p<0.01$) respiratory capacity, as well as respiratory control ratio (88±2%, $p<0.01$) (Figure 3.1).

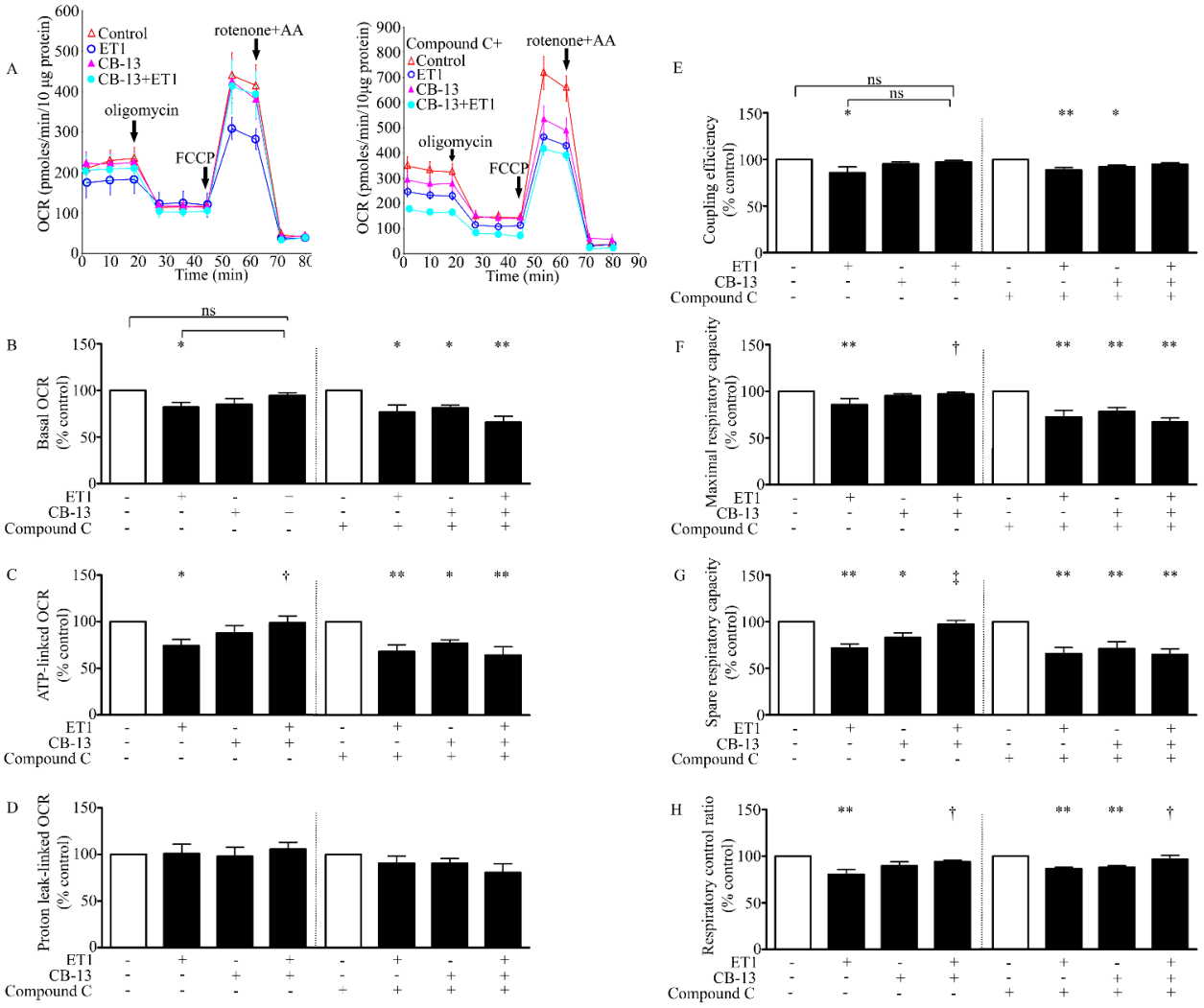

Figure 3.1. CB13 attenuates ET1-depression of fatty acid oxidation-related respiration. Serum-deprived myocytes were pre-treated with CB13 (1 µM; 2 h) followed by addition of ET1 (0.1 µM; 4 h), and provided palmitate/BSA conjugates (200 µM) as energy substrate. A, Representative plots. Left panel B-H, quantitative data demonstrate that ET1 reduced B, basal OCR, C, ATP-linked OCR, E, coupling efficiency, F, maximal and G, spare respiratory capacity, as well as H, respiratory control ratio. CB13 attenuated ET1 effects. D, Proton leak-linked OCR was unaffected by ET1 or CB13. Right panel B-H, quantitative data demonstrate that the ability of CB13 to attenuate ET1-induced reductions in B, basal OCR, C, ATP-linked OCR, E, coupling efficiency, F, maximal and G, spare respiratory capacity were attenuated, at least in part, by compound C. D, Proton leak-linked OCR and H, respiratory control ratio were unaffected. n=4-7 (5 replicates/n), *p<0.05 and **p<0.01 vs. control (open bars); ns=not significant; †p<0.05 and ‡p<0.01 vs. ET1. mean ± SEM.

3.4.3. ET1-induced mPT is prevented by CB13.

Myocytes were first pretreated with CB13 or its vehicle, DMSO, followed by loading of calcein-AM and $CoCl_2$. Images were acquired pre- (t = 0 min) and post-treatment (t = 15 min) with ET1 or H_2O. Fluorescence contrast between mitochondria and cytosol was measured to reflect the status of mPTPs. Lower fluorescence contrast indicates greater calcein leak from mitochondria to cytosol and is evidence of higher levels of mPT. As shown in Figure 3.2, ET1 induced a significant reduction in fluorescence contrast compared to H_2O (ET1: 31±6% *vs.* H_2O: 84±9%, $p<0.01$), suggesting an increase in mPT. In contrast, myocytes pretreated with CB13 exhibited similar fluorescence contrast after treatment with H_2O or ET1 (ET1: 64±2% *vs.* H_2O: 75±3%, not significant), suggesting CB13 prevented ET1-dependent mPT. At the end of the experiment, myocytes from all groups were treated with ionomycin (2 μM; 5 min). Ionomycin causes Ca^{2+} overload and induces mPT, and thus served as positive control. Mitochondrial fluorescence puncta were dissipated by ionomycin in all groups (data not shown).

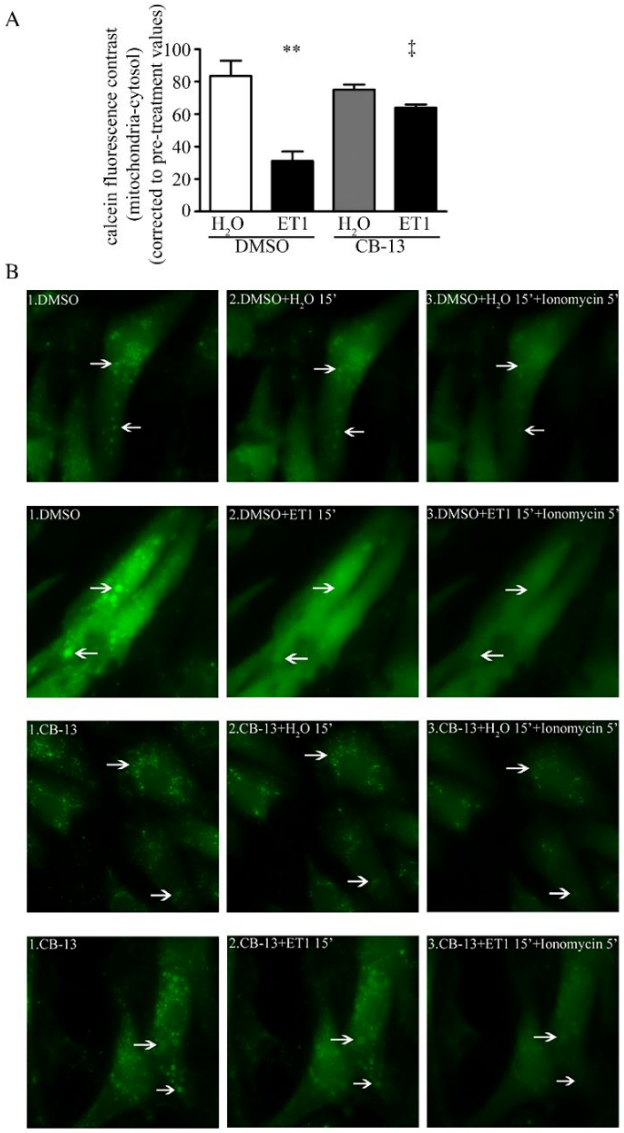

Figure 3.2. CB13 ameliorates ET1-induced mPT. Serum-deprived myocytes were pre-treated with CB13 (1 μM, 1 h) or DMSO (vehicle for CB13), followed by addition of ET1 (0.1 μM, 15 min) or H_2O in media containing palmitate/BSA (200 μM) as substrate. Calcein fluorescence contrast between mitochondria and cytosol, an indicator that negatively correlates with mPT, was measured within randomly selected myocytes before (t = 0 min) and after (t = 15 min) ET1/H_2O treatments. Results are presented as percent of post-treatment:pre-treatment fluorescent contrast. Addition of ET1 (0.1 μM) to myocytes for 15 min significantly dissipated fluorescence calcein contrast between mitochondria and cytosol compared to H_2O-treatment, suggesting increased mPT. In the presence of CB13 (1 μM), ET1 failed to reduce fluorescence calcein contrast between mitochondria and cytosol, suggesting preserved mPT. n=3. 15 mitochondrial regions from 5 myocytes were analyzed per replicate. **$p<0.01$ *vs.* H_2O treatment with DMSO (open bar); ‡$p<0.01$ *vs.* ET1 treatment with DMSO. mean ± SEM.

3.4.4. CB13 prevents ET1-induced mitochondrial membrane depolarization in an AMPK-independent manner.

The ratio of red J-aggregates-to-green monomer declined in ET1-treated cells (80±3%, $p<0.05$ *vs.* control), reflecting membrane depolarization (Figure 3.3A). Depolarization was attenuated by CB13 pre-treatment (106±10%, $p<0.05$ *vs.* ET1). The ability of CB13 to prevent mitochondrial depolarization was unaffected by the AMPK chemical inhibitor, compound C (Figure 3.3B).

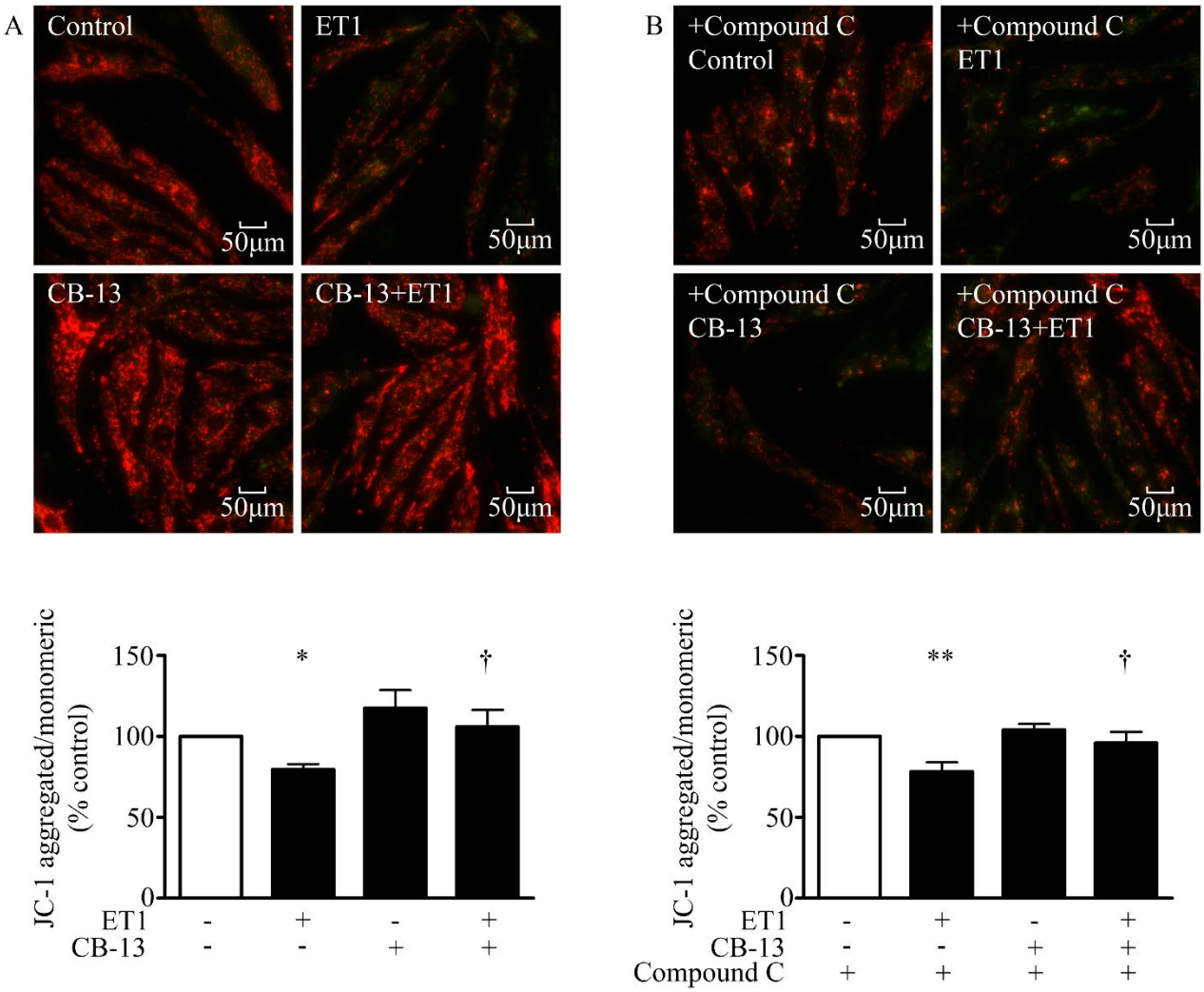

Figure 3.3. In the presence of palmitate as energy substrate, CB13 prevents ET1-induced mitochondrial membrane depolarization in an AMPK-independent manner Serum-deprived myocytes were pre-treated with CB13 (1 µM, 2 h) in the presence or absence of compound C (AMPK inhibitor, 1 µM; 1 h), followed by addition of ET1 (0.1 µM; 4 h) in media containing palmitate/BSA (200 µM) as substrate. Results are presented as representative fluorescent images and percent of normalized red/green fluorescence ratio vs. control (open bar). A, The ability of ET1 to induce mitochondrial membrane depolarization, indicated by decreased ratio of JC-1 aggregated red signal to monomeric green signal, was attenuated by pre-treatment with CB13. B, Rescue of mitochondrial membrane potential by CB13 was unaffected by compound C. n=7-8 (≥3 replicates per n-value). *$p<0.05$ and **$p<0.01$ vs. control (open bars); †$p<0.05$ vs. ET1. mean ± SEM.

3.4.5. CB13 attenuates ET1-reduced expression of PGC-1α and CPT-1β through AMPK.

CB13 treatment (4 h) increased phosphorylation of AMPKα at Thr172 (303±60%, $p<0.01$ *vs.* control) (Figure 3.4A), which is an indicator of AMPK activation status.(258, 259) PGC-1α, a central regulator of mitochondrial metabolism,(260) was reduced by ET1 by 41±7% ($p<0.01$ *vs.* control), and this was prevented by CB13 (96±2%, $p<0.05$ *vs.* ET1). CB13 alone increased PGC-1α (140±27%, $p<0.01$ *vs*. control). We next performed knockdown of AMPK$\alpha_{1/2}$ to ascertain its contribution to CB13 effects. Infection of cardiomyocytes with lentiviral constructs expressing shRNA against AMPKα_1 and AMPKα_2 produced significant and simultaneous reductions in AMPKα_1 and AMPKα_2 (supplemental data, Figure S7.5). shRNA knockdown of AMPKα_1 and AMPKα_2 abrogated the ability of CB13 to increase PGC-1α (Figure 3.4B); in fact, CB13 then reduced PGC-1α expression, whether in the presence (32±7%, $p<0.01$ *vs.* control) or absence (59±10%, $p<0.01$ *vs.* control) of ET1 (Figure 3.4B).

We next examined CPT-1, which is a rate-limiting enzyme that facilitates the transport of fatty acids into the mitochondria for use as energy substrates.(261) CPT-1β, the predominant isoform of CPT-1 in the heart,(262) was assessed by real-time PCR. ET1 reduced CPT-1β expression to 82±4% ($p<0.05$ vs. control), and this was attenuated by CB-13 (91±6%, ns from control or ET1) (Figure 3.4C). However, simultaneous knockdown of AMPKα_1 and AMPKα_2 abrogated the ability of CB13 to rescue CPT-1β (73±8%, $p<0.05$ *vs.* control) (Figure 3.4C).

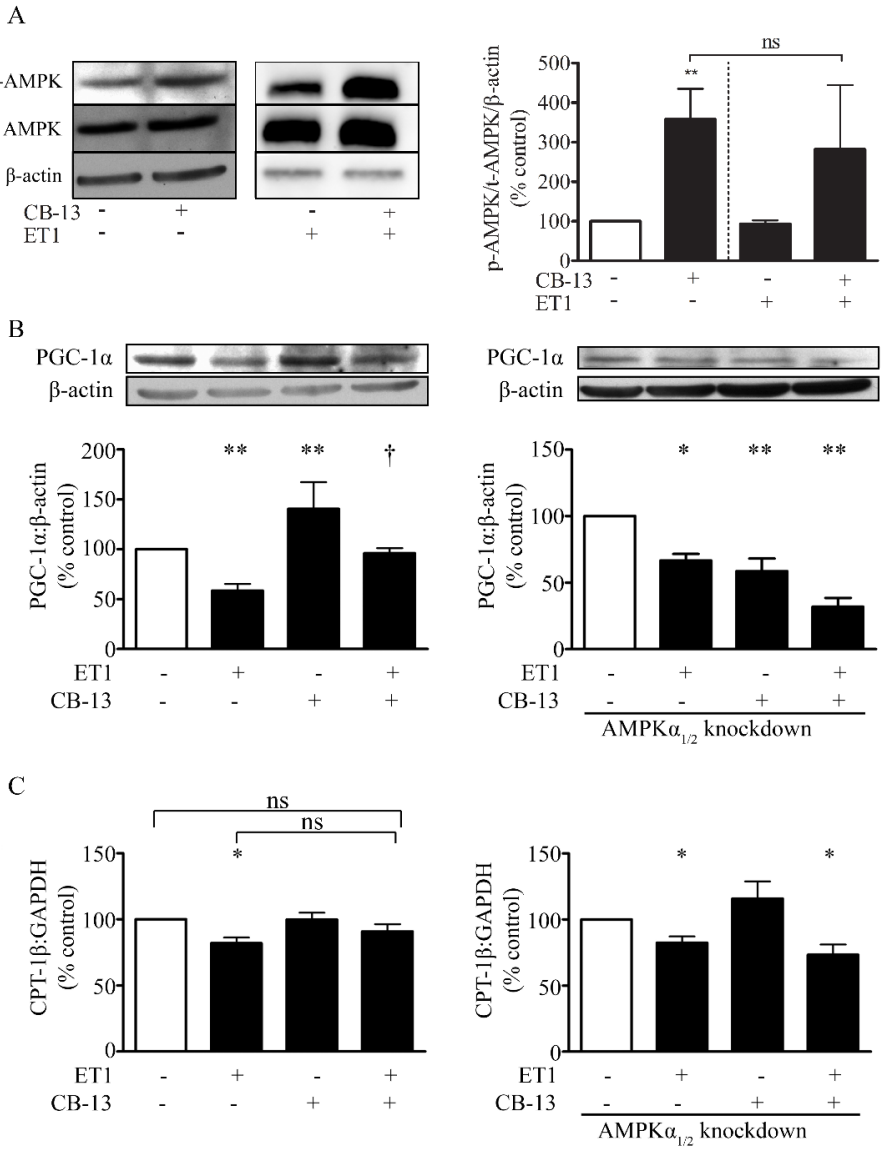

Figure 3.4. ET1-induced down-regulation of PGC-1α and CPT-1β is attenuated by CB13 in an AMPK-dependent manner. *A*, Exposure to CB13 (1 μM) significantly increased phosphorylation of AMPKα at Thr172, which is an indicator of AMPK activation status. AMPK phosphorylation in the presence of CB13 and ET1 is comparable to AMPK phosphorylation levels in the presence of CB13 alone. n=3-9. **p<0.01 vs. control (open bar). *B*, PGC-1α was reduced by ET1 (0.1 μM; 4 h), and this was prevented by CB13. Up-regulation of PGC-1α by CB13 in untreated myocytes was abolished by AMPKα$_1$/α$_2$ knockdown. Likewise, the ability of CB13 to restore PGC-1α expression in ET1-treated myocytes was blocked by AMPKα$_1$/α$_2$ knockdown. n=3-12. *p<0.05 and **p<0.01 vs. control (open bars); †p<0.05 vs. ET1. *C,* ET1 decreased CPT-1β RNA expression, and this was partially attenuated by CB13. AMPKα$_1$/α$_2$ knockdown blocked CB13 effects. n=5-8. (≥3 replicates per n-value). *p<0.05 vs. control (open bars); ns=not significant vs. control (open bars). mean ± SEM.

3.5. Discussion

Mitochondrial aberrations have been linked to numerous aspects of cardiovascular disease such as ischemia reperfusion injury,(245) cardiomyopathy,(246) and heart failure.(141) In fact, mitochondrial dysfunction purportedly contributes to the development of cardiac hypertrophy vis-à-vis, for example, altered mitochondrial biogenesis, decreased energy production/state, worsened redox status, and impaired Ca^{2+} homeostasis. Accordingly, improvement of mitochondrial function has been proposed as a therapeutic target toward the treatment of cardiac hypertrophy.(184) The present study shows that activation of the endocannabinoid system attenuates mitochondrial aberrations in cardiac myocytes subjected to an acute, pre-hypertrophic exposure of ET1. CB13, a dual CB1R/CB2R agonist,(233, 238) attenuated ET1-induced depression of fatty acid-dependent respiration (a surrogate marker of FAO), mitochondrial mPT, and mitochondrial inner membrane depolarization. These protective effects of CB13 were largely dependent on AMPK and were associated with rescued expression of two key regulators of mitochondrial function: PGC-1α and CPT-1β.

3.5.1. Acute exposure to ET1 impairs FAO-dependent mitochondrial bioenergetics.

Our data suggest that an early response to ET1 is depressed FAO. ET1 reduced palmitate-dependent basal OCR (Figure 3.1). This was attributable solely to a decrease in ATP-linked OCR and translated into compromised coupling efficiency (i.e. efficiency of ATP production).

In ET1-treated cardiac myocytes, the net result of depressed FAO is a decrease in oxidative phosphorylation, yet hypertrophic growth, for example, is an energy-consuming process. From a bioenergetic perspective, this may explain, at least in part, the contribution of prolonged hypertrophy to the development of heart failure and functional decompensation.(263-265) We

previously reported that ET1 impaired contractile function of cardiac myocytes by reducing shortening and re-lengthening velocities (125), and a link exists between decreased conduction velocities, mitochondrial dysfunction and inefficient cellular ATP utilization.(266, 267) Moreover, maximal and spare respiration capacities, which reflect the ability of mitochondria to respond to higher energy demand, were also reduced by ET1. This predicts a limited capacity to adjust to conditions such as hemodynamic overload that require extra ATP, rendering myocytes vulnerable to secondary stress.(253)

3.5.2. Mitochondrial membrane integrity in ET1-treated cardiac myocytes in the presence of palmitate

Mitochondrial $\Delta\Psi_m$ results from the electrochemical gradient across the inner membrane, which is established as protons are pumped from the mitochondrial matrix to the intermembrane space by ETC complexes I, III, and IV (extrusion). In contrast, $\Delta\Psi_m$ might be dissipated via proton leak and the ATP synthase pore (re-entry). Thus, $\Delta\Psi_m$ is influenced by the rates of proton extrusion and re-entry.

Our data suggest that ET1-induced mitochondrial depolarization was attributable to reductions in proton extrusion (Figure 3.3). In the presence of palmitate, ET1 reduced net proton re-entry (as evidenced by reduced ATP-linked OCR and unaffected proton leak; Figure 3.1). Nevertheless, mitochondrial $\Delta\Psi_m$ was reduced, indicating that the decline in proton extrusion exceeded the decline in proton re-entry. Thus, dissipation of $\Delta\Psi_m$ was due to a reduction in active proton extrusion.

CB13 restored $\Delta\Psi_m$ in ET1-treated myocytes, and this appeared to be AMPK-independent (Figure 3.3). In the latter, the failure of compound C to abolish protective CB13 effects on $\Delta\Psi_m$

does not seem to reconcile with ablation of CB13 effects on ATP-linked OCR (i.e. proton re-entry; Figure 3.1C). This disparity might be explained by a concomitant further decrease in proton extrusion, where treatment with ET1+compound C+CB13 reduced not only proton re-entry via ATP synthase (Figure 3.1C), but also proton extrusion. This would yield a normalized mitochondrial $\Delta\Psi_m$. This might be achieved by a blunting of ETC complexes I, III, and IV expression and/or activity in the absence of AMPK signaling. Decreased AMPK activity and ETC complex expression were observed in pulmonary artery endothelial cells from fetal lambs with persistent pulmonary hypertension.(268) Decreased AMPK activity (269, 270) and reduced gene expression of Complex I and ATP synthase were also detected in rat ventricles,(271) and in the spontaneously hypertensive rat, hypertrophy is linked to suppressed activities of Complex I and AMPK.(272) Another mechanism by which loss of AMPK might impair proton extrusion is via reduced CPT-1β levels, as shown in response to ET1+CB13+AMPK knockdown treatment (Figure 3.4C). Suppression of CPT-1β would reduce mitochondrial fatty acid uptake and entry into the TCA cycle, electron donor concentrations ($NADH/FADH_2$), and therefore ETC-dependent proton extrusion. Thus, our findings suggest that during FAO, disrupting AMPK abolishes the ability of CB13 to maintain both proton extrusion rate and proton re-entry, yielding a net non-effect on mitochondrial $\Delta\Psi_m$. Thus, rather than suggesting non-involvement of AMPK, the inability of compound C to reverse CB13 rescue of $\Delta\Psi_m$ reflects a parallel loss of CB13/AMPK effects on proton extrusion and re-entry.

3.5.3. Effects of liganded CB receptor activation on mitochondrial signaling cascades

We identified PGC-1α as a candidate mediator of CB13 actions. PGC-1α is a key transcriptional co-activator that regulates mitochondrial function. ET1, angiotensin II, and phenylephrine in

myocytes (273) or pressure overload *in vivo* (274) down-regulate PGC-1α. Activators of AMPK increase PGC-1α expression, and when PGC-1α is absent, the expression of several target mitochondrial genes of AMPK is ablated.(275) AMPK might also stimulate PGC-1α by increasing NAD^+:NADH, thereby activating sirtuin-1 (SIRT1), an NAD^+- dependent deacetylase. SIRT-1 activates PGC-1α by deacetylating lysine sites,(276, 277) and AMPK and SIRT1 reciprocally up-regulate each other.(278, 279) PGC-1α regulates mitochondrial biogenesis, ATP synthesis, and ROS defense mechanisms,(280, 281) and PGC-1α overexpression rescues cardiac mitochondrial function.(184) ET1 reduced PGC-1α and, consistent with reports that deactivation of the PPARγ/PGC-1α complex leads to down-regulation of FAO genes,(276, 282, 283) CPT-1β expression (Figure 3.4) as well. Up-regulation of CPT-1 involves AMPK (284), so while CB13 rescued PGC-1α and CPT-1β expression, $AMPK\alpha_{1/2}$ knockdown abrogated CB13 effects.

When we disrupted AMPK signaling, by shRNA knockdown or using compound C, CB13 treatment alone reduced PGC-1α (Figure 3.4B) and, as would then be expected, FAO-related mitochondrial respiration (Figure 3.1). We speculate that CB13 activates AMPK via CB2Rs, whereas CB1Rs invoke other signaling. JWH-133, a CB2R-selective agonist, activates AMPK (data not shown), and a CB2R agonist is sufficient to stimulate PGC-1α.(285) This suggests that without AMPK signaling, CB13 might be stimulating other signaling cascades to reduce PGC-1α, thus depressing fatty acid oxidation-related mitochondrial bioenergetics. CB13 is a dual agonist of CB1R and CB2R; our previous findings showed that anandamide, which is equally potent at CB1R and CB2R,(286) stimulates PGC-1α expression in the SD rat heart, and moreover, JWH-133 stimulates AMPK activity (data not shown). In addition, Zheng *et al.* reported that a CB2R agonist activated PGC-1α.(285) Therefore, we speculate that CB1-induced signaling emerges to exert opposing effects when CB2R/AMPK signaling is inhibited. Indeed, Tedesco *et al.* observed

decreased AMPK activity and eNOS expression, as well as depressed mitochondrial biogenesis in liver, muscle and white adipose tissues in mice treated with a CB1-selective agonist.(287) Perwitz *et al.* also showed that blockage of CB1R enhanced mitochondrial respiration and increased AMPK activity and PGC-1α expression in adipocytes.(288) Other studies also reported the opposite effects of CB1R and CB2R, where CB1R is detrimental and CB2R is beneficial.(289-291) Therefore, an explanation for our finding that CB13 impairs fatty acid oxidation when AMPK signaling is inhibited might be that CB1R (deleterious) and CB2R (salutary) act in opposition, at least in cardiac myocyte mitochondria, and that CB2R-stimulated AMPK pathways dominate over CB1R signaling in cardiac myocytes to achieve regulation of mitochondrial function by CB13. This remains to be tested.

3.6. Conclusion

We previously reported that manipulation of the endocannabinoid system represents a viable strategy to prevent cardiac hypertrophy.(125) Here, activation of CBRs exerted early protective effects on mitochondrial function in cardiac myocytes exposed to a pro-hypertrophic agonist. Dual agonism of CB1R and CB2R restored mitochondrial $\Delta\Psi_m$ and prevented depression of FAO-related mitochondrial bioenergetics. AMPK played a central role, at least in part by up-regulating PGC-1α and CPT-1β, which are key regulators of FAO. Given that fatty acids are the primary energy source in the heart, the ability of CB13 to restore FAO strengthens its cardioprotective potential. Thus, activation of peripheral CB1R/CB2R may be a new therapeutic approach to address mitochondrial dysfunction in the context of cardiac disease.

3.7. Connecting Text

Ventricular hypertrophy increases the risk of cardiac arrhythmias.(170, 171) More specifically it is associated with increased risk of progression from paroxysmal to persistent/permanent AF.(170, 171) During prolonged periods of stress within the myocardium, and specifically during AF, cardiomyocytes revert to the fetal phenotype and undergo myocyte dedifferentiation; this includes upregulation of ventricular dominant genes and downregulation of atrial-specific genes.(17, 18, 292) Molecular abnormalities that occur during the development of AF substrate are similar to pathophysiological changes that develop in ventricular hypertrophy, heart failure, and ischemia.(221) Additionally, anti-hypertensive medication used to treat underlying LVH symptoms decrease not only LV mass, but also the prevalence of AF.(172)

Cannabinoids exhibit antiarrhythmic effects in the context of ischemia,(222) and prevent endothelial dysfunction in coronary arteries.(198, 230, 231) eCBs decrease the risk of arrhythmia through CBRs.(222) Furthermore, cannabinoids interact with ion channels such as Kv1.5 channels and may influence APD and AP shape.(232) Chapter 4 extends on the findings described in this chapter and describes the effects of CB13 in tachypaced atria using a novel *ex vivo* Langendorff hanging heart technique in SD rats.

Chapter 4

Cannabinoid Receptor Agonist Inhibits Atrial Electrical Remodeling in a Tachypaced *Ex Vivo* Rat Model

4. Cannabinoid Receptor Agonist Inhibits Atrial Electrical Remodeling in a Tachypaced *Ex Vivo* Rat Model

This section contains collaborative work that has been published as an original research article in the journal;

"Cannabinoid Receptor Agonist Inhibits Atrial Electrical Remodeling in a Tachypaced Ex Vivo Rat Model"

Frontiers in Pharmacology. 2021 Apr 22;12:642398. doi:10.3389/fphar.2021.642398.

Danielle I. Lee,[1,2] Michael Murninkas,[3,4] Sigal Elyagon,[3,4] Yoram Etzion,[3,4†] Hope D. Anderson[1,2†]

[1]College of Pharmacy, Rady Faculty of Health Sciences, University of Manitoba, Winnipeg, Canada. 750 McDermot Avenue, Winnipeg, Canada. R3E 0T5.
[2]Canadian Centre for Agri-Food Research in Health and Medicine (CCARM), Albrechtsen Research Centre, St Boniface Hospital, 351 Taché Avenue, Winnipeg, Canada. R2H 2A6.
[3]Cardiac Arrhythmia Research Laboratory, Department of Physiology and Cell Biology, Faculty of Health Sciences, Ben-Gurion University of the Negev, Beer-Sheva, Israel.
[4]Regenerative Medicine and Stem Cell Research Center, Ben-Gurion University of the Negev, Beer-Sheva, Israel.
[†] Equal contribution, co-corresponding authors

Author contributions:

DIL: Contributed to the conception and design of the study, performed all experiments, analyzed all data, generated all figures, prepared the first draft of the manuscript and completed submission of the manuscript (e.g. submitted manuscript, responded to reviewers and made appropriate revisions).
MM, SE: Provided experimental assistance.
YE and HDA: Conceived and designed the study, guided the data analysis and design of the figures, and led completion of the manuscript.
All authors contributed to preparation of the manuscript and approved the submitted version.

4.1. Abstract

Introduction: Atrial fibrillation (AF) leads to rate-dependent atrial changes collectively defined as atrial remodeling (AR). Shortening of the atrial effective refractory period (AERP) and decreased conduction velocity are among the hallmarks of AR. Pharmacological strategies to inhibit AR, thereby reducing the self-perpetual nature of AF, are of great clinical value. Cannabinoid receptor (CBR) ligands may exert cardioprotective effects; CB13, a dual CBR agonist with limited brain penetration, protects cardiomyocytes from mitochondrial dysfunction induced by endothelin-1. Here, we examined the effects of CB13 on normal physiology of the rat heart and development of tachypacing-induced AR.

Methods: Rat hearts were perfused in a Langendorff set-up with CB13 (1μM) or vehicle. Hemodynamic properties of non-paced hearts were examined conventionally. In a different set of hearts, programmed stimulation protocol was performed before and after atrial tachypacing for 90 min using a mini-hook platinum quadrupole electrode inserted on the right atrium. Atrial samples were further assessed by western blot analysis.

Results: CB13 had no effects on basal hemodynamic properties. However, the compound inhibited tachypacing-induced shortening of the AERP. Protein expression of PGC1α was significantly increased by CB13 compared to vehicle in paced and non-paced hearts. Phosphorylation of AMPKα at residue threonine 172 was increased suggesting upregulation of mitochondrial biogenesis. Connexin43 was downregulated by tachypacing. This effect was diminished in the presence of CB13.

Conclusions: Our findings support the notion that peripheral activation of CBR may be a new treatment strategy to prevent AR in patients suffering from AF, and therefore warrants further study.

4.2. Introduction

Atrial fibrillation (AF) is a common, recalcitrant-to-treatment arrhythmia associated with severe complications including thromboembolic events, heart failure progression, reduced quality of life and increased mortality.(52, 58, 293) The prevalence of AF doubles every decade of life and is associated with multiple comorbidities including, but not limited to, structural heart disease, arterial hypertension, obesity, diabetes and sleep apnea.(54-57, 148) Current approaches for rhythm control in AF patients are far from optimal. Ablation therapies are invasive and limited by cost, complexity, potential life-threatening complications and uncertain long-term outcome.(294) Available drugs are only modestly effective, and some have unfavorable side effects including predisposition to life-threatening arrhythmias.(295)

AF has a self-perpetuating and self-exacerbating nature; thus, AF patients are progressively more prone to recurrence and persistence of the arrhythmia. The susceptibility of atrial tissue to AF (i.e. AF substrate) is developed through structural and electrical remodeling in ways that are still being elucidated.(296, 297) Increasing evidence indicates that cardiac dysmetabolism plays a central role in the pathophysiology of AF-related atrial remodeling as well as in the AF substrate of diabetic/pre-diabetic patients.(298) In fact, dysfunction of adenosine monophosphate-activated protein kinase (AMPK), which is a major regulator of cardiac metabolism, can lead to cellular abnormalities and increase AF substrate.(299, 300)

During cardiovascular distress such as ischemia-reperfusion injury, the endocannabinoid system (ECS) is activated and reportedly produces beneficial effects.(230, 301) The ECS is composed of cannabinoid receptors (CBR), endocannabinoid (eCB) ligands, and enzymes to biosynthesize, degrade and transport eCBs.(193) All components of the ECS are present in the heart.(195, 215, 216) Furthermore, in response to endogenous and external stimuli, eCBs are

produced and interact with CBRs to exert regulatory actions toward the maintenance of internal homeostasis through adaptive cellular modification.(193) Therefore, exogenous cannabinoid interactions with the cardiovascular ECS and CBRs may elicit beneficial effects to modulate complications of cardiomyopathies, such as arrhythmias.(301)

CBRs are G protein-coupled receptors of which there are two types. CBR type 1 (CB1R) predominates in the central nervous system, and is the key signaling effector of any CB-dependent psychoactive actions.(194, 209) In contrast, ligand activation of CBR type 2 (CB2R) typically leads to immunomodulation such as immune cell migration and cytokine release.(213) Agonists that bind to CB2R lack the psychoactive effects elicited by CB1R agonists in the brain.(209, 213) CB1R and CB2R are also found in the periphery and regulate processes in organs such as the gastrointestinal tract, lungs, skin, bone, heart and liver.(195-198)

Exogenous cannabinoids, whether plant-derived or synthetic, have a wide range of physiological effects through interaction with the ECS. While eCB actions are presumably limited to the cellular site in which they are synthesized and released, the delivery of exogenous cannabinoids into the body results in excess compound concentrations that are more widely distributed.(193) Thus, exogenous cannabinoid effects are much more prolonged compared to eCBs.(193) Synthetic cannabinoids, originally developed to act as pharmacological probes of the ECS, are derivatives of phytocannabinoids and eCBs.(203) Hundreds of varieties of new and novel synthetic cannabinoids exist, as minor modifications to the chemical structure alter the affinity and selectivity to CBRs.(203)

Using CB13, a CB1R and CB2R dual agonist that does not cross the blood-brain barrier, we previously reported antihypertrophic effects and attenuated mitochondrial dysfunction in cardiomyocytes via activation of AMPK signaling pathways.(125, 302) We hypothesize that the

beneficial effects of CB13 may be relevant to stressed atria as well. Here, we used a Langendorff-perfused rat heart to assess the effects of CB13 on basic physiology of the heart as well as on the atrial electrophysiology following acute atrial tachypacing to mimic an atrial tachyarrhythmia. Our findings support the notion that the beneficial effects of CB13 are indeed relevant in the stressed atria and may serve as a new therapeutic strategy to attenuate AF-related atrial remodeling.

4.3. Materials and Methods

4.3.1. Animals

Adult male Sprague-Dawley rats (n=26, 200–250g) obtained from Envigo Laboratories (Jerusalem, Israel) were used in the study. Experiments were approved by the institutional ethics committee of Ben-Gurion University of the Negev, Israel (Protocol No. IL-05-09-2018A) and were carried out in strict accordance with the Guide for the Care and Use of Laboratory Animals of the National Institutes of Health. The animals were kept under standardized conditions: 12:12 light:dark cycles at 20–24°C and 30–70% relative humidity. Animals were free-fed autoclaved rodent chow and had free access to reverse osmosis-filtered water. Hearts were excised from the animals under deep pentobarbital anesthesia.

4.3.2. Isolated perfused heart preparation and basic physiological measurements

Isolated heart experiments were performed as previously described(188, 303) with slight modifications as detailed below. Briefly, following intraperitoneal (IP) injection of heparin (1000 units), each rat was anesthetized with pentobarbital (IP; 60 mg/Kg) and the heart was excised into cold, oxygenated Tyrode's buffer (mM: 140 NaCl, 5.4 KCl, 0.5 $MgCl_2$, 2.5 $CaCl_2$, 0.39 NaH_2PO_4, 10 HEPES, and 11 glucose, pH 7.4). The aorta was cannulated and perfusion was initiated with

oxygenated, pre-heated (37ºC) Tyrode's solution. Perfusion rate was adjusted to maintain a constant coronary perfusion pressure of ~80 mmHg. To obtain hemodynamic measurements, the left atrium was excised and a fluid-filled latex balloon was inserted into the left ventricle (LV) cavity through the mitral valve. The balloon was then inflated to an end-diastolic pressure of ~5 mmHg. Electrophysiological signals from the right atria (RA) and LV were recorded using miniature-bipolar hook electrodes.(188) Coronary perfusion pressure and LV pressure were recorded by a pressure amplifier (ETH-256C amplifier and PB-100 probes, iWorx, NH, USA). Electrical signals were filtered (1-2 kHz) and recorded by two voltage amplifiers (Model 3000, A-M Systems, Carlsborg, WA, USA). Signals were interfaced with a PC using an A/D converter (PCI-6024E, National Instruments, Austin, TX, USA) and a custom-designed program developed with LabView programing language (National Instruments, Austin, TX, USA) to control signal acquisition, data saving and off-line analysis. Basic physiological measurements included spontaneous beating rate, atrioventricular (AV) interval, LV developed pressure, +dP/dt and -dP/dt. Parameters were recorded following a 20 min recovery period (Figure 4.1.A). Thereafter, CB13 or vehicle were applied and measurements were repeated every 15 minutes for 1h.

4.3.3. Atrial electrophysiology and atrial tachypacing experiments

For atrial electrophysiology experiments, hearts were perfused as described above but a balloon was not inserted to the LV cavity and both atria remained intact. A custom-designed quadripolar-electrode was inserted on the RA for simultaneous pacing and recording.(304) The electrode contained two pairs of platinum-iridium poles (one for pacing and one for recordings) with an inter-pair interval of 4 mm. The electrode was fixed to the atria by two delicate stainless steel pins and RA pacing and recording were verified. Hearts were continuously exposed to CB13 or vehicle

throughout the experiments. A programmed S1S2 stimulation protocol was performed using a double threshold intensity, to measure atrial effective refractory period (AERP). The protocol consisted of 10 S1-S1 intervals of 150 ms followed by an S1-S2 interval that was reduced by 1 ms each time until atrial capture failed 3 consecutive times (Figure 4.1.B). Conduction time was measured during constant atrial pacing at 150-ms cycle length (CL) as the interval between the end of the stimulus applied to one side of the electrode and the first peak of the atrial signal that was recorded in the other side. (304) In addition to AERP and conduction time (CT) measurements, burst pacing was applied to the RA to evaluate for possible arrhythmia induction. This protocol included 10 consecutive 20 s bursts at a cycle length of 20 ms. Following baseline measurements, the RA was continuously tachypaced for 90 min at double diastolic threshold. Tachypacing cycle length was adjusted dynamically and maintained 5 ms above the minimal cycle length in which 1:1 atrial capture was observed (Figure 4.1.C). Following tachypacing, AERP and arrhythmia induction protocols were repeated and the LA and a sample of the LV were snap frozen in liquid nitrogen for further biochemical analysis.

4.3.4. Pharmacological treatments

CB13 (1-naphthalenyl[4-(pentyloxy)-1-naphthalenyl]methanone) was from Cayman Chemical (Ann Arbor, Michigan). Tyrode's buffer was supplemented with vehicle (0.1% v/v DMSO) or CB13 (1 μM, 0.1% v/v DMSO). Treatments remained in buffer for the remainder of the experiment. The concentration of CB13 was based on our previous findings in cardiomyocytes *in vitro*.(125, 302)

4.3.5. Western blotting

Lysates were prepared in radioimmune precipitation assay (RIPA) buffer with phosphatase and protease inhibitors using a bead mill homogenizer and clarified by centrifugation. Total protein concentration was determined by BCA assay (Thermo Fisher Scientific, Massachusetts, USA). Equal amounts of protein were loaded on Mini-PROTEAN TGX stain-free gels (Bio-Rad, California, USA) and transferred to PVDF membrane (Bio-Rad). Membranes were blocked using Tris-buffered saline with 0.1% Tween-20 (TBST) and 5% bovine serum albumin (BSA; Sigma Aldrich, Oakville, Ontario). Primary antibodies Phospho-AMPKα (Thr172) (1:1000, cat. 2535), AMPKα (1:1000, cat. 2603), phospho-LKB1 (1:1000, cat. 3482), LKB1 (1:1000, cat. 3047) were from Cell Signaling Technology (Danvers, Massachusetts) and PGC-1α (1:1000, cat. ab72230), connexin 43 (1:7500, cat. ab11370), CB1R (1:500, cat. ab23703), and CB2R (1:5000, cat. ab45942) antibodies were from Abcam (Toronto, Ontario). Primary antibodies were incubated overnight at 4°C. Affinity-purified horseradish peroxidase-linked secondary antibodies were from Cell Signaling. As applicable, membranes were stripped and reprobed. Membranes were normalized to total protein concentration (TPN) using Bio-Rad stain-free technology, measured using a Bio-Rad Chemidoc^{TM} MP Imaging system and analyzed using Image Lab Software (Mississauga, Ontario) to account for variation in loading amongst lanes.

4.3.6. Statistical analysis

Data are expressed as mean ± SEM. GraphPad Prism 9 software was used for analysis. Normality assumptions were tested using the Shapiro-Wilk test for normality. For analysis between more than two groups: when 1 or more groups did not pass the normality test, a Kruskal-Wallis test followed by Dunn's *post hoc* for multiple comparisons was performed. For normally distributed

data a one-way analysis of variance (ANOVA) followed by Holm-Sidak *post hoc* test for multiple comparisons was performed. Unpaired student t-test or Mann-Whitney test were used to compare the differences between two groups. Two-way ANOVA was used to compare two independent variables between two or more normally distributed groups. The specific tests that were used for each data set are reported in the relevant figure legends. A p-value of ≤ 0.05 was considered significant.

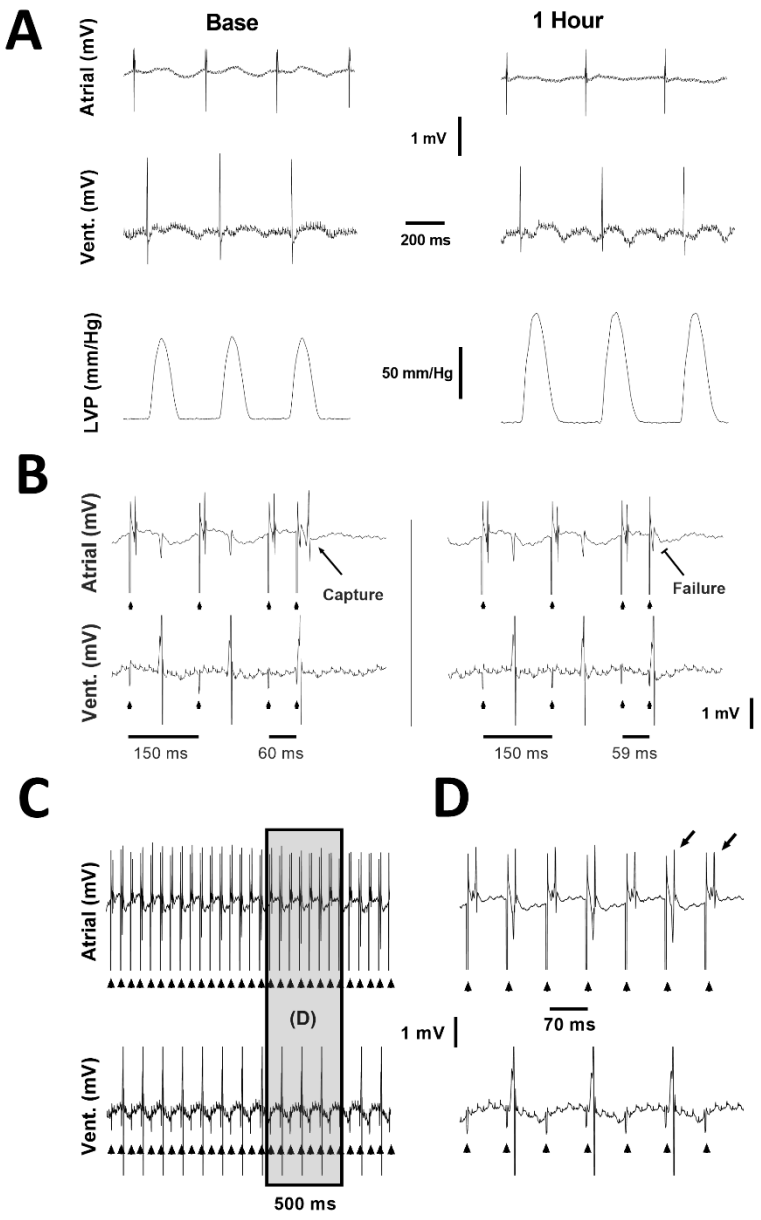

Figure 4.1. Example recordings from the ex vivo experimental setup. (A) Baseline (left) and 1 hour (right) recordings demonstrating the atrial and ventricular electrical signals and LVP signal used to evaluate the effects of CB-13 under standard conditions without pacing. (B) Conventional S1S2 programmed stimulation protocol applied using a quadripolar electrode attached to the right atrium. Left, Atrial capture following S1S2 of 60ms. Right, Failure of atrial capture following S1S2 of 59ms. (C) Continuous assessment of atrial and ventricular signals during atrial tachypacing study. (D) Enlarged segment of the recording in C demonstrating the clear and precise ability to determine 1:1 atrial capture during the tachypacing protocol used in this study. Note beat-to-beat oscillation in the shape of the atrial signal (alternans) often observed when the fast pacing cycle length was reaching the minimal value that was able to maintain 1:1 atrial capture.

4.4. Results

4.4.1. Absence of chronotropic, dromotropic or hemodynamic effects of CB13 in the non-paced rat heart.

The physiological effects of CB13 on the intact heart were not determined previously. Thus, we began by evaluating the effects of the compound in isolated, non-paced rat hearts; the effects of CB13 (1 μM, n=5) were compared to vehicle treatment (n=5) in regard to heart rate (RR interval), AV conduction delay (AV interval) and LV hemodynamic properties over a period of 1 hour (Figure 4.2). RR interval and AV interval remained stable throughout the experimental period without any significant differences at t = 60 min compared to vehicle (323.0 ± 19.0 ms vs. 313.4 ± 24.8, and 53.50 ± 1.59 ms vs. 52.35 ± 2.98 ms, respectively). Likewise, there was no change in LV developed pressure (106.0 ± 16.0 vs. 105.9 ± 15.1 mm Hg vehicle). Furthermore, positive and negative maximal slopes of the LV contraction (+dP/dt, 2581 ± 478 vs. 2822 ± 392 mm Hg/s) or relaxation (-dP/dt, -1654 ± 219 vs. -1846 ± 248 mm Hg/s) were also maintained between groups. Overall, these findings demonstrate both stability in technical terms and lack of notable effects of CB13 on intact rat heart physiology.

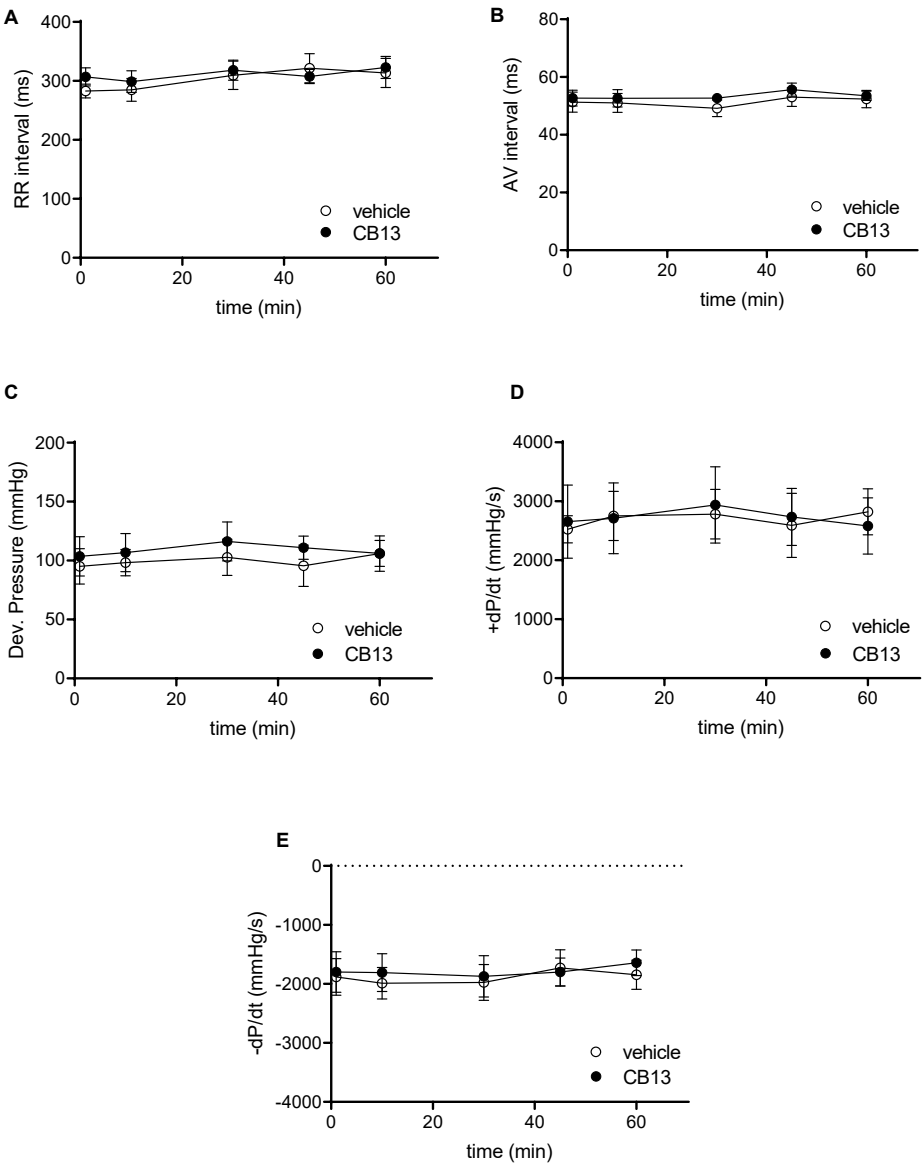

Figure 4.2. Absence of chronotropic, dromotropic or hemodynamic effects of CB13 in the non-paced rat heart. Isolated rat heart preparations were exposed to either 1 μM CB13 or vehicle alone, and (A) RR interval, (B) atrioventricular (AV) interval, (C) developed pressure (D) maximal rate of rise of LVP (+dP/dt), and (E) maximal rate of decay of LVP (-dP/dt) were assessed. All parameters demonstrated stability over time with no difference between the CB13 and vehicle preparations. (n=5). Data presented as mean ± SEM.

4.4.2. CB13-treatment inhibited tachypacing-induced atrial electrical remodeling.

As previously described,(188) *ex vivo* atrial tachypacing reduced AERP in vehicle-treated hearts compared to baseline (45 ± 4 vs. 54 ± 3 ms; $p<0.05$; Figure 4.3, A and B.). In contrast, the AERP of CB13-treated hearts remained unchanged after atrial tachypacing compared to baseline (56 ± 3 vs. 55 ± 3 ms; ns; Figure 4.3.A.B). Therefore, during tachypacing, CB13 treatment preserved AERP, which contrasts with the AERP shortening observed in vehicle-treated hearts (103.6 ± 9.2 vs. 82.3 ± 4.4% of baseline, respectively; $p<0.05$) (Figure 4.3, A and B.). Importantly, prior to tachypacing, there was no difference in AERP with CB13 perfusion compared to vehicle (55 ± 3 vs. 55 ± 3 ms, ns; Figure 4.3.A and B.). Of note, conduction time analysis demonstrated a trend of lengthening in vehicle treated tachypaced hearts relative to the CB13 treated hearts. However, this trend did not reach significance ($p=0.09$, Figure 4.3C). Since tachypacing cycle length (CL) was adjusted during the pacing protocol (see Methods for details), it was important to verify that the CL did not differ between groups. Indeed, average atrial tachypacing CL was not different between the CB13 and vehicle groups (Figure 4.3, D and E.). Comparison of the spontaneous RR interval before and after 1.5 hours of atrial tachypacing indicated a mild, statistically significant tendency of prolongation which did not differ significantly between the two treatments (Figure 4.3, D and E.). AF induction by burst pacing episodes failed to induce arrhythmia in both treatment groups both before and after the tachypacing (except in sporadic cases). Thus, the obtained results were inconclusive and are not shown.

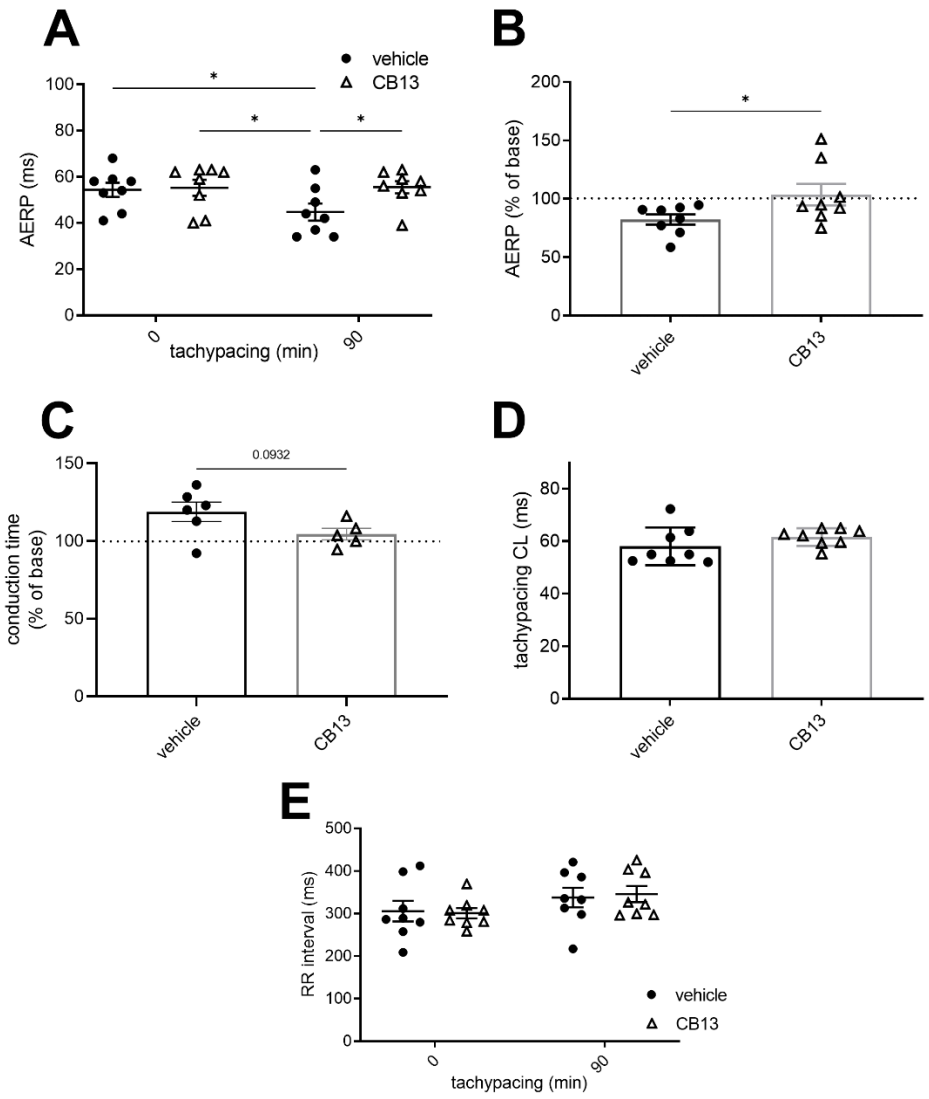

Figure 4.3. CB13-treatment inhibited tachypacing-induced atrial electrical remodeling. (A) AERP before and after 90 min of atrial tachypacing; (B) Scatter plot demonstrating the effect of atrial tachypacing on the AERP represented as % of baseline value in each experiment. CB13 treatment prevented reduction in AERP following tachypacing. (C) Conduction time analysis demonstrated a trend of lengthening in vehicle treated tachypaced hearts relative to the CB13 treated hearts. (D) Average pacing CL over the 90 min of atrial tachypacing. The CL was adjusted continuously and maintained 5 ms above the minimal CL to maintain 1:1 atrial capture. Note no difference between the CB13 group and vehicle group in this regard. (E) Spontaneous RR interval measured before and after 90 min of atrial tachypacing in both groups. Note a mild tendency of RR interval prolongation which reached significance in the CB13 group only. n=8 for each group. Data are presented as mean ± SEM. *$p < 0.05$. CL, cycle length; AERP, atrial effective refractory period. Based on the normality test statistical significance was determined using two-way ANOVA with Newman-Keuls test for multiple comparisons (A and E), Mann-Whitney test (B)

4.4.3. Biochemical effects of CB13 in the tachypaced atria

In order to further reveal the effects of CB13 in the context of atrial tachypacing, biochemical analyses of relevant signaling effectors were performed in LA tissue homogenates. Protein expression levels of CB1R or CB2R did not differ between non-paced control tissues and tachypaced preparations (Figure 4.4, A and B), nor between CB13 and vehicle treatments during tachypacing (Figure 4.4, A and B). In contrast, tachypacing significantly reduced phosphorylation of AMPKα at Thr172, and this effect was partially attenuated by CB13 perfusion during tachypacing (Figure 4.5A). Neither tachypacing nor CB13 affected LKB1 expression or phosphorylation (Figure 4.5B), which indicates that the aforementioned changes in AMPK signaling are not induced through LKB1 modulation (see discussion). PGC1α is phosphorylated by AMPK and acts as a fundamental co-activator for transcription of genes that regulate mitochondrial function. Expression levels of PGC1α were comparable in non-paced and tachypaced atrium (Figure 4.5C). However, tachypacing in the presence of CB13 upregulated PGC1α compared to both non-paced and tachypaced atrium (Figure 4.5C). Of note, there were no changes in total AMPK or total LKB1 levels in our experimental settings (Figure 4.6).

Connexin 43 (Cx43) is a major gap junction protein in the heart which was recently linked to AMPK signaling in the context of AF.(124) Cx43 was downregulated in tachypaced atria compared to non-paced controls (Figure 4.7). Although there appeared to be a trend of recovery of this effect in the presence of CB13, this effect did not reach statistical significance.

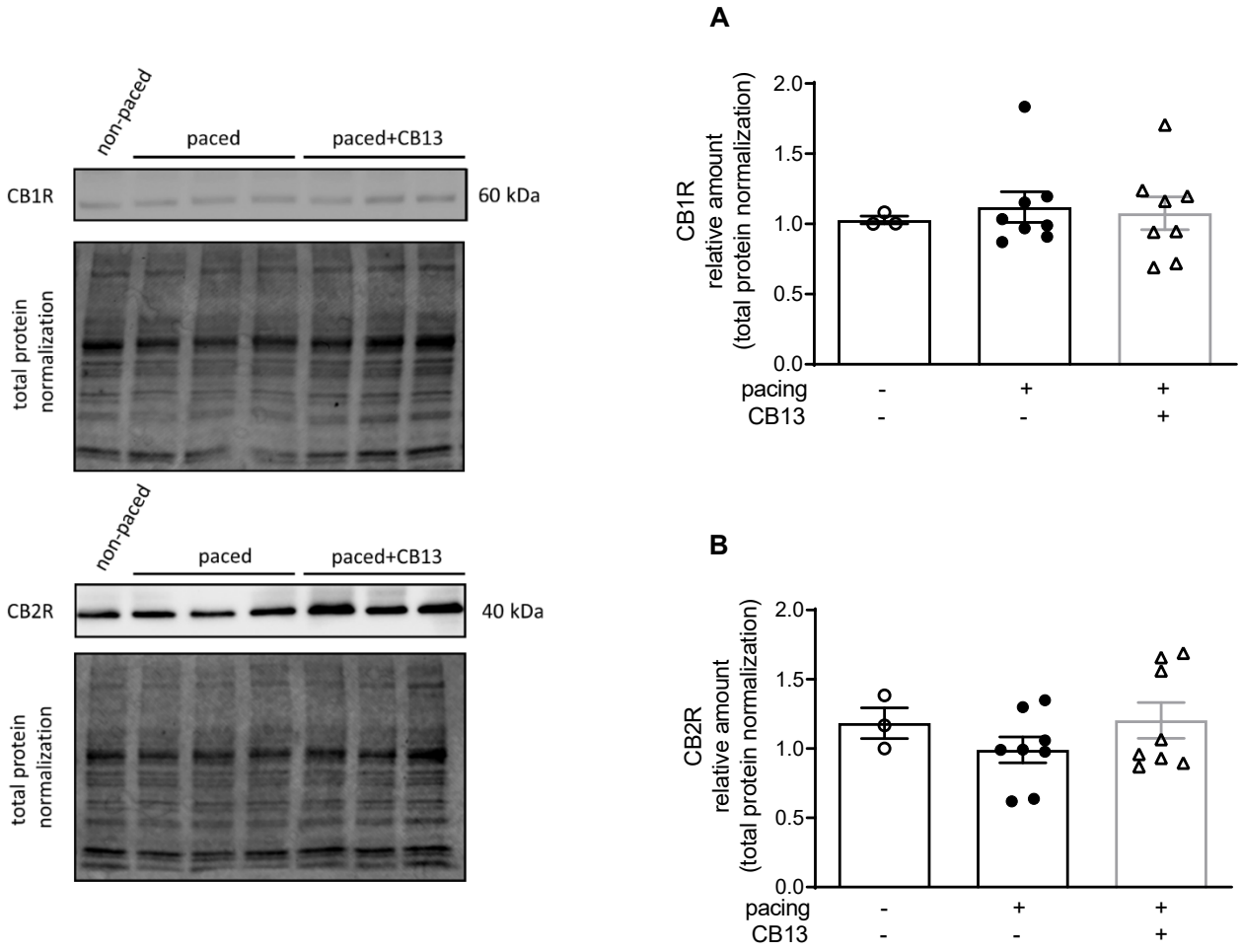

Figure 4.4. Cannabinoid receptor protein levels remain unaltered in atrial tissue. (A) CB1R and (B) CB2R protein levels within atrial tissue exhibit no significant changes between groups. n=3-5. Data presented as mean ± SEM. Data was tested for normality using Shapiro-Wilk normality test. Statistical significance was determined for non-normal data by Kruskal-Wallis with Dunn's post-hoc for multiple comparisons (A and B).

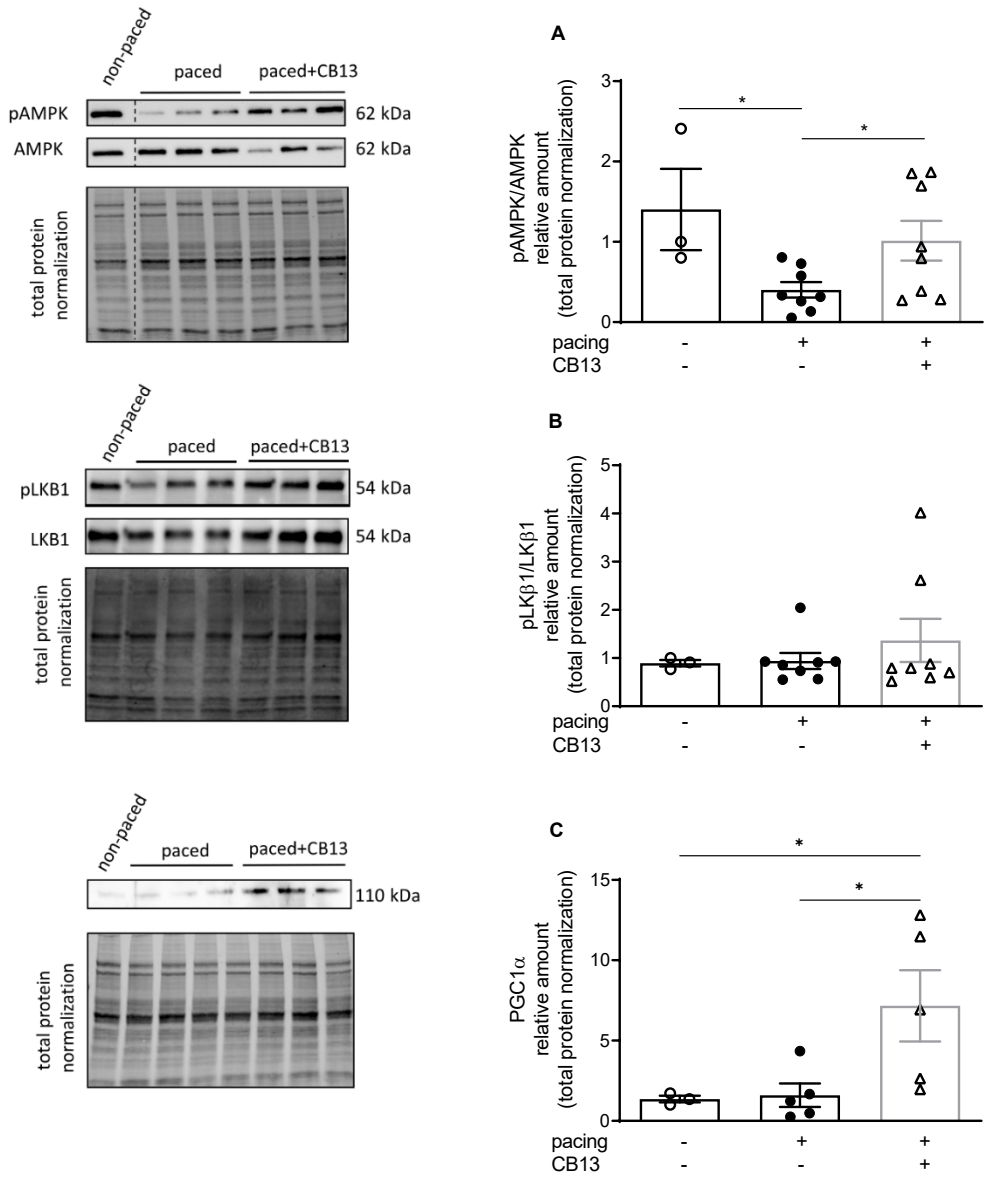

Figure 4.5. Tachypacing induced reduction of phosphorylated AMPK, while CB13 treatment abrogated tachypacing effects and increased PGC1α signaling (A) Tachypacing for 1.5 hours significantly reduced pAMPK compared to non-paced atrial tissue, while CB13 perfusion during tachypacing rescued pAMPK. (B) pLKB1 levels did not change between groups. (C) Protein expression levels of PGC1α were unaltered in both non-paced and tachypaced atrium whereas CB13 perfusion during tachypacing significantly upregulated PGC1α. *p ≤ 0.05. n=3-8. Data presented as mean ± SEM. Data was tested for normality using Shapiro-Wilk normality test. Accordingly, statistical analysis was performed by one-way ANOVA with Holm-Sidak post-hoc for multiple comparisons (A and C) and by Kruskal-Wallis with Dunn's post-hoc for multiple comparisons (B).

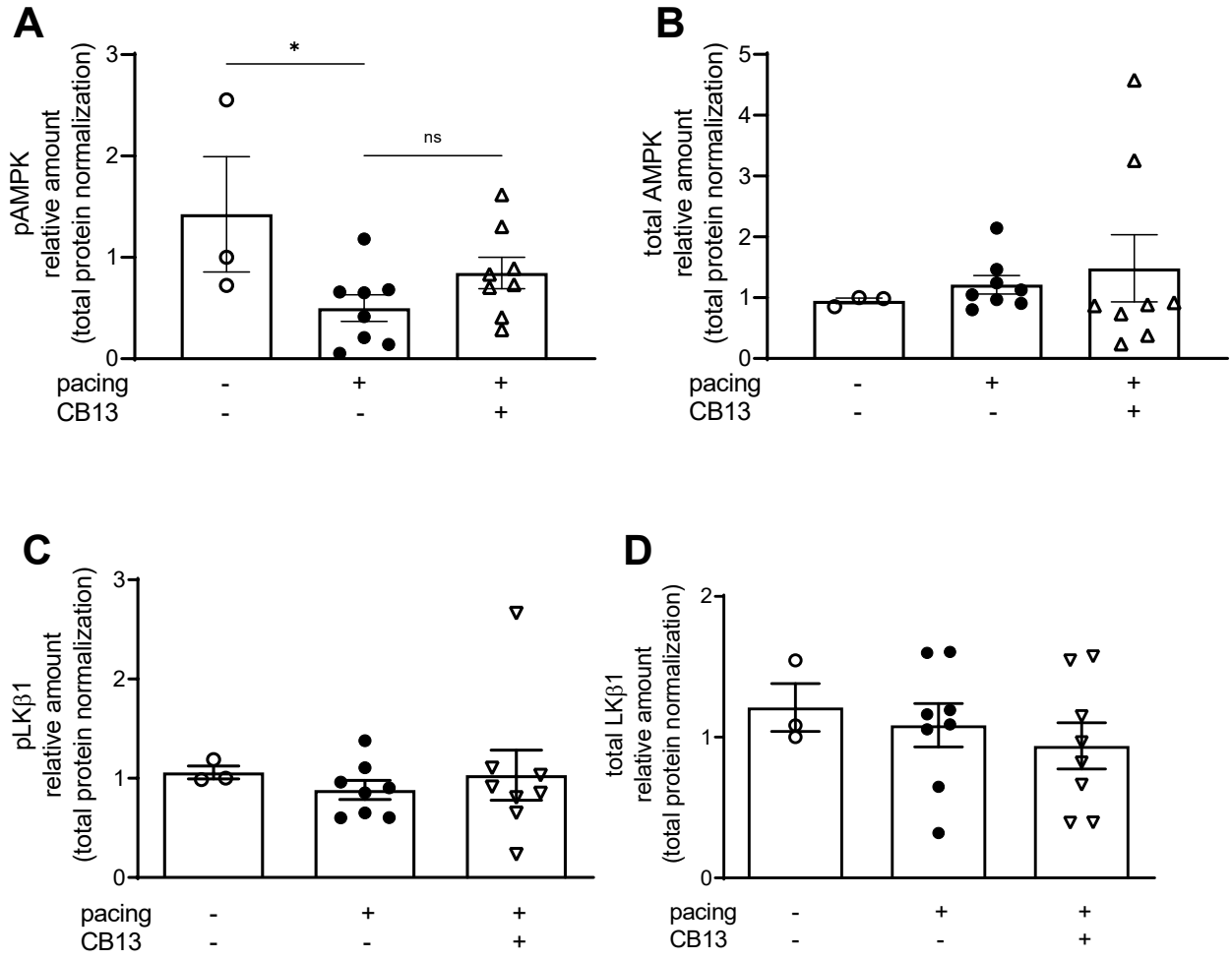

Figure 4.6. Total AMPK and total LKB1 were not altered in atrial tissue. (A) Tachypacing for 1.5 hours significantly reduced pAMPK compared to non-paced atrial tissue (B) but did not alter total AMPK. (C) Phospho-LKB1 and (D) total LKB1 protein expression did not change between groups. See Figure 4.5A and 4.5B for representative blots. *$p \leq 0.05$. ns; not significant. n=3-8. Data presented as mean ± SEM. Data was tested for normality using Shapiro-Wilk normality test. Accordingly, statistical significance was determined by one-way ANOVA with Holm-Sidak post-hoc for multiple comparisons (A).

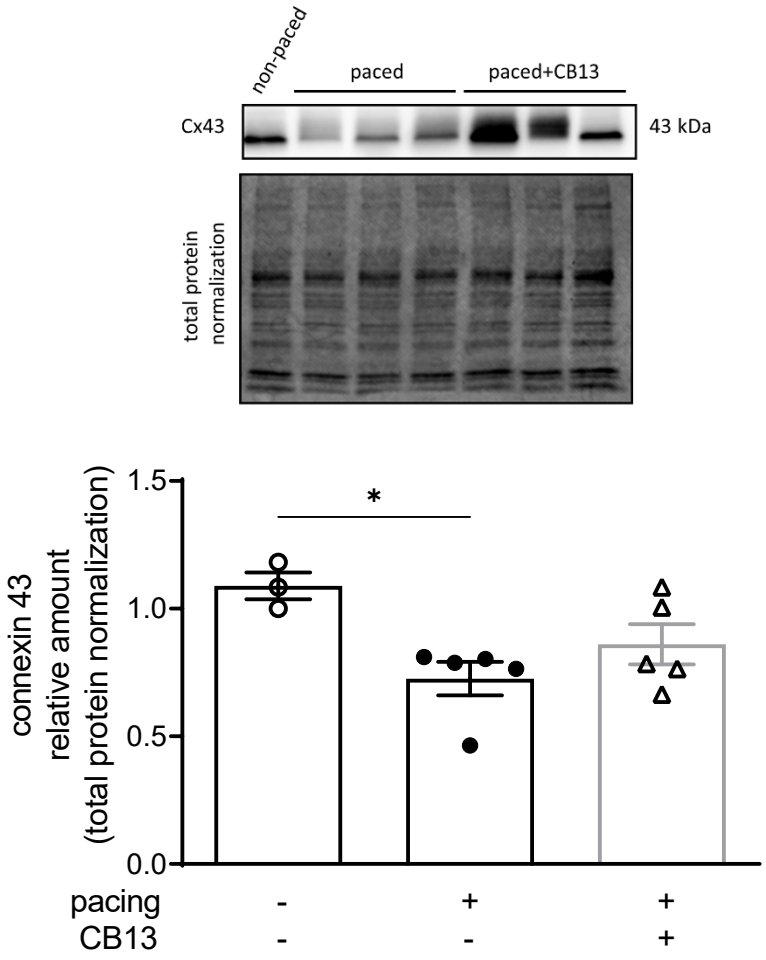

Figure 4.7. Tachypacing-induced reduction of connexin 43 is diminished by CB13. (A) Cx43 is downregulated in tachypaced atrium compared to non-paced atrium. This effect of tachypacing demonstrated a lower tendency in the presence of CB13. *$p \leq 0.05$. n=3-5. Data presented as mean ± SEM. Data was tested for normality using Shapiro-Wilk normality test. Accordingly, statistical analysis was performed by Kruskal-Wallis with Dunn's post-hoc for multiple comparisons.

4.5. Discussion

The present study extends extant evidence indicating possible beneficial effects of ECS activation in the stressed myocardium.(125, 230, 302) Overall, this study demonstrated three salient findings regarding the cardiac effects of the peripherally restricted, dual CBR agonist CB13 in rats: i) lack of CB13-dependent chronotropic, dromotropic or hemodynamic effects in the non-paced ex-vivo preparation; ii) an ability of CB13 to antagonize the AERP remodeling induced by acute atrial tachypacing; iii) AMPK activation may contribute to the ability of CB13 to protect against tachypacing-induced atrial remodeling. These topics are further discussed in detail below.

Our findings address the paucity of knowledge regarding the direct effects of CBR agonists on the intrinsic properties of the intact heart,(305) and support the notion that combined activation of CB1R and CB2R probably does not markedly alter the basic electrophysiology, Ca^{2+} handling and electromechanical coupling of the normal rat myocardium. Indeed, our data indicate that CB13 treatment does not alter chronotropy, dromotropy, or hemodynamics in the spontaneously beating rat heart. Activation of solely CB1Rs reportedly induces negative inotropic effects in isolated human atrial muscle.(195) Likewise, the CB1R agonist, HU-210, induced negative inotropic effects in the LV of the isolated rat heart, (306) although a recent study also using HU-210 did not report such effect.(307) Interestingly, in the presence of the CB1R antagonist AM251, anandamide exerted a CB2R-mediated positive inotropic effect in rat atria.(308) Thus, it is conceivable that the absence of CB13 effects on intrinsic cardiac properties results from opposing effects of CB1R activation and CB2R activation which manifest as a net zero effect. This is consistent with previous reports of opposing CB1R *versus* CB2R effects. In fact, CB2R activation has been linked to cardioprotective effects including antiarrhythmic effects,(222) whereas CB1R activation leads to a myriad of cardiodeleterious effects.(309-316) Thus, Lu *et al.* proposed that, in the context of

attenuating cardiac myocyte hypertrophy, activation of CB2Rs is necessary to negate any adverse effects produced by CB1Rs. Further pharmacological studies will be required to systematically explore this possibility in terms of chronotropy, dromotropy, or hemodynamics in the spontaneously beating rat heart.

Atrial tachypacing is an important experimental approach to mimic AF-related remodeling. In large mammals, sustained tachypacing modifies atrial properties so that AF susceptibility and sustainability gradually increase over time.(91, 297) Studies have indicated that the rapid atrial activity and consequent cellular Ca^{2+} overload within atrial cardiomyocytes lead to secondary changes which converge to increase AF substrate. Shortening of AERP is a hallmark of AF-related remodeling and an important factor that promotes multiple circuit re-entry in the atria.(53, 297) In rodents the long-term effects of atrial tachypacing are less clear. However, short-term tachypacing consistently leads to AERP shortening.(188) In addition, we recently demonstrated that atrial tachypacing of freely moving rats increases AF substrate and promotes molecular changes that resemble those reported in large mammalian models.(317) Moreover, tachypacing of atrial cells *in vitro* leads to molecular changes that recapitulate those observed in the atrial tissue of AF patients.(318, 319) Our current findings indicate that CB13 inhibits the AERP shortening induced by acute atrial tachypacing in the *ex vivo* rat heart. This finding supports the notion that activation of CBRs may be a new therapeutic target in the context of AF-related remodeling. However, further studies are needed to delineate the long-term effects of this new therapeutic strategy *in vivo*. In addition, since AF susceptibility of the normal rat heart is very low, it is challenging to induce AF even following atrial tachypacing and AERP shortening in the current experimental setup. Therefore, the effect of CB13 on AF induction will rely on future preparations that are more prone to AF induction (e.g. the atria of rats with heart failure post myocardial infarction).(320)

The biochemical findings of our study suggest that AMPK activation is involved in the protective effect of CB13 against tachypacing-induced atrial remodeling. AMPK is an essential signaling molecule that contributes to the maintenance of intracellular ATP levels.(321) To this end, AMPK controls energy homeostasis and senses changes in AMP:ATP to in turn control ATP-consumption and catabolic pathways.(321) Reduced AMPK activation in atrial cardiomyocytes appears to be deleterious in regards to regulating metabolic and oxidative stress.(117) Importantly, multiple risk factors for AF such as heart failure, myocardial ischemia, and hypertrophy are associated with metabolic stress and cellular dysfunction.(299) By virtue of ameliorating these metabolic abnormalities, AMPK activation may thus be implicated in improving arrhythmias.(299) In fact, Ozcan *et al.* demonstrated that liver kinase-B1 (LKB1; an AMPK kinase that is linked to activation of AMPK) knockout mice exhibit impaired contraction and decreased AMPK activity.(117) This LKB1 knockout model replicates human disease progression as it develops spontaneous AF that develops into persistent AF.(117)

Our data indicate that acute atrial tachypacing *ex vivo* leads to downregulation of phosphorylated AMPK, similar to that found in humans experiencing persistent AF.(121) In this context, CB13 abrogated AMPK downregulation and increased phosphorylation at its activation site, presumably improving metabolic and cellular function. Although we did not demonstrate a direct link between the electrophysiological effects and metabolic findings, we speculate that improved metabolic conditions of atrial cells in the presence of CB13 lead to less oxidative stress-dependent AERP shortening.(322, 323) However, this hypothesis will have to be addressed more directly in future studies. Furthermore, AERP reduction may also be caused by other factors; for example Ozgen *et al.* demonstrated involvement of Ca^{2+}-activated K^+ currents in action potential duration and atrial remodeling.(324) Additionally, AMPK activation by CB13 is likely not

mediated through LKB1 activation (Figure 4.5B) and is therefore likely achieved through changes in cellular Ca^{2+} levels, particularly since Ca^{2+}/calmodulin-dependent protein kinase kinases (CAMKKs) and reactive oxygen species (ROS), which promote AF, have been implicated to alter AMPK signaling.(119, 325) In fact, CAMKKα and CAMKKβ phosphorylate AMPK at its activation site,(326-328) and CBR ligands can signal through CAMKKs.(329) An important future direction will be to utilize a CAMKK inhibitor to validate this hypothesis.

Information regarding the mediator between AMPK and arrhythmia development, tissue remodeling, or modification of AF substrate remains limited.(299) However, there does appear to be a relationship between cardiac EP and metabolic changes that involve a key role of AMPK and AF substrate.(124, 300) In the current experimental setup, we identified PGC-1α as a candidate mediator for CB13-dependent effects (Figure 4.5C). PGC-1α regulates mitochondrial function vis-à-vis its function as a key transcriptional co-activator that modulates mitochondrial biogenesis, ATP synthesis, and reactive oxygen species (ROS) defense mechanisms.(280, 281) Activation of AMPK results in a downstream cascade that increases PGC-1α expression.(275) Notably, PGC-1α overexpression rescues cardiac mitochondrial function.(330) Tachypacing had no effect on PGC-1α compared to non-pacing controls (Figure 4.5C). However, CB13 treatment caused a significant upregulation of PGC-1α. We previously speculated that CB13 activates AMPK via CB2R whereas CB1R invoke other signaling pathways.(302) In addition, Zheng *et al.* demonstrated that JWH-133, a CB2R-selective agonist, adequately activated AMPK to stimulate PGC-1α, without CB1R interaction.(285) Here we elucidated that CB13 treatment during tachypacing induces a CBR/AMPK (possibly CB2R, specifically) signaling cascade, resulting in PGC-1α activation. While we have previously shown that CB13 has altered mitochondrial bioenergetics and mitochondrial membrane potential in hypertrophied ventricular cardiomyocytes,

an important next step is to determine the effects of CB13 on mitochondrial dysfunction in atrial cardiomyocytes, and the role of the AMPK signaling cascade therein.

Lastly, our data indicate that tachypacing reduces the atrial expression of Cx43, and this reduction was attenuated by with CB13 treatment. Cx43 is a major gap junction in the connexin family and is abundantly found within the atrial and ventricular myocardium.(114) Cx43 has been investigated in several AF-related remodeling studies; for example, in dog pacing models Cx43 reduction has been demonstrated after tachypacing for 3 days, with reduction being preserved for up to 21 days.(115) In rabbit atrial tachypacing experiments Cx43 reduction has been shown to promote atrial fibrillation development.(116) Additionally, Ozcan *et al.* demonstrated that AMPK activation may inhibit atrial fibrillation in LKB1 knockout mice, and similarly found LKB1 knockout mice had a reduction in Cx43 that was rescued by AMPK activation.(38) In contrast, Alesutan *et al.* demonstrated inhibition of Cx43 by AMPK;(331) thus Cx43 and its interaction with AMPK in the context of electrical remodeling remains inconclusive. Furthermore, downregulation of Cx43 would lead to reduced EP coupling between atrial cardiomyocytes, which in turn would slow conduction velocity and increase AF susceptibility in atrial tissue.(332) While we did not demonstrate a change in conduction velocity between groups there was a trend towards conduction lengthening in the vehicle treatment group. It is possible that the short-term tachypacing in our model did not allow for more prominent effects to be observed. Of note, oxidative stress associated with rapid atrial activity has been shown to cause Cx43 alterations;(297, 333) and this may be modulated by AMPK activation.(124) Further studies to examine the interplay between CB13, AMPK, and Cx43 are clearly warranted.

4.6. Conclusion

In conclusion, our data demonstrating the ability of CB13 treatment to prevent tachypacing-induced AERP shortening and Cx43 reduction, as well as to activate known cardioprotective signaling mediators in terms of metabolic dysfunction (i.e. AMPK and PGC-1 α), are collectively in favor of a putative beneficial effect of this drug as a new upstream modality that might be utilized to prevent atrial electrical remodeling. Considering the possible beneficial effects of such treatment in the context of pathological hypertrophy,(125, 302) which shares many of the risk factors for AF, this therapeutic strategy is even more attractive for further investigation.

4.7. Limitations

Electrophysiologic properties of the atria differ between that of rodents and humans, and thus represent a limitation of our study. Dependent on species, the atria have altered electrophysiological properties, including action potential duration and action potential repolarization.(79) Nevertheless, the relevance of rodent models to AF studies are becoming increasingly recognized.(186, 320, 334) In addition, there are multiple studies indicating that tachypacing induces oxidative stress and affects the molecular biology of rodent cardiomyocytes in a highly clinically relevant manner.(317, 319, 335, 336) Furthermore, while we suspect that AMPK activation is linked to ameliorating metabolic abnormalities and improving atrial remodeling through mechanisms including altering AERP, the exact link between AERP and AMPK activation remains to be determined. Assessment of activation status (i.e. phosphorylated levels) of AMPK and presumably LKB1 is reasonable within 1.5 h, and the ability of CB13 to increase PGC1 is likewise plausible as a downstream effector of AMPK signaling. However, detection of changes in CB1R and CB2R expression levels might require more than 1.5 h of

experimental intervention. Further experiments will be crucial to elucidate the underlying mechanisms, and to delineate relevant ionic mechanisms. Of note, we recently introduced a methodology enabling comprehensive EP measurements and AF susceptibility testing in ambulatory rats over time.(304) Thus, based on the current findings it will be interesting to explore the effects of CB13 on longer periods of tachypacing in unanesthetized rats in the near future.

4.8. Connecting Text

Chronic stress exhibited in cardiovascular disease results in hypertrophic remodeling, metabolic shift, opening of mPTP, changing mitochondrial $\Delta\Psi_m$, and AERP augmentation.(189, 273, 297, 302, 337) Chapter 3 describes our findings that CB13 alters mPT, and $\Delta\Psi_m$ in NRVM. Activation of CBR was protective against a pro-hypertrophic agonist and improved mitochondrial function in cardiomyocytes. Dual agonism of CBR restored mitochondrial $\Delta\Psi_m$ and prevented reduction in FAO-related mitochondrial bioenergetics in ET1-treated NRVM. Furthermore, in Chapter 4 CB13 exhibited an ability to alter metabolic dysfunction induced by tachypacing by activating known cardioprotective signaling mediators (i.e. AMPK and PGC-1α). CB13 treatment altered EP parameters, and prevented tachypacing-induced AERP shortening. However, while not statistically significant a possible mechanism may include the depression of Cx43 *ex vivo,* additional experiments must be completed in the future to determine the role of gap junction signaling. Chapter 5 continues to extend my findings in NRVM and tachypaced-atria, as it defines the effects of CB13 on AngII-treated NRAM. The following chapter bridges mitochondrial dysfunction and AF, thereby strengthening the link between CB13, AF and mitochondrial interactions.

Chapter 5

Modulation of Cannabinoid Receptors Attenuates Hypertrophy and Mitochondrial Dysfunction in Rat Atrial Cardiomyocytes

5. Cannabinoid Receptor Agonist Attenuates Angiotensin II–Induced Hypertrophy and Mitochondrial Dysfunction in Rat Atrial Cardiomyocytes

This section contains unpublished collaborative work, including text and figures, by Danielle I. Lee in Dr. Hope Anderson's lab at the St. Boniface Albrechtsen Research Centre, University of Manitoba, Canada, in collaboration with Dr. Yoram Etzion at Ben Gurion University of the Negev, Israel.

"*Cannabinoid Receptor Agonist Attenuates Angiotensin II–Induced Hypertrophy and Mitochondrial Dysfunction in Rat Atrial Cardiomyocytes*"

Danielle I. Lee,[1,2] Yoram Etzion,[3,4] and Hope D. Anderson[1,2]

[1]College of Pharmacy, Rady Faculty of Health Sciences, University of Manitoba, Winnipeg, Canada. 750 McDermot Avenue, Winnipeg, Canada. R3E 0T5.
[2]Canadian Centre for Agri-Food Research in Health and Medicine (CCARM), Albrechtsen Research Centre, St Boniface Hospital, 351 Taché Avenue, Winnipeg, Canada. R2H 2A6.
[3]Cardiac Arrhythmia Research Laboratory, Department of Physiology and Cell Biology, Ben-Gurion University of the Negev, Beer-Sheva, Israel.
[4]Regenerative Medicine and Stem Cell Research Center, Ben-Gurion University of the Negev, Beer-Sheva, Israel.

Author contributions:

DIL: Contributed to the conception and design of the study, performed all experiments, analyzed all data, generated all figures, prepared the first draft of the manuscript.
YE: Conceived and designed the study, and contributed to the completion of the manuscript
HDA: Conceived and designed the study, guided the data analysis and design of the figures, and led the completion of the manuscript.
All authors contributed to the preparation of the manuscript.

5.1. Abstract

Atrial fibrillation (AF) is a common and complex medical challenge with a progressive nature and multiple complications. Activation of the renin-angiotensin system (RAS) appears to play important roles in the pathophysiology of AF, particularly in patients with cardiovascular risk factors. RAS activation is an important factor contributing to atrial tissue changes defined as atrial remodeling, which makes tissue more prone to the arrhythmia upon arrival of electrical triggers. Structural remodeling resulting from enhanced RAS activation results in atrial hypertrophy and prolongation of P-wave duration. In addition, atrial cardiomyocytes are electrically coupled via gap junctions, and electrical remodeling of connexins may result in dysfunction of coordinated wave propagation within the atria. Currently, there is a lack of effective therapeutic strategies that target atrial remodeling and address atrial substrate (i.e. tissue susceptibility to AF). Recently we found that cannabinoid receptors (CBR) may have cardioprotective qualities. CB13 is a dual cannabinoid receptor agonist that activates AMPK signaling in ventricular cardiomyocytes. We recently reported that CB13 attenuates tachypacing-induced shortening of atrial refractoriness and inhibition of AMPK signaling in the rat atria. Here, we evaluated the effects of CB13 on neonatal rat atria cardiomyocytes (NRAM) stimulated by angiotensin II (AngII) in terms of atrial myocyte hypertrophy and mitochondrial function. CB13 inhibited atrial hypertrophy induced by AngII in an AMPK-dependent manner. CB13 also inhibited mitochondrial membrane potential deterioration in the same context. However, AngII and CB13 did not affect mitochondrial permeability transition pore opening. We further demonstrate that CB13 increased Cx43 compared to AngII-treated NRAM. Overall, our results support the notion that CBR activation promotes atrial AMPK activation, and prevents pathological hypertrophy, mitochondrial depolarization and

Cx43 destabilization. Therefore, peripheral CBR activation should be further tested as a novel treatment strategy in the context of AF.

5.2. Introduction

Atrial fibrillation (AF) is the most common cardiac arrhythmia and is prevalent worldwide.(338, 339) Over the next decade, it is estimated that over 12 million people will suffer from AF within the United States.(338, 339) AF is a progressive condition that often transforms from paroxysmal episodes to persistent arrhythmia over time and is associated with several risks, including heart failure progression, reduced quality of life and devastating thromboembolic events. AF substrate, or tissue susceptibility to arrhythmia, can occur due to multiple factors including age, genetic predisposition, and underlying cardiovascular disease.(78) Cardiovascular comorbidities including hypertension, heart failure, and valvular disease contribute to the development of AF substrate.(340) These underlying cardiovascular risk factors result in atrial remodeling making tissue vulnerable to triggers, re-entry, and ectopic firing, thus initiating arrhythmic episodes.(78, 341) Current pharmacotherapies for AF treatment focus on maintenance of heart rate and rhythm through ion channel blockade. However, they are only modestly effective and can paradoxically lead to the development of life-threatening arrhythmias as well as additional side effects.(295). Patients with underlying cardiovascular diseases are prone to AF development and progression.(341, 342) Enhanced activation of the renin-angiotensin system (RAS) in these patients results in structural and electrical atrial remodeling that markedly increases AF substrate.(343) Enhanced levels of angiotensin II (AngII) leads to left atrial enlargement and prolongation of P-wave duration, indicative of structural and electrical atrial remodeling.(341, 342, 344) Thus, AngII likely plays an important mechanistic role in AF development.

In contrast, adenosine monophosphate-activated protein kinase (AMPK) activation during AF appears to improve atrial structural, contractile, and electrical properties by regulating atrial metabolism and adenosine triphosphate (ATP) expenditure.(34, 345) AMPK is a signaling protein sensor that monitors cellular energy level and is present in all mammalian cells, including atrial and ventricular cardiomyocytes.(299, 346) The increased activation rate of atrial cardiomyocytes during AF increases metabolism and energy consumption, resulting in depletion of ATP.(8, 347) Compounds that activate AMPK may mitigate the metabolic demands resulting from AF.(121, 345) In this regard, our group has found that cannabinoid receptor (CBR) ligands exert cardioprotective effects in ventricular hypertrophy models *in vitro* and *in vivo* presumably due to activation of AMPK (125, 302) Recently, we also demonstrated that CB13, a dual CBR agonist with limited brain penetration, is an AMPK activator that prevents tachycardia-induced electrical remodeling and improves energy metabolism in rat atria *ex vivo*. (189) In addition to activating AMPK, CB13 appears to alter gap the junction, Cx43, a signal conduction protein that connects cardiomyocytes and is important for synchronous atrial contraction.(124, 189) More recently Cx43 has been demonstrated to be a potential downstream signaling mediator of AMPK activation.(124) Thus, CB13, as an activator of AMPK, warrants further study as a potential therapeutic to attenuate pathological remodeling of atrial cardiomyocytes.

In this study, we examined the effect of CB13 on AngII-induced atrial hypertrophy and mitochondrial dysfunction, as characteristics of AF, using NRAM. Our findings demonstrate that CB13 has cardioprotective effects via AMPK activation and prevents structural, metabolic and gap junction abnormalities.

5.3. Materials and Methods

5.3.1. Materials

AngII was from Sigma Aldrich (St. Louis, MO). CB13 (1-Naphthalenyl[4-(pentyloxy)-1-naphthalenyl]methanone), compound C (dosmorphin, (6-[4-(2-Piperidin-1-ylethoxy) phenyl]-3-pyridin-4-ylpyrazolo [1,5-a]pyrimidine)), JC-1 (tetraethylbenzimidazolylcarbocyanine iodide) Mitochondrial Membrane Potential assay kit and Mitochondrial Permeability Transition Pore (mPTP) assay kit were from Cayman Chemical (Ann Arbor, MI). Primary antibodies from Cell Signaling Technology (Danvers, Massachusetts) for phospho-AMPKα (Thr172) (1:1000, cat. 2535), AMPKα (1:1000, cat. 2603), phospho-LKB1 (1:1000, cat. 3482), LKB1 (1:1000, cat. 3047) and Abcam (Toronto, Ontario) connexin 43 (1:7500, cat. ab11370), CB1R (1:500, cat. ab23703), and CB2R (1:5000, cat. ab45942) were used.

5.3.2. Neonatal rat atrial cardiomyocytes

This study was approved by the University of Manitoba Animal Care Committee and follows Canadian Council on Animal Care guidelines. This protocol is adapted from our NRVM protocol.(248, 302) Atria were isolated from 1 to 3 day-old neonatal Sprague-Dawley rats and digested at 37℃ with 0.1% trypsin and 0.002% DNase in Ca^{2+}- and bicarbonate-free Hanks HEPES (CBFHH) buffer with agitation in repeating 5 minute cycles. After each digestion cycle the digested cells were suspended in bovine calf serum (BCS) in 50 ml conical tubes on ice; once the 50 ml conical tube was full it was centrifuged at 60 rpm for 15 min to obtain the cell pellet. Cell pellets were filtered through a 100 μm strainer. To distinguish non-cardiomyocytes from NRAM, cells were seeded (i.e. pre-plated) on T75 tissue culture flasks for 75 min in Dulbecco's Modified Eagle Medium (DMEM) containing 10% cosmic calf serum (CCS) and 1% penicillin-

streptomycin (P/S). Pre-plating allowed non-cardiomyocytes to adhere to the tissue culture flask, whereas most NRAM remained suspended in the culture medium. NRAM were collected from flasks and seeded in 0.1% gelatin-coated 6, 12, 24, and 48 well culture plates in 10% CCS DMEM for 24 h. Cells were serum-starved overnight prior to experiments/treatments in 0% CCS DMEM.

5.3.3. Treatments

NRAM were rendered quiescent by serum starvation for 24 h and pre-treated for 1 h with CB13 (1 μM) in the presence or absence of chemical inhibitors of AMPK (compound C; 1 μM; 1 h).(302) Following the 1 h pretreatment, all treatments (compound C and CB13) remained in the culture media for the entirety of the experimental protocol. Atrial cardiomyocyte hypertrophy and mitochondrial dysfunction were stimulated in NRAM by AngII (10 μM; 24 h).(344, 348, 349)

5.3.4. Cell surface area measurements

NRAM were cultured in 12-well plates (1.5×10^6 cells/ml) and treated as required. NRAM were fixed with 4% paraformaldehyde, followed by permeabilization with phosphate-buffered saline (PBS) containing 0.1% Triton X-100 and blocked with PBS containing 2% bovine serum albumin (BSA), as previously described.(350) NRAM were incubated with mouse anti-rat sarcomeric α-actinin primary antibody overnight. NRAM were washed three times with PBS and incubated with Alexa Fluor® 488-conjugated secondary anti-mouse IgG1 antibody (ThermoFisher Scientific) for 1 h at room temperature. After washing with PBS, NRAM were viewed using an Olympus IX81 brightfield fluorescence microscope. Surface areas of individual cells were quantified using Image J software.

5.3.5. Mitochondrial membrane potential ($\Delta\Psi_m$) imaging

To assess relative changes in mitochondrial membrane potential ($\Delta\Psi_m$) in NRAM, the JC-1 Mitochondrial Membrane Potential assay kit was used, as per the manufacturer's protocol (Cayman Chemical), and as previously described.(302) JC-1 is a lipophilic fluorescent reagent; in healthy mitochondria with high $\Delta\Psi_m$, JC-1 concentrates as J-aggregates and emits red fluorescence. In mitochondria with reduced $\Delta\Psi_m$, JC-1 is monomeric and emits green fluorescence.

NRAM were cultured in 24-well plates (7.5 x 10^5 cells/well). Following treatments, NRAM were incubated with JC-1 for 30 min at 37ºC. NRAM images were acquired using an Olympus IX81 brightfield fluorescence microscope. Samples were fluoresced at ex/em at 485/535 nm for monomer green fluorescence and 560/595 nm for aggregate red fluorescence. The ratio of aggregate to monomer (red:green) fluorescence was measured as an indicator of changes in $\Delta\Psi_m$ via corrected total cell fluorescence (CTCF) using ImageJ software, where;

CTCF = integrated density – (area of cell x mean fluorescence of background)

and compared as aggregate CTCF:monomer CTCF.

5.3.6. Mitochondrial Permeability Transition (mPT) imaging

Mitochondrial Membrane Permeability Transition (mPT) Pore assays were performed by measuring mPT pore (mPTP) status opening in NRAM using a commercially available kit (Cayman Chemical, Michigan, USA) according to manufacturer specifications, and as previously described.(302) This mPTP assay kit utilizes a calcein:cobalt technique that is multiplexed with TMRE. Calcein:cobalt dual staining is a recognized method to assess the degree of mPTP opening. Fluorescence contrast between the mitochondrial puncta and cytosol was measured to quantify mPTP.

NRAM were cultured in 48-well plates ($5x10^5$ cells/well) and treated as required. NRAM were coloaded with calcein, cobalt and TMRE for 15 min, followed by a 5 min wash with PBS. The wavelengths for calcein ex/em 485/535 and TMRE ex/em 545/57l, approximately. Fluorescence was measured using an Olympus IX81 inverted fluorescence microscope. Fluorescence contrast was determined as the difference in fluorescent calcein intensity between mitochondrial puncta and cytosol using Image J. For each replicate, images were captured for 5 cells, and fluorescent calcein intensity was measured in three distinct fields.

5.3.7. Western blotting

NRAM were seeded in 12-well plates (1.5×10^6 cells/well) and treated as required. NRAM lysates were prepared in radioimmune precipitation assay (RIPA) lysis buffer with phosphatase and protease inhibitor cocktails, as previously described.(189) Protein concentration was determined by bicinchoninic (BCA) assay (Thermo Fisher Scientific, Massachusetts, USA). NRAM samples were loaded on Mini-PROTEAN TGX stain-free gels (Bio-Rad, California, USA) at 10 µg/lane and transferred to PVDF membrane (Bio-Rad). Membranes were blocked and primary antibodies were incubated overnight at 4°C. Primary antibody dilutions are listed under *Materials*. Secondary antibodies were from Cell Signaling. As applicable, membranes were stripped and reprobed. Blots were imaged with Bio-Rad Chemidoc™ MP Imaging system and analyzed using Bio-Rad stain-free technology, Proteins of interest were normalized to total protein on the same stain-free membrane and quantified with Image Lab Software (Bio-Rad, Mississauga, Ontario).

5.3.8. Statistical analysis

Data are reported as mean±SEM. Experimental data were analyzed using GraphPad Prism 9 software. Normality assumptions were tested using the Shapiro-Wilk test for normality. For normally distributed data, a one-way analysis of variance (ANOVA) followed by Tukey *post hoc* test for multiple comparisons was performed. A p-value of ≤ 0.05 was considered significant.

5.4. Results

5.4.1. CB13 suppresses AngII-induced hypertrophy in an AMPK-dependent manner.

In patients with cardiovascular diseases, enhanced activation of the RAS system gives rise to atrial remodeling and increased risk for AF.(342) Here, we first examined whether CB13 would reduce hallmarks of pathological hypertrophy in atrial cardiomyocytes (Figure 5.1). Indeed, AngII, increased NRAM surface area compared to control cells (124.6% ± 5.0% vs control; $p \leq 0.01$) (Figure 5.1A). However, CB13 markedly reduced the AngII-dependent NRAM enlargement (97.9% ± 1.5% vs. 124.6% ± 5.0%; $p \leq 0.01$) (Figure 5.1A) indicating that CB13 suppresses atrial cardiomyocyte hypertrophy induced by RAS system activation.

We previously demonstrated that CB13 inhibits hypertrophy in ET1-treated NRVM and that disruption of AMPK signaling using a chemical inhibitor, compound C, abolished this effect.(125) Thus, to determine whether CB13 suppresses hypertrophy in NRAM through an AMPK-dependent mechanism, we treated cells with compound C (Figure 5.1B). AngII increased NRAM surface area (136.0% ± 3.5% vs. control, $p<0.01$). However, the ability of CB13 to prevent AngII-induced hypertrophy in NRAM was completely abolished by compound C (137.0% ± 4.4% vs. 136.0% ± 3.5%; ns) (Figure 5.1B). This suggests that CB13 prevents NRAM hypertrophy in an AMPK-dependent manner.

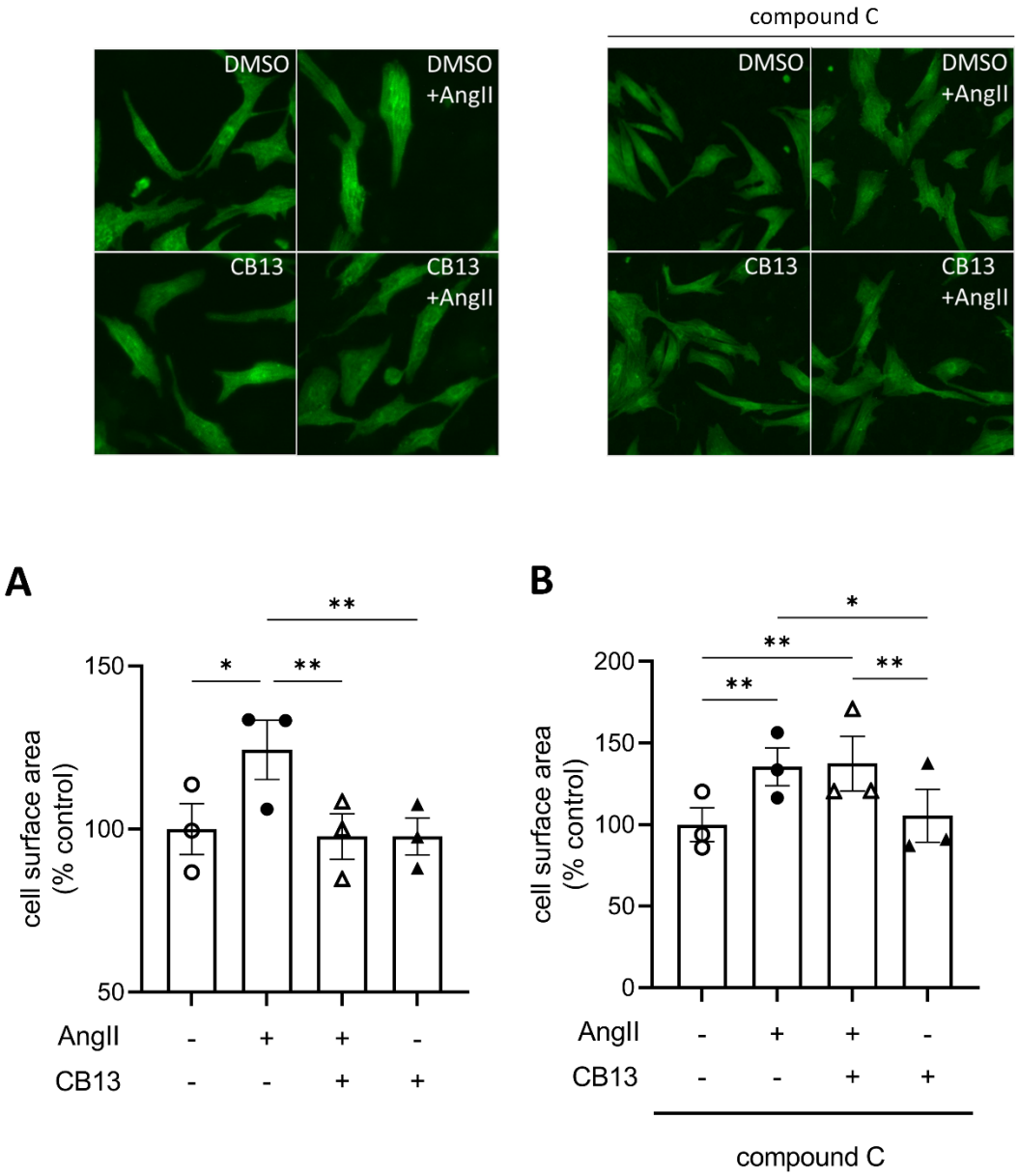

Figure 5.1. CB13 suppressed AngII-induced hypertrophy in an AMPK-dependent manner. (A) The ability of AngII to induce hypertrophy in NRAM was abolished by CB13 treatment. (B) Treatment of NRAM with compound C, an AMPK inhibitor, prevented CB13s ability to suppress hypertrophy. Serum-deprived NRAM were pre-treated with CB13 (1 μM, 1 h) in the presence or absence of compound C (1 μM, 1 h), followed by treatment with AngII (10 μM). All treatments remained in media for 24 h. Results are presented with representative fluorescent images. Data are presented as mean ± SEM. n=3. *$p \leq 0.05$ and **$p < 0.01$.

5.4.2. CB13 prevents AngII-induced mitochondrial membrane depolarization in an AMPK-dependent manner.

Mitochondrial dysfunction underlies atrial metabolic remodeling.(34, 351) Therefore, mitochondrial membrane depolarization was measured as a parameter of metabolic remodeling. $\Delta\Psi_m$ is determined by the ratio between red J-aggregates to green monomers. The lipophilic and cationic dye, JC-1, selectively enters the mitochondria and changes from green to red as $\Delta\Psi_m$ increases. When cells are healthy, and the $\Delta\Psi_m$ is high, JC-1 forms red J-aggregates. When cells are apoptotic and unhealthy JC-1 remains in monomeric form and will form green monomers. AngII induced a decline in red aggregate:green monomer (67.3% ± 4.1% vs. control; $p<0.05$), indicating reduced $\Delta\Psi_m$ (Figure 5.2A). Mitochondrial membrane depolarization was prevented by CB13 in AngII-treated cells. (100.1% ± 9.4% vs. 67.3% ± 4.1%; $p<0.05$). When NRAM were pre-treated with compound C, CB13 no longer attenuated the decline in red:green (i.e. mitochondrial membrane depolarization) compared to AngII (59.3% ± 13.8 vs. 58.8% ± 8.7%; ns) (Figure 5.2B). Therefore, CB13 attenuated AngII-induced mitochondrial membrane depolarization in an AMPK-dependent manner.

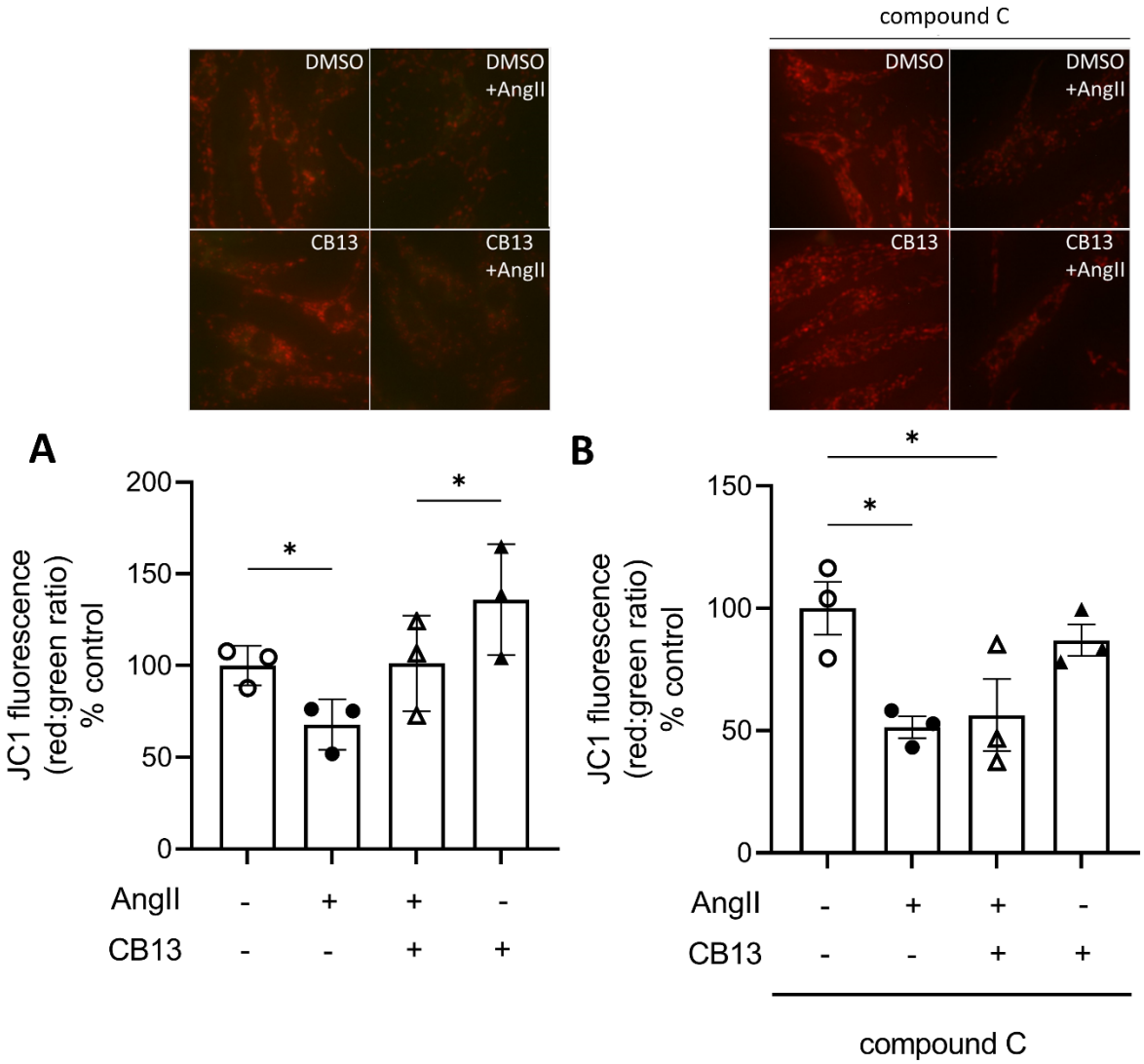

Figure 5.2. CB13 prevented AngII-induced mitochondrial membrane depolarization in an AMPK-dependent manner. The ratio of red aggregates to green monomers (red:green) reflects membrane depolarization. (A) CB13 treatment prevents AngII-induced mitochondrial membrane depolarization. AngII induces membrane depolarization, as indicated by a decrease in red:green, which is attenuated by CB13. (B) Compound C, an AMPK inhibitor, prevented the ability of CB13 to alter mitochondrial membrane depolarization. Serum-deprived NRAM were pre-treated with CB13 (1 μM, 1 h) in the presence or absence of compound C (1 μM, 1 h), followed by treatment with AngII (10 μM). All treatments remained in media for 24 h. Results are presented with representative fluorescent images. Data are presented as mean±SEM. n=3. *$p \leq 0.05$ *and* ***$p < 0.001$.

5.4.3. Mitochondrial permeability transition pore (mPTP) is not altered by AngII.

NRAM treated with AngII did not exhibit alterations in mPTP opening, nor did CB13 influence mPT either in the presence or absence of AngII (Figure 5.3).

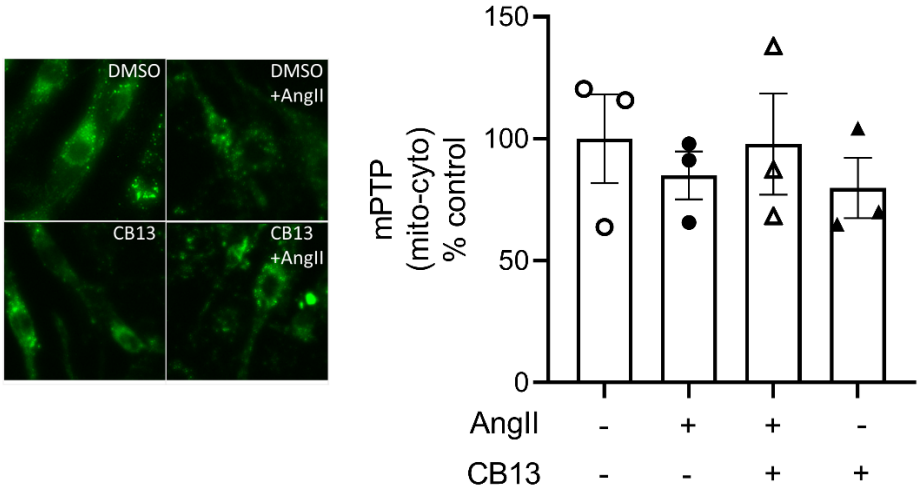

Figure 5.3. Mitochondrial permeability transition pore (mPTP) was not altered by AngII treatment. NRAM treated with AngII did not undergo changes in mPTP opening. Calcein fluorescence was measured as the contrast between the cytosol and mitochondrial puncta. Serum-deprived NRAM were pre-treated with CB13 (1 μM, 1 h) in the presence or absence of compound C (1 μM, 1 h), followed by treatment with AngII (10 μM). All treatments remained in media for 24 h. Results are presented with representative fluorescent images. Data are presented as mean±SEM. n=3.

5.4.4. Biochemical effects of CB13 in atrial cardiomyocytes exposed to AngII

Biochemical analyses of relevant signaling mediators were performed using NRAM protein lysates. We began by investigating phosphorylation of AMPKα at Thr172, an indicator of activation status. AngII treatment decreased phosphorylation of AMPKα (0.62 ± 0.07 vs. control; $p < 0.05$) (Figure 5.4A). CB13 treatment abolished the inhibitory effects on AMPKα activation elicited by AngII (1.05 ± 0.05 vs. 0.62 ± 0.07; $p < 0.05$) (Figure 5.4A). Neither AngII nor CB13 altered phosphorylation or native LKB1 (Figure 5.4D and E). Note also there were no changes in protein expression between native AMPKα nor native LKB1 regardless of treatment (Figure 5.4B and 5.4E).

The gap junction, connexin 43 (Cx43), is a major connexin in the heart that mediates cardiomyocyte electrical coupling; underexpression of this key protein is linked to AF.(117) More recently, Cx43 has been associated as a downstream signaling mediator of AMPK.(124, 352) CB13 increased Cx43 levels compared to cells treated with AngII (1.3 ± 0.2 fold; $p<0.05$). CB13 also tended to increase Cx43 levels in the presence of AngII, but the latter effect did not reach significance (Figure 5.5A). NRAM treated with compound C+CB13 did not have different Cx43 levels when compared to control NRAM (Figure 5.5B).

Lastly, we investigated the expression levels of cannabinoid receptor 2 (CB2R) and cannabinoid receptor 1 (CB1R). CB2R was downregulated by AngII in NRAM (0.48 ± 0.15 vs. control; $p<0.05$) (Figure 5.6A). In contrast, CB1R was unaltered by AngII and/or CB13 treatment (Figure 5.6B)

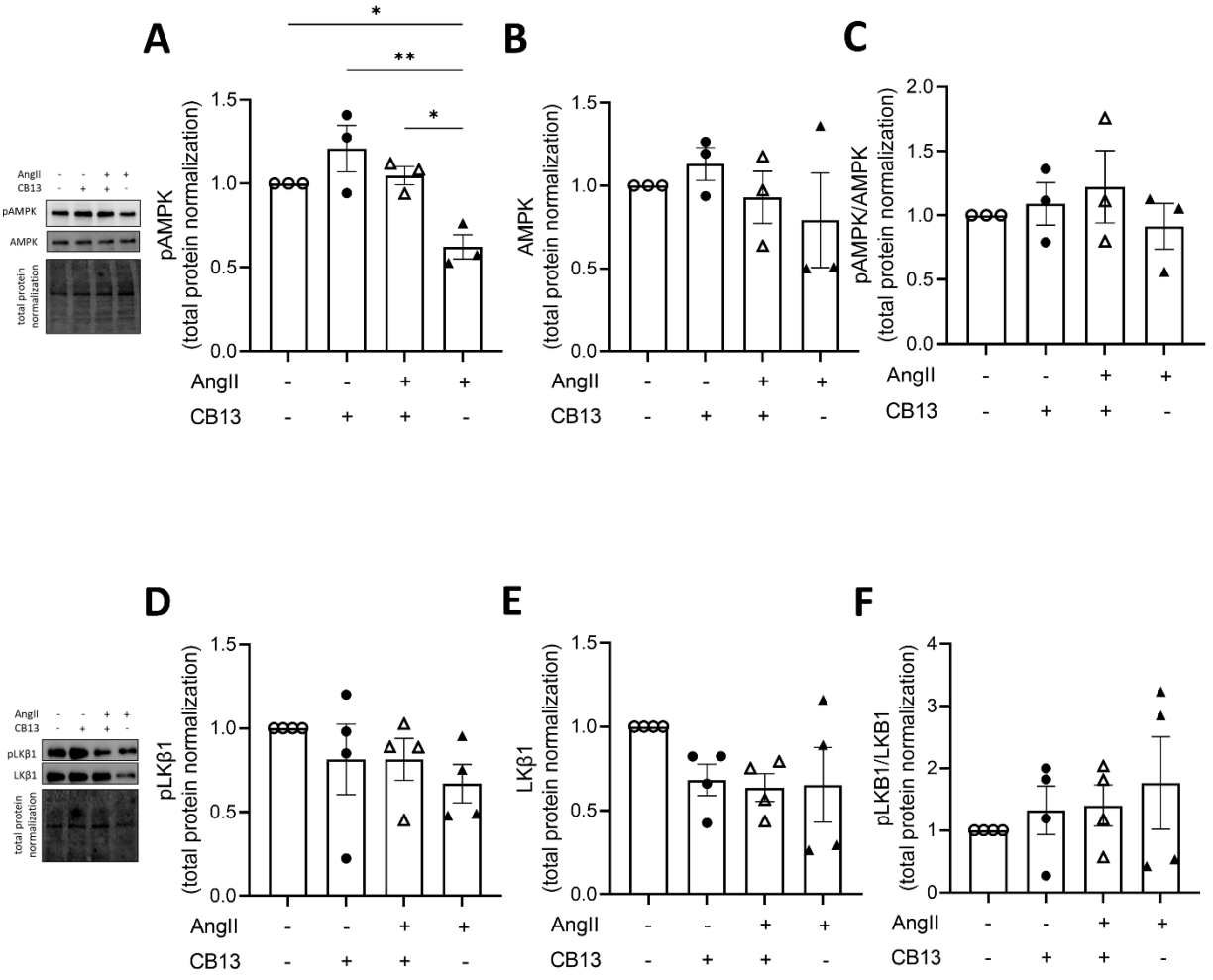

Figure 5.4. CB13 rescued AngII-induced reduction of phosphorylated AMPK. (A) CB13 treatment resulted in phosphorylation of AMPK in NRAM at Thr172 (an indicator of AMPK activation status) compared to control, and rescued AngII-induced downregulation of p-AMPK. (B) Total AMPK was unaltered by AngII and CB13 treatment. (C) pAMPK over total AMPKa. (D) p-LKB1 (D) total and (E) pLKB1 over total LKB1 were unchanged by AngII and CB13. Data are presented as mean±SEM. n=3-4. **p≤0.05 and **p<0.01.*

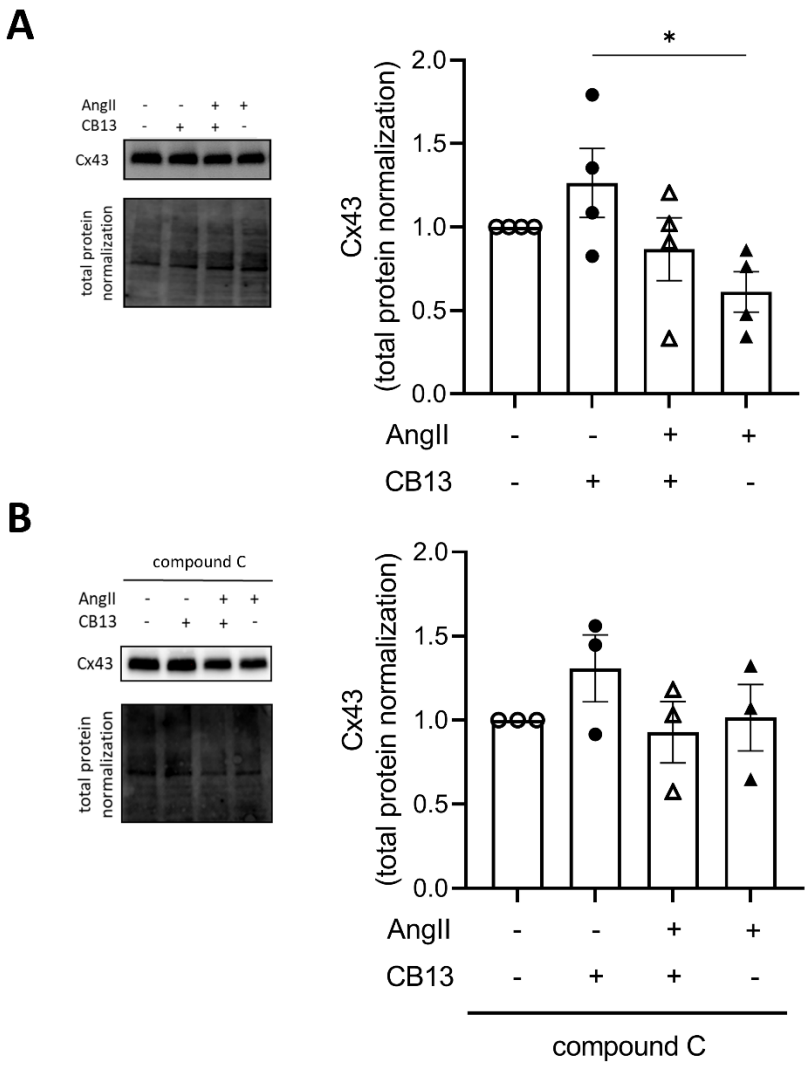

Figure 5.5. CB13 increased the gap junction, Cx43, compared to AngII controls. (A) CB13 increased Cx43 levels compared to NRAM treated with AngII. CB13 also tended to increase Cx43 levels in the presence of AngII, but the latter effect did not reach significance (B) NRAM treated with compound C+CB13 did not have different Cx43 levels when compared to control NRAM. Data are presented as mean±SEM. n=3-4. *$p \leq 0.05$.

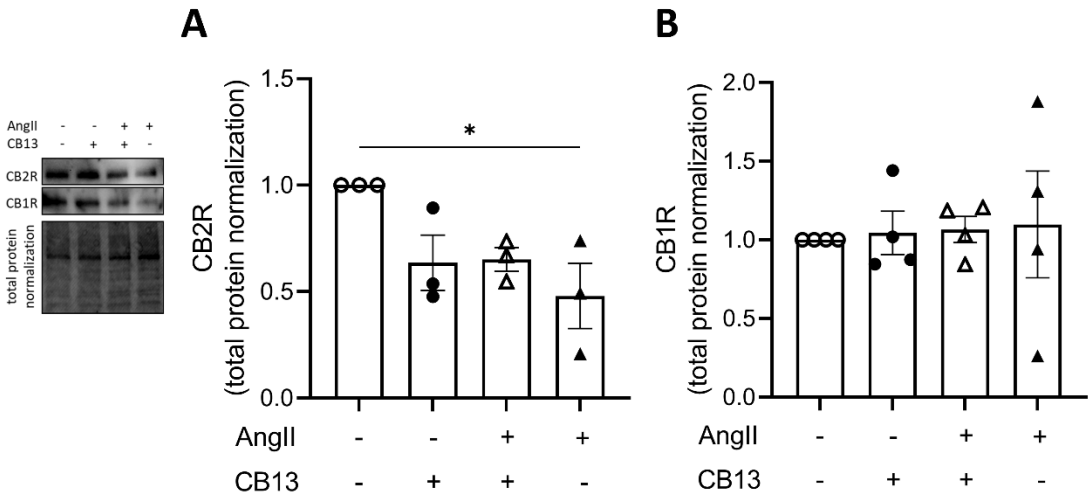

Figure 5.6. Cannabinoid receptor 2 expression was downregulated in NRAM by AngII.(A) CB2R was decreased by AngII-treatment. (B) CB1R was unaltered by AngII and CB13. Data are presented as mean±SEM. n=3. *$p \leq 0.05$.

5.5. Discussion

Our findings demonstrate that the CBR ligand, CB13, attenuates atrial hypertrophy and mitochondrial dysfunction in NRAM through an AMPK signaling mechanism, building upon previous evidence for beneficial effects of CBR ligands in stressed cardiomyocytes.(125, 189, 302) In addition, our data may suggest that AMPK-dependent changes in Cx43 expression also contribute to the possible beneficial effect of CBR ligands. Overall, this study demonstrates three novel findings regarding the effects of CB13 in NRAM: 1) the anti-hypertrophic ability of CB13, previously detected in ventricular cardiomyocytes, extends to atrial cardiomyocytes and is AMPK-dependent; 2) CB13 inhibits mitochondrial depolarization in a manner dependent on AMPK, but independent of mPTP; 3) AMPK activation and Cx43 are effectors of cardioprotection against AngII-induced atrial stress.

RAS activation appears to play a key role in AF development and progression, particularly in patients with cardiovascular diseases.(39, 344) Increased RAS activation leads to multiple alterations in the atria including hypertrophy and abnormal contractile function of the tissue.(39, 343) AF by itself can ultimately affect ventricular filling rate, thereby giving rise to further pathological cardiac complications and RAS activation.(8, 302, 343) Our findings show that CB13 prevented the AngII-induced increase in cell surface area of NRAM. These findings extend upon our previous results of growth inhibition in NRVM and demonstrate the global nature of beneficial CBR activation in the heart.(125). Since many cardiovascular patients with AF also have increased ventricular hypertrophy, this finding may have important translational applications that should be further explored based on the current results. Furthermore, we demonstrated that AMPK inhibition, using compound C blocked the anti-hypertrophic effect of CB13. This indicates that the molecular mechanism behind the beneficial effect of CBR activation is logically related to metabolic terms.

Furthermore this finding is consistent with the multiple recent reports regarding the possible beneficial effects of AMPK activation in the context of AF.(34, 121, 353, 354)

Metabolic stress, leading to a reduction in ATP and an increase in ROS, is an important contributor to atrial remodeling.(34) During AF the rapid atrial rate results in energy depletion and acute metabolic stress. This in turn activates AMPK as a compensatory mechanism.(121, 299) In fact, interventions that promote AMPK activation have been found to protect patients with paroxysmal AF from arrhythmia persistence.(121) In contrast, patients presenting with persistent AF demonstrate a decrease in AMPK activation.(34) Thus, reduced AMPK activation may be an underlying mechanism that leads to AF progression. Our findings show activation of AMPK mediates the antihypertrophic effect of CB13 in NRAM, and may therefore prevent progression of paroxysmal to persistent AF. Ikeda *et al.* also demonstrated that deletion of LKB1, an upstream signaling mediator of AMPK, led to hypertrophy, AF and overall cardiac dysfunction.(353) In addition, Ozcan *et al.* reported that LKB1 knockout mice develop spontaneous AF and bi-atrial enlargement.(117). In this context our group recently demonstrated that CBR ligand activation prevented AMPK inhibition and atrial electrical remodeling following atrial tachypacing *ex vivo*.(189) Overall, the current results, in conjunction with previous reports, support the notion that AMPK activation may be a viable treatment modality in the context of AF. Given the apparent safety of CBR activation in hemodynamic terms,(189) this treatment modality might be an attractive therapeutic option in this regard.

An additional aspect of metabolic remodeling is mitochondrial dysfunction. $\Delta\Psi_m$ was reduced in AngII-treated NRAM, indicating a decline in proton motive force and an overall reduction in free energy available to generate ATP.(24) However, $\Delta\Psi_m$ was restored to control levels by CB13 in an AMPK-dependent manner. This contrasts with the AMPK-independent

ability of CB13 to prevent reduced mitochondrial depolarization in NRVM.(302) However, this finding was likely not due to complete lack of AMPK involvement but rather simultaneous loss of CB13/AMPK effect on the mitochondrial electron transport chain.(302)

The role of mPT in cardiovascular injury is well-studied, as opening of mPTPs results in apoptosis and cell death in myocardial infarction and left ventricular dysfunction.(355-361) However, in the context of arrhythmia and AF, the role of mPTP activity remains unclear.(24) While the collapse in $\Delta\Psi_m$ has been demonstrated in numerous studies and leads to arrhythmias(302, 362-365), the mechanistic basis is poorly understood.(24, 366, 367) AngII-induced atrial mitochondrial membrane depolarization is not linked to mPT, as opposed to the $\Delta\Psi_m$-mPTP coupling in ET-1-treated NRVM. The contradictory involvement of mPTP in CB13-treated NRAM but not CB13-treated NRVM is possibly explained by functional differences of ion complexes within the inner membrane that are involved in $\Delta\Psi_m$. For example, blocking the inner membrane ion channel, IMAC, was protective against arrhythmias by preventing $\Delta\Psi_m$ reduction, improving left ventricular developed pressure, and preventing action potential shortening.(363, 367, 368) As noted above, we recently reported that CB13 treatment prevents atrial refractoriness shortening in an *ex vivo* rat model exposed to atrial tachypacing, suggesting prevention of action potential shortening by CB13.(189) It is plausible that CB13 counteracted the tachypacing-related remodeling by modulating $\Delta\Psi_m$ via IMAC. However, this possibility should be further confirmed in future studies. Overall, AngII induces mitochondrial dysfunction in NRAM, and utilizing therapeutics that target metabolic alterations and preserve $\Delta\Psi_m$ may prevent the development of arrhythmias.

In AF, the aforementioned structural remodeling is accompanied by metabolic and electrical remodeling. (34) In addition to AMPK activation, our data suggest that Cx43 may be a

downstream effector of CB13. Cx43 is a major gap junction assembled from connexin proteins that are necessary for cell-to-cell electrical communication. Found in both ventricular and atrial myocardial tissue,(114, 369) Cx43 is downregulated during several AF-related remodeling studies and contributes to AF etiology.(115, 116, 189) Ozcan *et al.* also demonstrated that aspirin and metformin, both activators of AMPK, preserved Cx43 protein levels and atrial size in an LKB1 knockout mouse model.(38) Our finding that CB13 preserves Cx43 levels offers insight into the potential effect of CB13 in terms of electrophysiological coupling between NRAM. Whether CB13/AMPK crosstalk is required for CB13 effects on Cx43 remain to be elucidated. Cx43 is reportedly a downstream signaling effector of AMPK activation, possibly through K_{ATP} channels.(124, 352) Our data show that in NRAM, AngII reduced phosphorylation of AMPK, CB13 rescued AMPK activation, and concomitantly prevented AngII-induced suppression of Cx43. We further demonstrate that CB13 increased Cx43 compared to AngII-treated NRAM, which is consistent with our previous report that CB13 rescued Cx43 in an acute tachypaced AF model.(189). This finding supports the notion that Cx43 expression levels are linked to AMPK activation status in a way that may be clinically relevant in the context of AF. However this finding should be interpreted cautiously, as CB13+AngII did not alter Cx43 differently than AngII alone. Further experiments *in vivo* investigating electrical coupling of Cx43 are warranted, as cell culture may not demonstrate electrical coupling between cells. Lastly, CB2R was downregulated in atrial cardiomyocytes by AngII. This may suggest that the inhibitory effect of AngII on CB2R is perhaps a route by which AngII prevents AMPK signaling.

In summary, our study demonstrates that CB13 prevents hallmarks of AngII-induced structural, metabolic, and possibly also electrical remodeling in a largely AMPK-dependent manner. Specifically, the CB13/AMPK axis prevents AngII-dependent NRAM hypertrophy,

restores $\Delta\Psi_m$, and may address electrophysiological aberrations by rescuing expression of Cx43. CBR-based interventions therefore warrant further study as a potential therapeutic approach to the clinical problem of AF.

Chapter 6

Discussion, Future Directions, and Conclusion

6.1. Discussion and Future Directions

This thesis reports three novel major findings: 1) CB13 exerts an anti-hypertrophic effect *in vitro* in both NRAM and NRVM, 2) CB13 attenuates mitochondrial dysfunction and alters metabolic signaling *in vitro* in NRAM and NRVM, and lastly, 3) CB13 alters electrical signaling through Cx43 *in vitro* and *ex vivo,* and prevents AERP shortening in *ex vivo* tachypaced hearts.

6.1.1. CB13 is anti-hypertrophic

Cardiomyocyte hypertrophy is a risk factor for AF and heart failure.(228) Furthermore, all components of the ECS are found within the heart.(195, 212, 215-218). However, CB1R/CB2R are not present in all cardiac cell types. Atrial and ventricular cardiomyocytes, endothelial cells, and smooth muscle cells express both CBR, while fibroblasts and certain immune cells only express CB2R.(212) The dual CBR agonist, CB13, attenuated hypertrophy in NRVM and NRAM.

Previously, Lu *et al.* probed CB1R and/or CB2R with several cannabinoids, and reported that CB1R and CB2R have distinct anti-hypertrophic effects.(125) CB1R activation prevented fetal gene activation, but not hypertrophy, while CB1R/CB2R activation prevented both hypertrophy and fetal gene activation.(125) Moreover, CB2R-deficient mice show greater cardiomyocyte hypertrophy compared to wild-type.(370) Thus, Duerr *et al.* state that CB2R likely prevent apoptosis by modulating contractile elements, increasing reactive oxygen scavenger enzymes and lowering the inflammatory response.(370) Furthermore, Duerr *et al.* reported that patients with aortic valve stenosis and cardiac hypertrophy had elevated levels of eCB, CB2R and FAAH, predominantly in cardiomyocytes.(371) Thus, CB2R likely modulates the damage associated with pressure-overload, as previously shown in experimental models of ischemia.(371) The ECS is also involved in regulating inflammation.(371) In fact, the ECS, and specifically CB2R

is associated with modulating macrophage function. In CB2R-deficient murine hearts, there is significantly higher macrophage density (proinflammatory) and suppression of IL-10 (anti-inflammatory).(370)

The effect of CB1R in cardiac hypertrophy remains inconclusive. CB1R has been associated with the attenuation of heart failure in murine models, and contradictorily involved in the development of ventricular dysfunction.(372, 373) To further confirm the anti-hypertrophic effect of CB13 through the ECS, *in vivo* experiments using SHR, spontaneously hypertensive heart failure (SHHF) rats, or TAC-induced animals may be useful. AMPK is reportedly protective in terms of TAC-induced hypertrophy, ventricular dysfunction and fibrosis.(143, 144) Therefore, CB13/AMPK signaling is likely to produce similar effects *in vivo*. Furthermore, *in vivo* experiments will provide greater understanding regarding CB1R/CB2R expression and inflammatory markers within the myocardium.

It is important to note that although CB1R/CB2R are the major CBR in the ECS, other receptors interact with cannabinoids. An alternative to the two major CBR, TRPV1, may induce the progression of hypertrophy. TRPV1 expression is upregulated in the hypertrophied heart and contributes to fibrosis, apoptosis and contractile function.(374) TRPV1 knockout preserved heart structure and function in TAC mice.(374, 375) Antagonism of TRPV1 with a non-cannabinoid resulted in protection from further hypertrophy, fibrosis and tissue remodeling.(374, 375) Importantly, cannabinoids such as THC, AEA, WIN55212-2 (synthetic high affinity CB2R agonist), and CB13 reduce TRPV1 sensitization.(376, 377)

As stated in Chapter 1, sex differences are reported in heart failure presentation.(165, 168) Similarly, there is recent research suggesting sex differences in the ECS.(378) For example females have higher density of CB1R in the amygdala compared to males.(379, 380) This

difference in CB1R density is due to the presence of estradiol in females.(380) Currently, research on the impact of sex differences in the ECS is mainly concentrated on CNS function. Thus, further investigation into sex differences involving the cardiovascular ECS is necessary.

Furthermore, AngII and ET-1 both stimulate hypertrophy through Gαq signalling.(381) Activation of Gαq-coupled receptors induce hypertrophy and cardiomyopathy, *in vitro* and *in vivo*, respectively. Gαq-overexpression in the mouse heart stimulates cardiac hypertrophy, however, intervention with GTP-ase activating proteins (GAPs), such as RSG4 and RGS2, attenuate hypertrophy.(381) Thus, signaling mediators controlled by GAPs and Gαq signaling may be of interest as cannabinoid intervention also demonstrates antihypertrophic effects in both ET-1 and AngII myocyte models. Furthermore, G-protein signaling, and regulators of G-protein signaling (RGS) interact with cannabinoid receptors in neuropathy.(382)

It should also be noted that *in vitro* cardiomyocyte characterization have limitations and may not represent the precise conditions of an *in vivo* injured heart. Cultured NRAM and NRVM respond differently compared to intact cardiac tissue as cultures lack surrounding tissue and cellular environment, such as fibroblasts, endothelial, and cardiomyocyte coupling interactions. Additionally, utilizing a single agonist (i.e. AngII or ET-1) may not capture the broad spectrum of disease progression that would be demonstrated in pathological *in vivo* settings.

6.1.2. CB13 alters mitochondrial dysfunction and metabolic signaling

Mitochondrial dysfunction reportedly contributes to cardiac hypertrophy.(330) CB13 attenuated ET1-induced aberrations of FAO-related mitochondrial bioenergetics and prevented AngII and ET1-induced reductions in $\Delta\Psi_m$. Lastly, CB13 activated AMPK, subsequently preventing the downregulation of PGC-1α and CPT-1β *in vitro.*

Metabolic alterations occur in both heart failure and AF.(33, 34) CB13 did not alter LKB1, an upstream activator of AMPK, as shown in Chapter 4 and Chapter 5. However, ROS, which promote AF, have been implicated as modulators of AMPK signaling.(119, 325) In contrast to my findings, Kim *et al.* showed that AMPK was activated in HL-1 cardiomyocytes through ROS generation at AT_1R.(344) However, this finding is not demonstrated in *in vivo* models. Murine models with functional AMPK knockdown had exacerbated LVH and impaired APD, K_{ATP} channels and AMPK cardioprotection.(383-385) Additionally, LKB1 knockout models exhibit spontaneous AF, which is thought to be due to the lack of the LKB1/AMPK signaling pathway.(386) In AF, AMPK downregulation may be a biomarker that results in transition from paroxysmal to persistent AF, and overall AF initiation, and this may explain the findings by Kim *et al*.(34) Therefore, AMPK activation in early stages of substrate development may prevent AF initiation.

As previously mentioned in Chapter 3, CB1R and CB2R may act in opposition within the mitochondria, where CB1R may be deleterious while CB2R is salutary. CB2R agonism using the synthetic cannabinoid, JWH133, prevents loss of $\Delta\Psi_m$ and mPTP opening in the ischemic heart.(289). Fisar *et al.* investigated CB1R-dependent changes in the mitochondria using a CB1R antagonist, inverse agonist, and several agonists.(291) It was demonstrated that AM251 (CB1R antagonist) was protective, and CB1R activation using THC inhibited mitochondrial respiration.(291) Additionally, mitochondrial effects of cannabinoids may not always be CBR-mediated. Accumulation of cannabinoids within the inner mitochondrial membrane can impair ETC complexes and inhibit mitochondrial respiration.(291) Furthermore, CBR signaling alters mitochondrial basal and ATP-linked OCR and respiratory capacity (Chapter 3). However, whether mitochondrial respiratory capacity changes Ca^{2+} flux has not been studied in detail.(387) As

AMPK is able to regulate ion channels and transport functions, it can also alter cardiac EP.(299) The role of AMPK and Ca^{2+}-handling within the heart has not been studied in detail. However, there is likely a link between SERCA2a, ROS, and AMPK.(299, 388)

Lastly, modulation of the ECS has been used as an approach to treat metabolic disease. The CB1R antagonist, rimonabant, effectively treats obesity.(389) However, due to CB1R blockade, rimonabant was associated with high risk of depression and anxiety, and clinical trials were terminated.(390) Alternatively, the CB2R agonist, JWH-015, reduced body weight and improved obesity-related inflammation, including increasing IL-10.(391) There are also sex differences within the metabolic processing of cannabinoids. THC has higher potencies in female rats compared to males due to differences in oxidative metabolism within the liver, more specifically oxidation of the 9-position methyl group in females.(392) These findings reinforce the negative side-effects of CB1R modulation, the importance of using peripherally restricted cannabinoids, and reinforce the need to investigate sex differences within the ECS.

6.1.3. CB13 affects electrical signaling via AERP and Cx43

Arrhythmias develop in heart failure, LVH, and AF. In fact, left ventricular dysfunction initiates multiple neurohormonal compensatory mechanisms, including a hyperadrenergic state, increasing the risk of AF.(393) CB13 preserved AERP in *ex vivo* tachypacing models and augmented Cx43 levels in both *in vitro* NRAM and *ex vivo* tachypacing models, likely through an AMPK/Cx43 signaling axis.

Cannabinoids are cardioprotective with regard to arrhythmia and infarction. The synthetic cannabinoid, WIN55212-2, reduced leukocyte-dependent myocardial damage from ischemia-reperfusion injury via CB2R.(226) Furthermore, Kola *et al.* demonstrated that THC acts by

stimulating AMPK activity in the rat heart.(126) This is supported by Joyeux *et al.* who further demonstrated eCBs acting through CB2R provide cardioprotection and reduced infarct size in myocardial ischemia after damage caused by heat stress.(394) Hajrasouliha *et al.* demonstrated that CB2R signaling is likely antiarrhythmic; eCB preconditioning in the rat heart reduced infarct size and arrhythmia incidence.(395) Furthermore, CB1R is reportedly proarrhythmic during surgery, and increased eCB levels may be detrimental to cardiac function.(395, 396) However, this study did not take into account that eCB levels may be elevated as a protective response during surgery.(396)

Chapter 4 reports data suggesting that CB13 treatment does not alter chronotropy, dromotropy, or hemodynamics in the spontaneously beating rat heart. This finding remedies the gap in knowledge of the direct effects of CB13 on the intact heart, and demonstrates that CB1R/CB2R activation likely does not pathologically affect basic cardiac EP. However, CB2R has been linked to cardioprotective antiarrhythmic effects, whereas CB1R is linked to cardiodeleterious effects. (222, 309-316) Studies suggest that activation of solely CB1R may be detrimental (See Chapter 4 discussion).(195, 306) Therefore, it is possible that the lack of CB13 effects on intrinsic cardiac properties results from opposing effects of CB1R and CB2R. This is consistent with previous reports of opposing CB1R (deleterious) versus CB2R (salutary) effects as discussed in Section 6.1.2.

Atrial tachypacing is an important experimental approach to mimic AF-related remodeling. However, AF susceptibility in rat hearts is low and hard to induce. A limitation of this work is that atrial tachypacing did not consistently induce arrhythmia using the current experimental setup. The effect of CB13 on AF induction will rely on future experiments that utilize models that are more susceptible to arrhythmia initiation. For example, myocardial infarction is a risk factor for

AF.(397) The Etzion laboratory has demonstrated that LAD coronary artery ligation (a model of MI) induces AF.(320) To further extend our previous findings *ex vivo,* investigation of the effect of tachypacing on ischemic cardiomyopathy may yield novel results regarding CB13 effects on arrhythmias. CB13 demonstrated cardioprotective effects *in vitro* and *ex vivo* in tachypaced SD rat hearts. Thus, these experiments will further test CB13 on more severe cardiac disease.

Furthermore, CB13 effects could be verified using a novel *in vivo* setup with our collaborator, Dr. Yoram Etzion. The Etzion lab has recently optimized a novel method implanting a quadripolar electrode-based system in conscious rats that are subjected to continuous right atrium tachypacing.(398) The Etzion lab has found that tachypacing for greater than 48 hours increases AF substrate in healthy rats.(398) Data also show that tachypacing induces molecular similarities to those in AF-related remodeling.(398) Under these conditions which mimic human AF, the efficacy of CB13 in reducing AF substrate, and the ability to alter molecular and metabolic markers of remodeling, may be evaluated. This *in vivo* experiment could delineate the long-term effects of CB13 as a new therapeutic strategy.

Lastly, in select case studies, *Cannabis* initiated arrhythmias.(399) While low doses of *Cannabis* initiate sympathetic stimulation, high doses of *Cannabis* containing THC result in parasympathetic stimulation.(399, 400) Vagal stimulation reduces APD and shortens refractory period, predisposing atrial tissue to re-entrant mechanisms and AF initiation.(400) Vagal-stimulated AF is found in patients without structural disease. Thus, arrhythmia initiation is due to triggering events, such as drug use. For example, in one case study, the patient's underlying hypertension initiated atrial flutter and elevated sympathetic response during *cannabis* use which subsequently triggered AF.(400) While recreational *Cannabis* use may result in cardiovascular complications, concomitant health conditions and recreational use of additional drugs largely

contribute to cases of *Cannabis*-induced initiation of AF. The contradiction of cannabinoids being antiarrhythmic and pro-arrhythmic may be a combination of factors, including but not limited to, CBR affinity, dosing, cannabis usage frequency, supplementary drug use, or additional factors.(195, 222, 306, 309-316, 399, 400)

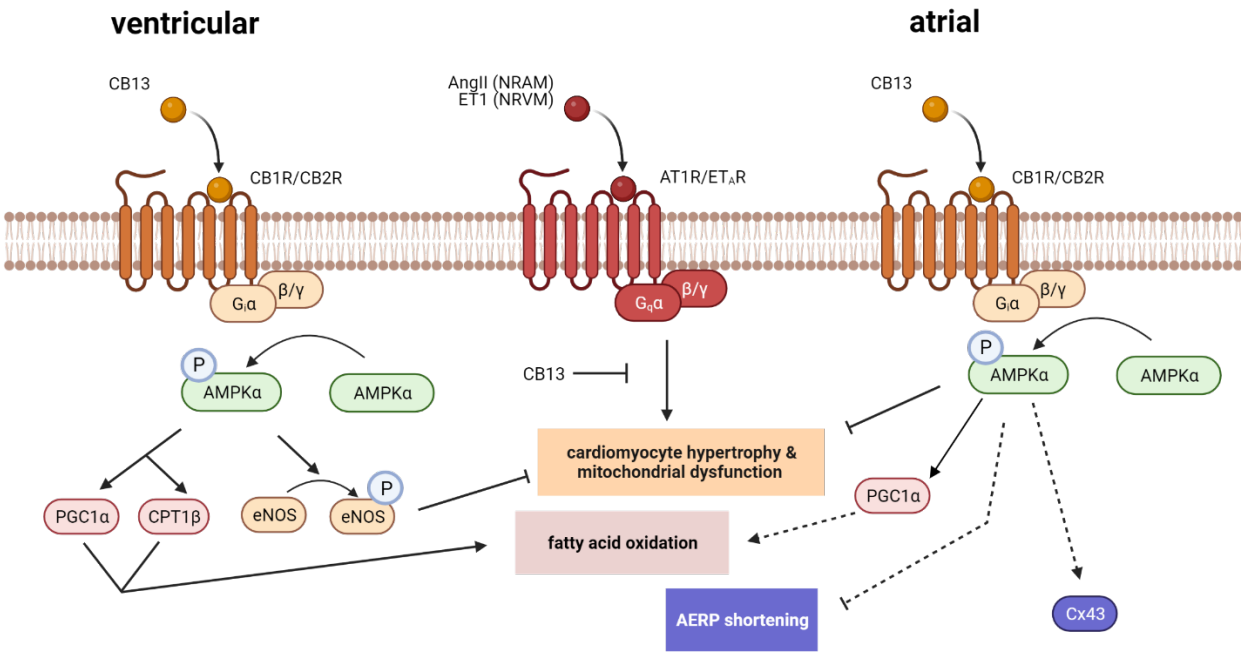

Figure 6.1. Summary Schematic. Schematic representation of putative mitochondrial and signaling events that are triggered by AngII or ET1 and the effects of cannabinoids CB13 in both ventricular and atrial cardiomyocytes. *Adapted from "GPCR Effector Pathways" template by Biorender.com (2022). Retrieved from https://app.biorender.com/biorender-templates.*

6.2. Overall Conclusion

This work establishes the foundation of CB13 as a potential therapeutic for ventricular hypertrophy and AF-related remodeling *in vitro* and *ex vivo*. Moreover, this thesis provides evidence for the protective effects of CB13 on hypertrophy, mitochondrial dysfunction and EP changes *in vitro* using NRAM and NRVM, and *ex vivo* using tachypaced SD rat hearts. Our understanding of the signaling axes between CB13/AMPK and AMPK/Cx43 is still emerging. Thus, greater understanding of these signaling pathways is necessary to conclusively link CB13 to metabolic and electrical signaling mechanisms. However, the ability to develop CB13 as a therapy for cardiovascular disease without compromising the CNS is ideal. This work has further advanced the therapeutic potential of cannabinoids, specifically CB13, for treating cardiac remodeling that results from AF and ventricular hypertrophy.

Chapter 7

Appendix

Appendix

7.1. Supplemental Data File for Chapter 3 - Activation of Cannabinoid Receptors Attenuates Endothelin-1-induced Mitochondrial Dysfunction in Neonatal Rat Ventricular Myocytes

S7.1. Optimization of working conditions for mitochondrial bioenergetics assays.

Mitochondrial bioenergetics of cardiac myocytes were assessed in the presence of glucose/pyruvate and palmitate as major substrates. It was important to first determine the optimal conditions for mitochondrial bioenergetics assays. Therefore, the glucose/pyruvate model was used to optimize cell seeding density and oligomycin concentration. Furthermore, as the maximal effective concentration of FCCP may vary depending on the different energy substrate provided (401), optimal concentrations of FCCP were ascertained for both glucose and palmitate.

Primary neonatal rat cardiac myocytes were seeded into 24-well X24 microplates with test densities: 100,000, 200,000, 300,000 and 400,000 cells/well. As shown in Figure S7.1, oxygen consumption rates (OCRs) declined with increases in cell density. In addition, Hill *et al.* detected a linear increase in OCR in neonatal rat ventricular myocytes within a range of 25,000 to 75,000 cells/well (255). Thus, OCR peaks at a seeding density of 75,000-100,000 cells/well, whereas underseeding or overseeding impacts the accuracy of OCR measurements. Here, 100,000 cells/well was chosen for future experiments.

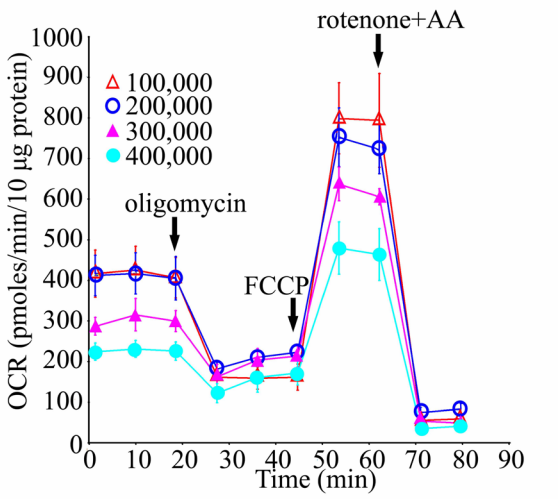

Supplemental Figure 7.1. OCR were measured using the Seahorse Bioscience XF24 analyzer in cultured neonatal rat cardiac myocytes at cell densities ranging from 100,000 to 400,000 myocytes per well. Basal OCRs were measured in media containing 10 mM glucose and 1 mM pyruvate, followed by the sequential addition of oligomycin (1 µg/mL), then FCCP (2 µM) and R/AA (rotenone, 1 µM and antimycin A, 1 µM). The results are presented as the OCR per 10 µg protein. A cell density of 100,000 myocytes per well resulted in the maximal protein-normalized OCR. n=5 replicate cultures (5 replicate wells/n).

Increasing concentrations of oligomycin were titrated with glucose/pyruvate as provided substrates. OCR plots were presented as percent values normalized to basal levels (basal OCR was set as a baseline of 100%) (Figure S7.2). Addition of increasing concentrations of oligomycin (0.5, 1.0, 5.0 and 10 µg/mL) reduced OCRs to similar degrees. A working oligomycin concentration of 1 µg/mL was selected for subsequent experiments.

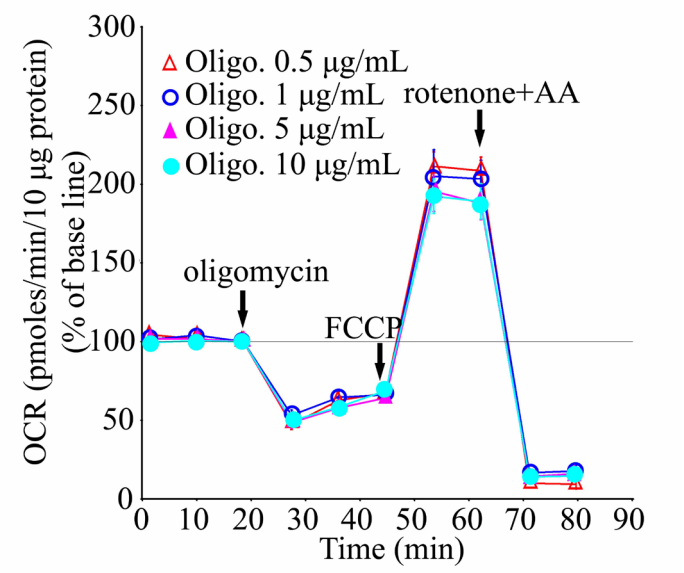

Supplemental Figure 7.2. OCRs of cultured myocytes at basal levels were measured using the Seahorse Bioscience XF24 Analyzer in media containing 10 mM glucose and 1 mM pyruvate, followed by the sequential addition of increasing concentrations of oligomycin (0.5-10 µg/mL), then FCCP (2 µM) and R/AA (rotenone, 1 µM and antimycin A, 1 µM). Results are presented as the percent values of basal OCR. There were no concentration-dependent differences in oligomycin-induced OCR reductions between groups. Oligomycin at 1 µg/mL was chosen for subsequent experiments. n=5 replicate cultures (5 replicate wells/n).

Effective concentrations of FCCP vary according to cell type and energy substrate (255, 401-403). Hence, it is important to determine the optimal concentration applicable to cardiac myocytes in the context of glucose or palmitate as substrate. Increasing concentrations of FCCP were tested in the presence of either palmitate/BSA or glucose/pyruvate. As shown in Figure S7.3A, during glucose oxidation, FCCP concentrations ranging from 1 µM to 10 µM did not generate significant differences, except perhaps only a minor increase at 2 µM. In contrast, the effect of FCCP on fatty acid oxidation was concentration-dependent, and 10 µM achieved the maximal response (Figure S7.3B). Therefore, 2 µM and 10 µM of FCCP were selected for glucose- and fatty acid-dependent OCR respectively.

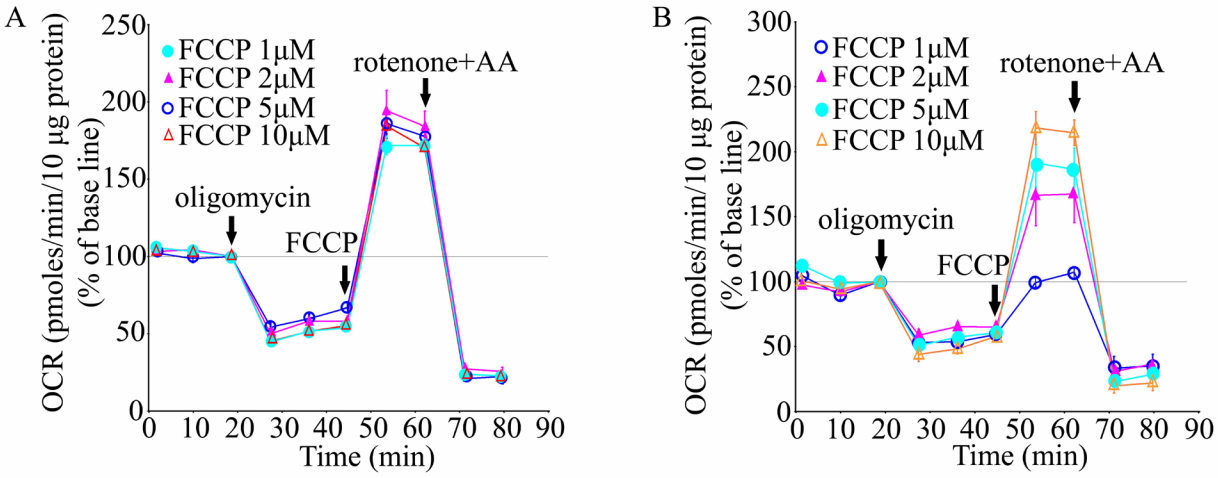

Supplemental Figure 7.3. OCRs of cultured myocytes at basal levels were measured using the Seahorse Bioscience XF24 Analyzer in media containing A) glucose (10 mM)/pyruvate (1 mM) and B) palmitate/BSA (200 µM), followed by the sequential addition of oligomycin (1 µg/mL), FCCP (1-10 µM) and R/AA (rotenone, 1 µM and antimycin A, 1 µM). Results are presented as the percent of basal OCR. When glucose/pyruvate were provided as the primary substrates, differences between groups are subtle; FCCP of 2 µM gives an apparent maximal rate of OCR. Whereas when palmitate/BSA was provided as the major substrate, FCCP at 10 µM gives a maximal response of increased OCR. n=5 replicate cultures (5 replicate wells/n).

S7.2. Determination of fatty acid oxidation-associated OCR in cultured neonatal rat cardiac myocytes.

OCR was measured using the Seahorse Bioscience XF24 analyzer to determine the capacity of mitochondrial respiration. Cultured neonatal rat cardiac myocytes were exposed to palmitate/BSA conjugates to facilitate the study of fatty acid-dependent respiration. To verify that responses were due to utilization of exogenous palmitate by mitochondria, subgroups were pretreated with etomoxir (40 μM) 15 min prior to the assay to inhibit CPT-1. As CPT-1 facilitates fatty acid transport across the mitochondrial membrane (261), etomoxir would inhibit oxidation of exogenous fatty acids. BSA, the carrier of palmitate, was injected to the cells in the presence or absence of etomoxir, and served as negative control. As shown in Figure S7.4, the addition of etomoxir dramatically inhibited palmitate-related OCR, and BSA only generated negligible OCR. These data confirm that here, oxygen consumption was due to oxidation of exogenous palmitate.

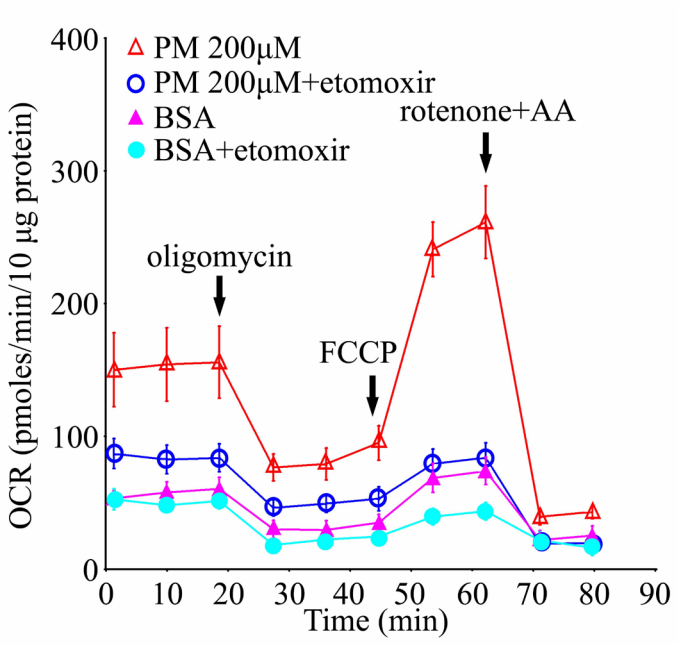

Supplemental Figure 7.4. OCRs at basal levels were measured in the Seahorse Bioscience XF24 Analyzer in cultured myocytes (100,000 cells per well) with palmitate/BSA complex (PM, 200 µM) or BSA (vehicle carrier) as the substrate, in the absence or presence of etomoxir (inhibits CPT-1 and therefore mitochondrial fatty acid uptake), followed by the sequential addition of oligomycin (1 µg/mL), FCCP (2 µM) and R/AA (rotenone, 1 µM and antimycin A, 1 µM). The difference between PM (Δ) and PM + etomoxir (○) suggests that exogenous fatty acids were utilized as substrate. n=5 replicate cultures (5 replicate wells/n).

S7.3. Determination of AMPKα1/2 knockdown in cultured neonatal rat cardiac myocytes

CB13 activated AMPKα by increasing phosphorylation at Thr172; therefore, we queried the role of AMPK in CB13-mediated mitochondrial protective effects. To ascertain the role of AMPK, neonatal rat cardiac myocytes were infected for 24 h with lentiviral vectors expressing shRNA against AMPKα_1 and α_2, followed by 72 h incubation. Degree of knockdown was confirmed by western blotting. As shown in Figure S7.5, this achieved significant, simultaneous reductions of AMPKα_1 and α_2.

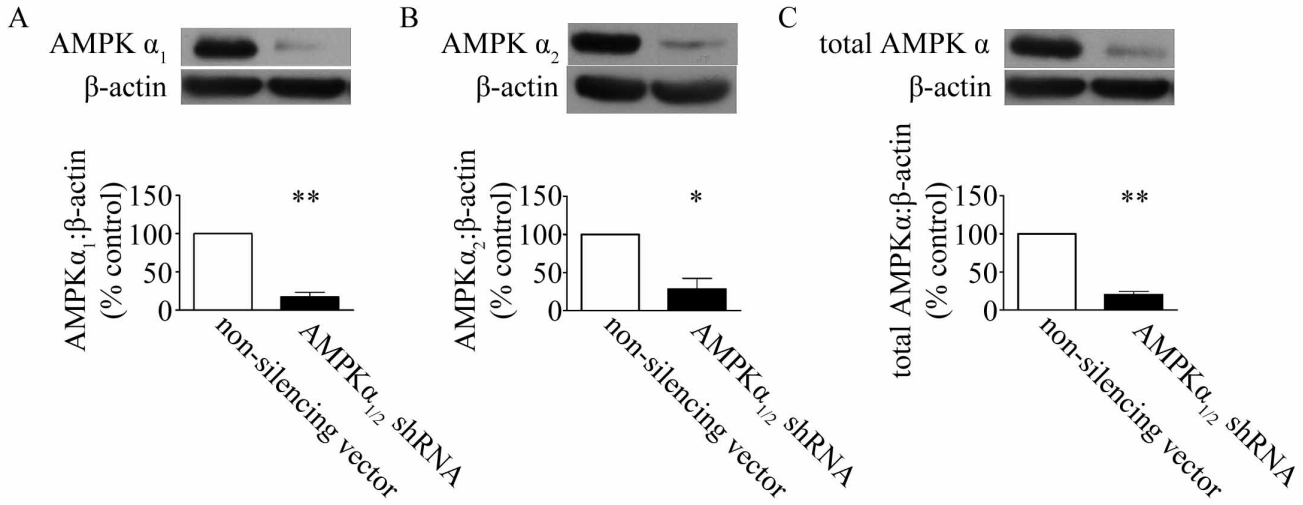

Supplemental Figure 7.5. Myocytes were infected with lentivirus carrying shRNA against AMPK α_1 and α_2 or non-silencing empty vector. 72 h post-infection, *A,* AMPKα_1, B, AMPKα_2, and C, total AMPKα were measured by conventional western blotting of total cell lysates. Results are presented as percent of normalized protein *vs.* empty vector-treated controls. n=3. *$p<0.05$ and **$p<0.01$ *vs*. non-silencing vector treated control (open bars).

S7.4. Quantification of cannabinoid receptor protein concentration in neonatal rat cardiomyocytes

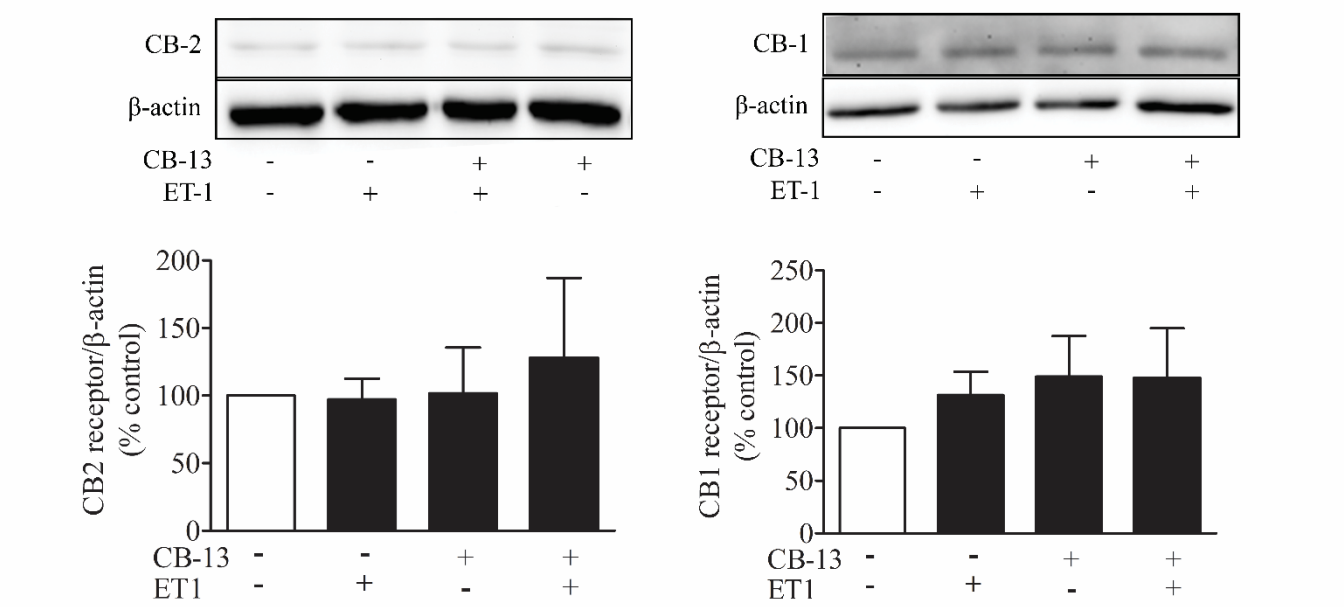

Supplemental Figure 7.6. Myocytes were exposed to ET1 (0.1 μM; 4 h) in the presence or absence of vehicle or CB13 (1 μM). *A*, representative blot, *B*, CB1R and *C*, CB2R expression following CB13 (1 μM) and ET1 (0.1 μM) treatment in neonatal rat cardiomyocytes. CB1R and CB2R levels were measured by conventional western blotting of total cell lysates and were not significantly different. n=3.

S7.5. Schematic of events as elucidated from experimental NRVM's results.

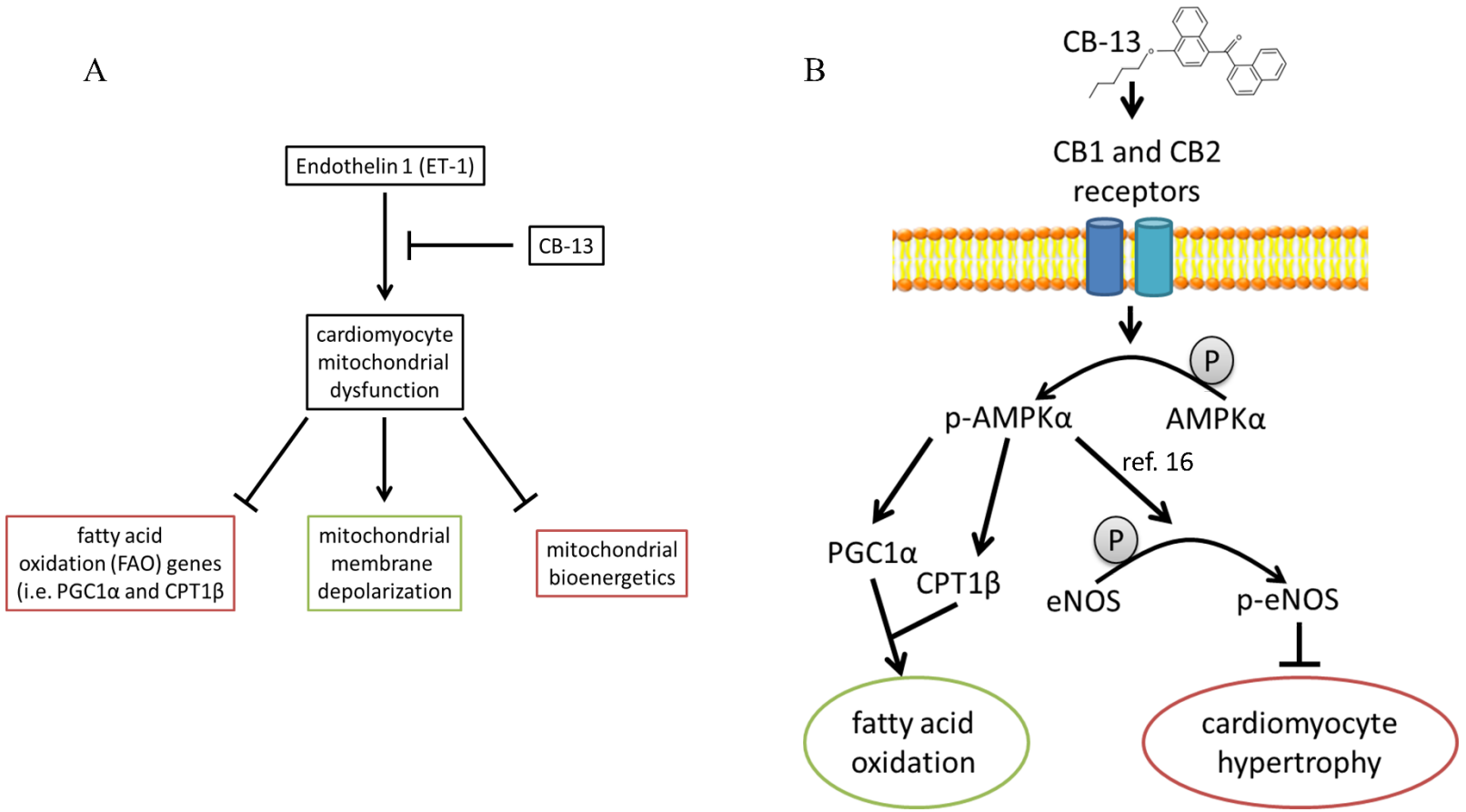

Supplemental Figure 7.7. Schematic representation of putative bioenergetic and signaling events triggered by *A,* endothelin-1 (ET-1) and *B*, CB13 in neonatal rat cardiac myocytes.

7.2. References:

1. Zhou P, Pu WT. Recounting Cardiac Cellular Composition. Circ Res. 2016;118(3):368-70.

2. Pinnell J. TS, Howell S. Cardiac muscle physiology. Continuing Education in Anaesthesia Critical Care & Pain. 2007;7(3):85-8.

3. Filgueiras-Rama D, Jalife J. Structural and Functional Bases of Cardiac Fibrillation. Differences and Similarities between Atria and Ventricles. JACC Clin Electrophysiol. 2016;2(1):1-3.

4. Pinnell J, Turner S, Howell S. Cardiac muscle physiology. Continuing Education in Anaesthesia Critical Care & Pain. 2007;7(3):85-8.

5. Eisner DA, Caldwell JL, Kistamas K, Trafford AW. Calcium and Excitation-Contraction Coupling in the Heart. Circ Res. 2017;121(2):181-95.

6. Ferrier GR, Howlett SE. Cardiac excitation-contraction coupling: role of membrane potential in regulation of contraction. Am J Physiol Heart Circ Physiol. 2001;280(5):H1928-44.

7. Bootman MD, Smyrnias I, Thul R, Coombes S, Roderick HL. Atrial cardiomyocyte calcium signalling. Biochim Biophys Acta. 2011;1813(5):922-34.

8. Brandenburg S, Arakel EC, Schwappach B, Lehnart SE. The molecular and functional identities of atrial cardiomyocytes in health and disease. Biochim Biophys Acta. 2016;1863(7 Pt B):1882-93.

9. Litvinukova M, Talavera-Lopez C, Maatz H, Reichart D, Worth CL, Lindberg EL, et al. Cells of the adult human heart. Nature. 2020;588(7838):466-72.

10. Pasek M, Brette F, Nelson A, Pearce C, Qaiser A, Christe G, et al. Quantification of t-tubule area and protein distribution in rat cardiac ventricular myocytes. Prog Biophys Mol Biol. 2008;96(1-3):244-57.

11. Smyrnias I, Mair W, Harzheim D, Walker SA, Roderick HL, Bootman MD. Comparison of the T-tubule system in adult rat ventricular and atrial myocytes, and its role in excitation-contraction coupling and inotropic stimulation. Cell Calcium. 2010;47(3):210-23.

12. Orchard C, Brette F. t-Tubules and sarcoplasmic reticulum function in cardiac ventricular myocytes. Cardiovasc Res. 2008;77(2):237-44.

13. Shaffer F, McCraty R, Zerr CL. A healthy heart is not a metronome: an integrative review of the heart's anatomy and heart rate variability. Front Psychol. 2014;5:1040.

14. Kolwicz SC, Jr., Purohit S, Tian R. Cardiac metabolism and its interactions with contraction, growth, and survival of cardiomyocytes. Circ Res. 2013;113(5):603-16.

15. Brown DA, Perry JB, Allen ME, Sabbah HN, Stauffer BL, Shaikh SR, et al. Mitochondrial function as a therapeutic target in heart failure. Nature Reviews Cardiology. 2017;14(4):238-50.

16. Barger PM, Kelly DP. Fatty acid utilization in the hypertrophied and failing heart: molecular regulatory mechanisms. Am J Med Sci. 1999;318(1):36-42.

17. Barth AS, Merk S, Arnoldi E, Zwermann L, Kloos P, Gebauer M, et al. Reprogramming of the human atrial transcriptome in permanent atrial fibrillation: expression of a ventricular-like genomic signature. Circ Res. 2005;96(9):1022-9.

18. Weil BR, Ozcan C. Cardiomyocyte Remodeling in Atrial Fibrillation and Hibernating Myocardium: Shared Pathophysiologic Traits Identify Novel Treatment Strategies? Biomed Res Int. 2015;2015:587361.

19. Allard MF, Schonekess BO, Henning SL, English DR, Lopaschuk GD. Contribution of oxidative metabolism and glycolysis to ATP production in hypertrophied hearts. Am J Physiol. 1994;267(2 Pt 2):H742-50.

20. Akhmedov AT, Marin-Garcia J. Mitochondrial DNA maintenance: an appraisal. Mol Cell Biochem. 2015;409(1-2):283-305.

21. Chess DJ, Khairallah RJ, O'Shea KM, Xu W, Stanley WC. A high-fat diet increases adiposity but maintains mitochondrial oxidative enzymes without affecting development of heart failure with pressure overload. Am J Physiol Heart Circ Physiol. 2009;297(5):H1585-93.

22. Gupta A, Akki A, Wang Y, Leppo MK, Chacko VP, Foster DB, et al. Creatine kinase-mediated improvement of function in failing mouse hearts provides causal evidence the failing heart is energy starved. J Clin Invest. 2012;122(1):291-302.

23. Nolfi-Donegan D, Braganza A, Shiva S. Mitochondrial electron transport chain: Oxidative phosphorylation, oxidant production, and methods of measurement. Redox Biol. 2020;37:101674.

24. Brown DA, O'Rourke B. Cardiac mitochondria and arrhythmias. Cardiovasc Res. 2010;88(2):241-9.

25. Urbani A, Prosdocimi E, Carrer A, Checchetto V, Szabo I. Mitochondrial Ion Channels of the Inner Membrane and Their Regulation in Cell Death Signaling. Front Cell Dev Biol. 2020;8:620081.

26. Baines AJ, Pinder JC. The spectrin-associated cytoskeleton in mammalian heart. Front Biosci. 2005;10:3020-33.

27. Wang YL, Zhao CX, Jing YL, Zheng HP, Cui GJ, Zhang SS. [The protective effects of ischemic preconditioning on the kidney injury following with ischemia/reperfusion of limbs and the possible mechanisms]. Zhongguo Ying Yong Sheng Li Xue Za Zhi. 2009;25(4):492-5.

28. Wang Y, Huang ZJ, Song JQ, Wu YN, Liu YX. [Cardioprotection of ramipril and BQ-123 against myocardial ischemia/reperfusion injury in vivo in rats]. Zhongguo Ying Yong Sheng Li Xue Za Zhi. 2009;25(4):478-82.

29. Piot C, Croisille P, Staat P, Thibault H, Rioufol G, Mewton N, et al. Effect of cyclosporine on reperfusion injury in acute myocardial infarction. N Engl J Med. 2008;359(5):473-81.

30. Javadov S, Karmazyn M, Escobales N. Mitochondrial permeability transition pore opening as a promising therapeutic target in cardiac diseases. J Pharmacol Exp Ther. 2009;330(3):670-8.

31. Shaheen M, Cheema Y, Shahbaz AU, Bhattacharya SK, Weber KT. Intracellular calcium overloading and oxidative stress in cardiomyocyte necrosis via a mitochondriocentric signal-transducer-effector pathway. Exp Clin Cardiol. 2011;16(4):109-15.

32. Beavis AD. Properties of the inner membrane anion channel in intact mitochondria. J Bioenerg Biomembr. 1992;24(1):77-90.

33. Li X, Liu J, Lu Q, Ren D, Sun X, Rousselle T, et al. AMPK: a therapeutic target of heart failure-not only metabolism regulation. Biosci Rep. 2019;39(1).

34. Brown SM, Larsen NK, Thankam FG, Agrawal DK. Regulatory role of cardiomyocyte metabolism via AMPK activation in modulating atrial structural, contractile, and electrical properties following atrial fibrillation. Can J Physiol Pharmacol. 2021;99(1):36-41.

35. Lopaschuk GD, Karwi QG, Tian R, Wende AR, Abel ED. Cardiac Energy Metabolism in Heart Failure. Circ Res. 2021;128(10):1487-513.

36. Li Y, Chen C, Yao F, Su Q, Liu D, Xue R, et al. AMPK inhibits cardiac hypertrophy by promoting autophagy via mTORC1. Arch Biochem Biophys. 2014;558:79-86.

37. Schips TG, Wietelmann A, Hohn K, Schimanski S, Walther P, Braun T, et al. FoxO3 induces reversible cardiac atrophy and autophagy in a transgenic mouse model. Cardiovasc Res. 2011;91(4):587-97.

38. Ozcan C, Dixit G, Li Z. Activation of AMP-Activated Protein Kinases Prevents Atrial Fibrillation. J Cardiovasc Transl Res. 2020.

39. Allessie MA, Boyden PA, Camm AJ, Kleber AG, Lab MJ, Legato MJ, et al. Pathophysiology and prevention of atrial fibrillation. Circulation. 2001;103(5):769-77.

40. Rudy Y. Molecular basis of cardiac action potential repolarization. Ann N Y Acad Sci. 2008;1123:113-8.

41. Nerbonne JM, Kass RS. Molecular physiology of cardiac repolarization. Physiol Rev. 2005;85(4):1205-53.

42. Tomaselli GF, Beuckelmann DJ, Calkins HG, Berger RD, Kessler PD, Lawrence JH, et al. Sudden cardiac death in heart failure. The role of abnormal repolarization. Circulation. 1994;90(5):2534-9.

43. Fatkin D, Otway R, Vandenberg JI. Genes and atrial fibrillation: a new look at an old problem. Circulation. 2007;116(7):782-92.

44. Santana LF, Cheng EP, Lederer WJ. How does the shape of the cardiac action potential control calcium signaling and contraction in the heart? J Mol Cell Cardiol. 2010;49(6):901-3.

45. Shiroshita-Takeshita A, Brundel BJ, Nattel S. Atrial fibrillation: basic mechanisms, remodeling and triggers. J Interv Card Electrophysiol. 2005;13(3):181-93.

46. Pandit SV. 31 - Ionic Mechanisms of Atrial Action Potentials. In: Zipes DP, Jalife J, Stevenson WG, editors. Cardiac Electrophysiology: From Cell to Bedside (Seventh Edition): Elsevier; 2018. p. 293-303.

47. King JH, Huang CL, Fraser JA. Determinants of myocardial conduction velocity: implications for arrhythmogenesis. Front Physiol. 2013;4:154.

48. Azevedo PS, Polegato BF, Minicucci MF, Paiva SA, Zornoff LA. Cardiac Remodeling: Concepts, Clinical Impact, Pathophysiological Mechanisms and Pharmacologic Treatment. Arq Bras Cardiol. 2016;106(1):62-9.

49. Burchfield JS, Xie M, Hill JA. Pathological ventricular remodeling: mechanisms: part 1 of 2. Circulation. 2013;128(4):388-400.

50. Nattel S, Burstein B, Dobrev D. Atrial remodeling and atrial fibrillation: mechanisms and implications. Circ Arrhythm Electrophysiol. 2008;1(1):62-73.

51. Dorn GW, 2nd. The fuzzy logic of physiological cardiac hypertrophy. Hypertension. 2007;49(5):962-70.

52. Wolf PA, Mitchell JB, Baker CS, Kannel WB, D'Agostino RB. Impact of atrial fibrillation on mortality, stroke, and medical costs. Arch Intern Med. 1998;158(3):229-34.

53. Wakili R, Voigt N, Kaab S, Dobrev D, Nattel S. Recent advances in the molecular pathophysiology of atrial fibrillation. J Clin Invest. 2011;121(8):2955-68.

54. Nattel S, Dobrev D. Controversies About Atrial Fibrillation Mechanisms: Aiming for Order in Chaos and Whether it Matters. Circ Res. 2017;120(9):1396-8.

55. Anter E, Di Biase L, Contreras-Valdes FM, Gianni C, Mohanty S, Tschabrunn CM, et al. Atrial Substrate and Triggers of Paroxysmal Atrial Fibrillation in Patients With Obstructive Sleep Apnea. Circ Arrhythm Electrophysiol. 2017;10(11):e005407.

56. Ehrlich JR, Nattel S, Hohnloser SH. Atrial fibrillation and congestive heart failure: specific considerations at the intersection of two common and important cardiac disease sets. J Cardiovasc Electrophysiol. 2002;13(4):399-405.

57. Hayashi K, Tada H, Yamagishi M. The genetics of atrial fibrillation. Curr Opin Cardiol. 2017;32(1):10-6.

58. Nattel S, Harada M. Atrial remodeling and atrial fibrillation: recent advances and translational perspectives. J Am Coll Cardiol. 2014;63(22):2335-45.

59. Iwasaki YK, Nishida K, Kato T, Nattel S. Atrial fibrillation pathophysiology: implications for management. Circulation. 2011;124(20):2264-74.

60. Heeringa J, van der Kuip DA, Hofman A, Kors JA, van Herpen G, Stricker BH, et al. Prevalence, incidence and lifetime risk of atrial fibrillation: the Rotterdam study. Eur Heart J. 2006;27(8):949-53.

61. Foundation HaS. Heart Conditions - Atrial Fibrillation [Website]. 2019 [Available from: https://www.heartandstroke.ca/heart/conditions/atrial-fibrillation.

62. Miyasaka Y, Barnes ME, Gersh BJ, Cha SS, Bailey KR, Abhayaratna WP, et al. Secular trends in incidence of atrial fibrillation in Olmsted County, Minnesota, 1980 to 2000, and implications on the projections for future prevalence. Circulation. 2006;114(2):119-25.

63. January CT, Wann LS, Alpert JS, Calkins H, Cigarroa JE, Cleveland JC, Jr., et al. 2014 AHA/ACC/HRS guideline for the management of patients with atrial fibrillation: executive summary: a report of the American College of Cardiology/American Heart Association Task Force on practice guidelines and the Heart Rhythm Society. Circulation. 2014;130(23):2071-104.

64. Khairy P, Nattel S. New insights into the mechanisms and management of atrial fibrillation. CMAJ. 2002;167(9):1012-20.

65. Verma A, Cairns JA, Mitchell LB, Macle L, Stiell IG, Gladstone D, et al. 2014 focused update of the Canadian Cardiovascular Society Guidelines for the management of atrial fibrillation. Can J Cardiol. 2014;30(10):1114-30.

66. Nattel S. New ideas about atrial fibrillation 50 years on. Nature. 2002;415(6868):219-26.

67. Chiba T, Kondo N, Takahara A. Influences of rapid pacing-induced electrical remodeling on pharmacological manipulation of the atrial refractoriness in rabbits. J Pharmacol Sci. 2016;130(3):170-6.

68. Kim SJ, Choisy SC, Barman P, Zhang H, Hancox JC, Jones SA, et al. Atrial remodeling and the substrate for atrial fibrillation in rat hearts with elevated afterload. Circ Arrhythm Electrophysiol. 2011;4(5):761-9.

69. Eckstein J, Verheule S, de Groot NM, Allessie M, Schotten U. Mechanisms of perpetuation of atrial fibrillation in chronically dilated atria. Prog Biophys Mol Biol. 2008;97(2-3):435-51.

70. Dzeshka MS, Lip GY, Snezhitskiy V, Shantsila E. Cardiac Fibrosis in Patients With Atrial Fibrillation: Mechanisms and Clinical Implications. J Am Coll Cardiol. 2015;66(8):943-59.

71. Dobrev D, Carlsson L, Nattel S. Novel molecular targets for atrial fibrillation therapy. Nat Rev Drug Discov. 2012;11(4):275-91.

72. Rucker-Martin C, Pecker F, Godreau D, Hatem SN. Dedifferentiation of atrial myocytes during atrial fibrillation: role of fibroblast proliferation in vitro. Cardiovasc Res. 2002;55(1):38-52.

73. Aime-Sempe C, Folliguet T, Rucker-Martin C, Krajewska M, Krajewska S, Heimburger M, et al. Myocardial cell death in fibrillating and dilated human right atria. J Am Coll Cardiol. 1999;34(5):1577-86.

74. Xu J, Cui G, Esmailian F, Plunkett M, Marelli D, Ardehali A, et al. Atrial extracellular matrix remodeling and the maintenance of atrial fibrillation. Circulation. 2004;109(3):363-8.

75. Verheule S, Tuyls E, van Hunnik A, Kuiper M, Schotten U, Allessie M. Fibrillatory conduction in the atrial free walls of goats in persistent and permanent atrial fibrillation. Circ Arrhythm Electrophysiol. 2010;3(6):590-9.

76. Deroubaix E, Folliguet T, Rucker-Martin C, Dinanian S, Boixel C, Validire P, et al. Moderate and chronic hemodynamic overload of sheep atria induces reversible cellular electrophysiologic abnormalities and atrial vulnerability. J Am Coll Cardiol. 2004;44(9):1918-26.

77. Woods CE, Olgin J. Atrial fibrillation therapy now and in the future: drugs, biologicals, and ablation. Circ Res. 2014;114(9):1532-46.

78. Heijman J, Voigt N, Nattel S, Dobrev D. Cellular and molecular electrophysiology of atrial fibrillation initiation, maintenance, and progression. Circ Res. 2014;114(9):1483-99.

79. Clauss S, Bleyer C, Schuttler D, Tomsits P, Renner S, Klymiuk N, et al. Animal models of arrhythmia: classic electrophysiology to genetically modified large animals. Nat Rev Cardiol. 2019;16:457-75.

80. Waks JW, Josephson ME. Mechanisms of Atrial Fibrillation - Reentry, Rotors and Reality. Arrhythm Electrophysiol Rev. 2014;3(2):90-100.

81. Finet JE, Rosenbaum DS, Donahue JK. Information learned from animal models of atrial fibrillation. Cardiol Clin. 2009;27(1):45-54, viii.

82. Comtois P, Kneller J, Nattel S. Of circles and spirals: bridging the gap between the leading circle and spiral wave concepts of cardiac reentry. Europace. 2005;7 Suppl 2:10-20.

83. Li D, Fareh S, Leung TK, Nattel S. Promotion of atrial fibrillation by heart failure in dogs: atrial remodeling of a different sort. Circulation. 1999;100(1):87-95.

84. Haissaguerre M, Jais P, Shah DC, Takahashi A, Hocini M, Quiniou G, et al. Spontaneous initiation of atrial fibrillation by ectopic beats originating in the pulmonary veins. N Engl J Med. 1998;339(10):659-66.

85. Nattel S. Basic electrophysiology of the pulmonary veins and their role in atrial fibrillation: precipitators, perpetuators, and perplexers. J Cardiovasc Electrophysiol. 2003;14(12):1372-5.

86. Kalifa J, Jalife J, Zaitsev AV, Bagwe S, Warren M, Moreno J, et al. Intra-atrial pressure increases rate and organization of waves emanating from the superior pulmonary veins during atrial fibrillation. Circulation. 2003;108(6):668-71.

87. Shinagawa K, Derakhchan K, Nattel S. Pharmacological prevention of atrial tachycardia induced atrial remodeling as a potential therapeutic strategy. Pacing Clin Electrophysiol. 2003;26(3):752-64.

88. Daoud EG, Bogun F, Goyal R, Harvey M, Man KC, Strickberger SA, et al. Effect of atrial fibrillation on atrial refractoriness in humans. Circulation. 1996;94(7):1600-6.

89. Gaspo R, Bosch RF, Talajic M, Nattel S. Functional mechanisms underlying tachycardia-induced sustained atrial fibrillation in a chronic dog model. Circulation. 1997;96(11):4027-35.

90. Elvan A, Wylie K, Zipes DP. Pacing-induced chronic atrial fibrillation impairs sinus node function in dogs. Electrophysiological remodeling. Circulation. 1996;94(11):2953-60.

91. Wijffels MC, Kirchhof CJ, Dorland R, Allessie MA. Atrial fibrillation begets atrial fibrillation. A study in awake chronically instrumented goats. Circulation. 1995;92(7):1954-68.

92. Ausma J, van der Velden HM, Lenders MH, van Ankeren EP, Jongsma HJ, Ramaekers FC, et al. Reverse structural and gap-junctional remodeling after prolonged atrial fibrillation in the goat. Circulation. 2003;107(15):2051-8.

93. Fozzard HA. Afterdepolarizations and triggered activity. Basic Res Cardiol. 1992;87 Suppl 2:105-13.

94. Tsai CF, Tai CT, Hsieh MH, Lin WS, Yu WC, Ueng KC, et al. Initiation of atrial fibrillation by ectopic beats originating from the superior vena cava: electrophysiological characteristics and results of radiofrequency ablation. Circulation. 2000;102(1):67-74.

95. Chen YJ, Chen SA, Chen YC, Yeh HI, Chang MS, Lin CI. Electrophysiology of single cardiomyocytes isolated from rabbit pulmonary veins: implication in initiation of focal atrial fibrillation. Basic Res Cardiol. 2002;97(1):26-34.

96. Chen YC, Chen SA, Chen YJ, Chang MS, Chan P, Lin CI. Effects of thyroid hormone on the arrhythmogenic activity of pulmonary vein cardiomyocytes. J Am Coll Cardiol. 2002;39(2):366-72.

97. Chen YJ, Chen SA, Chen YC, Yeh HI, Chan P, Chang MS, et al. Effects of rapid atrial pacing on the arrhythmogenic activity of single cardiomyocytes from pulmonary veins: implication in initiation of atrial fibrillation. Circulation. 2001;104(23):2849-54.

98. Brundel BJ, Henning RH, Kampinga HH, Van Gelder IC, Crijns HJ. Molecular mechanisms of remodeling in human atrial fibrillation. Cardiovasc Res. 2002;54(2):315-24.

99. Morillo CA, Klein GJ, Jones DL, Guiraudon CM. Chronic rapid atrial pacing. Structural, functional, and electrophysiological characteristics of a new model of sustained atrial fibrillation. Circulation. 1995;91(5):1588-95.

100. Grandi E, Pandit SV, Voigt N, Workman AJ, Dobrev D, Jalife J, et al. Human atrial action potential and Ca2+ model: sinus rhythm and chronic atrial fibrillation. Circ Res. 2011;109(9):1055-66.

101. Burstein B, Nattel S. Atrial fibrosis: mechanisms and clinical relevance in atrial fibrillation. J Am Coll Cardiol. 2008;51(8):802-9.

102. Hunyady L, Catt KJ. Pleiotropic AT1 receptor signaling pathways mediating physiological and pathogenic actions of angiotensin II. Mol Endocrinol. 2006;20(5):953-70.

103. Shinagawa K, Shi YF, Tardif JC, Leung TK, Nattel S. Dynamic nature of atrial fibrillation substrate during development and reversal of heart failure in dogs. Circulation. 2002;105(22):2672-8.

104. Nattel S. Atrial electrophysiological remodeling caused by rapid atrial activation: underlying mechanisms and clinical relevance to atrial fibrillation. Cardiovasc Res. 1999;42(2):298-308.

105. Sun H, Chartier D, Leblanc N, Nattel S. Intracellular calcium changes and tachycardia-induced contractile dysfunction in canine atrial myocytes. Cardiovasc Res. 2001;49(4):751-61.

106. Yue L, Melnyk P, Gaspo R, Wang Z, Nattel S. Molecular mechanisms underlying ionic remodeling in a dog model of atrial fibrillation. Circ Res. 1999;84(7):776-84.

107. Yue L, Feng J, Gaspo R, Li GR, Wang Z, Nattel S. Ionic remodeling underlying action potential changes in a canine model of atrial fibrillation. Circ Res. 1997;81(4):512-25.

108. Gaspo R, Bosch RF, Bou-Abboud E, Nattel S. Tachycardia-induced changes in Na+ current in a chronic dog model of atrial fibrillation. Circ Res. 1997;81(6):1045-52.

109. Grandi E, Dobrev D, Heijman J. Computational modeling: What does it tell us about atrial fibrillation therapy? Int J Cardiol. 2019.

110. Yagi T, Pu J, Chandra P, Hara M, Danilo P, Jr., Rosen MR, et al. Density and function of inward currents in right atrial cells from chronically fibrillating canine atria. Cardiovasc Res. 2002;54(2):405-15.

111. Cha TJ, Ehrlich JR, Zhang L, Nattel S. Atrial ionic remodeling induced by atrial tachycardia in the presence of congestive heart failure. Circulation. 2004;110(12):1520-6.

112. Ehrlich JR, Cha TJ, Zhang L, Chartier D, Villeneuve L, Hebert TE, et al. Characterization of a hyperpolarization-activated time-dependent potassium current in canine cardiomyocytes from pulmonary vein myocardial sleeves and left atrium. J Physiol. 2004;557(Pt 2):583-97.

113. Kato T, Iwasaki YK, Nattel S. Connexins and atrial fibrillation: filling in the gaps. Circulation. 2012;125(2):203-6.

114. Severs NJ, Bruce AF, Dupont E, Rothery S. Remodelling of gap junctions and connexin expression in diseased myocardium. Cardiovasc Res. 2008;80(1):9-19.

115. Akar FG, Nass RD, Hahn S, Cingolani E, Shah M, Hesketh GG, et al. Dynamic changes in conduction velocity and gap junction properties during development of pacing-induced heart failure. Am J Physiol Heart Circ. 2007;293(2):H1223-H30.

116. Yan J, Kong W, Zhang Q, Beyer EC, Walcott G, Fast VG, et al. c-Jun N-terminal kinase activation contributes to reduced connexin43 and development of atrial arrhythmias. Cardiovasc Res. 2013;97(3):589-97.

117. Ozcan C, Battaglia E, Young R, Suzuki G. LKB1 knockout mouse develops spontaneous atrial fibrillation and provides mechanistic insights into human disease process. J Am Heart Assoc. 2015;4(3):e001733.

118. Igarashi T, Finet JE, Takeuchi A, Fujino Y, Strom M, Greener ID, et al. Connexin gene transfer preserves conduction velocity and prevents atrial fibrillation. Circulation. 2012;125(2):216-25.

119. Lin CC, Lin JL, Lin CS, Tsai MC, Su MJ, Lai LP, et al. Activation of the calcineurin-nuclear factor of activated T-cell signal transduction pathway in atrial fibrillation. Chest. 2004;126(6):1926-32.

120. Kim GE, Ross JL, Xie C, Su KN, Zaha VG, Wu X, et al. LKB1 deletion causes early changes in atrial channel expression and electrophysiology prior to atrial fibrillation. Cardiovasc Res. 2015;108(1):197-208.

121. Harada M, Tadevosyan A, Qi X, Xiao J, Liu T, Voigt N, et al. Atrial Fibrillation Activates AMP-Dependent Protein Kinase and its Regulation of Cellular Calcium Handling: Potential Role in Metabolic Adaptation and Prevention of Progression. J Am Coll Cardiol. 2015;66(1):47-58.

122. Mummidi S, Das NA, Carpenter AJ, Kandikattu H, Krenz M, Siebenlist U, et al. Metformin inhibits aldosterone-induced cardiac fibroblast activation, migration and proliferation in vitro, and reverses aldosterone+salt-induced cardiac fibrosis in vivo. J Mol Cell Cardiol. 2016;98:95-102.

123. Tabony AM, Yoshida T, Galvez S, Higashi Y, Sukhanov S, Chandrasekar B, et al. Angiotensin II upregulates protein phosphatase 2Calpha and inhibits AMP-activated protein kinase signaling and energy balance leading to skeletal muscle wasting. Hypertension. 2011;58(4):643-9.

124. Qiu J, Zhou S, Liu Q. Phosphorylated AMP-activated protein kinase slows down the atrial fibrillation progression by activating Connexin43. Int J Cardiol. 2016;208:56-7.

125. Lu Y, Akinwumi BC, Shao Z, Anderson HD. Ligand activation of cannabinoid receptors attenuates hypertrophy of neonatal rat cardiomyocytes. J Cardiovasc Pharmacol. 2014;64(5):420-30.

126. Kola B, Hubina E, Tucci SA, Kirkham TC, Garcia EA, Mitchell SE, et al. Cannabinoids and ghrelin have both central and peripheral metabolic and cardiac effects via AMP-activated protein kinase. J Biol Chem. 2005;280(26):25196-201.

127. Gradman AH, Alfayoumi F. From left ventricular hypertrophy to congestive heart failure: management of hypertensive heart disease. Prog Cardiovasc Dis. 2006;48(5):326-41.

128. Report from the Canadian Chronic Disease Surveillance System: Heart Disease in Canada, 2018: Public Health Agency of Canada; 2018 [1/25/2022]. Available from: https://www.canada.ca/en/public-health/services/publications/diseases-conditions/report-heart-disease-Canada-2018.html.

129. Yildiz M, Oktay AA, Stewart MH, Milani RV, Ventura HO, Lavie CJ. Left ventricular hypertrophy and hypertension. Prog Cardiovasc Dis. 2020;63(1):10-21.

130. Tham YK, Bernardo BC, Ooi JY, Weeks KL, McMullen JR. Pathophysiology of cardiac hypertrophy and heart failure: signaling pathways and novel therapeutic targets. Arch Toxicol. 2015;89(9):1401-38.

131. Gosse P. Left ventricular hypertrophy as a predictor of cardiovascular risk. J Hypertens Suppl. 2005;23(1):S27-33.

132. Swynghedauw B. Molecular mechanisms of myocardial remodeling. Physiol Rev. 1999;79(1):215-62.

133. Kamo T, Akazawa H, Komuro I. Cardiac nonmyocytes in the hub of cardiac hypertrophy. Circ Res. 2015;117(1):89-98.

134. Gonzalez A, Ravassa S, Lopez B, Moreno MU, Beaumont J, San Jose G, et al. Myocardial Remodeling in Hypertension. Hypertension. 2018;72(3):549-58.

135. McLenachan JM, Henderson E, Morris KI, Dargie HJ. Ventricular arrhythmias in patients with hypertensive left ventricular hypertrophy. N Engl J Med. 1987;317(13):787-92.

136. McMaster WG, Kirabo A, Madhur MS, Harrison DG. Inflammation, immunity, and hypertensive end-organ damage. Circ Res. 2015;116(6):1022-33.

137. Zhan H, Xia L. Excitation-contraction coupling between human atrial myocytes with fibroblasts and stretch activated channel current: a simulation study. Comput Math Methods Med. 2013;2013:238676.

138. Chrispin J, Jain A, Soliman EZ, Guallar E, Alonso A, Heckbert SR, et al. Association of electrocardiographic and imaging surrogates of left ventricular hypertrophy with incident atrial fibrillation: MESA (Multi-Ethnic Study of Atherosclerosis). J Am Coll Cardiol. 2014;63(19):2007-13.

139. Okin PM, Wachtell K, Devereux RB, Harris KE, Jern S, Kjeldsen SE, et al. Regression of electrocardiographic left ventricular hypertrophy and decreased incidence of new-onset atrial fibrillation in patients with hypertension. JAMA. 2006;296(10):1242-8.

140. Bernardo BC, Weeks KL, Pretorius L, McMullen JR. Molecular distinction between physiological and pathological cardiac hypertrophy: experimental findings and therapeutic strategies. Pharmacol Ther. 2010;128(1):191-227.

141. Doenst T, Nguyen TD, Abel ED. Cardiac metabolism in heart failure: implications beyond ATP production. Circ Res. 2013;113(6):709-24.

142. Chan AY, Dolinsky VW, Soltys CL, Viollet B, Baksh S, Light PE, et al. Resveratrol inhibits cardiac hypertrophy via AMP-activated protein kinase and Akt. J Biol Chem. 2008;283(35):24194-201.

143. Li HL, Yin R, Chen D, Liu D, Wang D, Yang Q, et al. Long-term activation of adenosine monophosphate-activated protein kinase attenuates pressure-overload-induced cardiac hypertrophy. J Cell Biochem. 2007;100(5):1086-99.

144. Zhang P, Hu X, Xu X, Fassett J, Zhu G, Viollet B, et al. AMP activated protein kinase-alpha2 deficiency exacerbates pressure-overload-induced left ventricular hypertrophy and dysfunction in mice. Hypertension. 2008;52(5):918-24.

145. Anderson ME, Brown JH, Bers DM. CaMKII in myocardial hypertrophy and heart failure. J Mol Cell Cardiol. 2011;51(4):468-73.

146. Li D, Benardeau A, Nattel S. Contrasting efficacy of dofetilide in differing experimental models of atrial fibrillation. Circulation. 2000;102(1):104-12.

147. Courtemanche M, Ramirez RJ, Nattel S. Ionic targets for drug therapy and atrial fibrillation-induced electrical remodeling: insights from a mathematical model. Cardiovasc Res. 1999;42(2):477-89.

148. Heijman J, Algalarrondo V, Voigt N, Melka J, Wehrens XH, Dobrev D, et al. The value of basic research insights into atrial fibrillation mechanisms as a guide to therapeutic innovation: a critical analysis. Cardiovasc Res. 2016;109(4):467-79.

149. Wijesurendra RS, Liu A, Eichhorn C, Ariga R, Levelt E, Clarke WT, et al. Lone Atrial Fibrillation Is Associated With Impaired Left Ventricular Energetics That Persists Despite Successful Catheter Ablation. Circulation. 2016;134(15):1068-81.

150. Lau DH, Nattel S, Kalman JM, Sanders P. Modifiable Risk Factors and Atrial Fibrillation. Circulation. 2017;136(6):583-96.

151. Pathak R, Lau DH, Mahajan R, Sanders P. Structural and Functional Remodeling of the Left Atrium: Clinical and Therapeutic Implications for Atrial Fibrillation. J Atr Fibrillation. 2013;6(4):986.

152. Cho HC, Marban E. Biological therapies for cardiac arrhythmias: can genes and cells replace drugs and devices? Circ Res. 2010;106(4):674-85.

153. Sardar MR, Saeed W, Kowey PR. Antiarrhythmic Drug Therapy for Atrial Fibrillation. Heart Fail Clin. 2016;12(2):205-21.

154. Tieleman RG, De Langen C, Van Gelder IC, de Kam PJ, Grandjean J, Bel KJ, et al. Verapamil reduces tachycardia-induced electrical remodeling of the atria. Circulation. 1997;95(7):1945-53.

155. Fareh S, Benardeau A, Nattel S. Differential efficacy of L- and T-type calcium channel blockers in preventing tachycardia-induced atrial remodeling in dogs. Cardiovasc Res. 2001;49(4):762-70.

156. Haghi D, Schumacher B. Current management of symptomatic atrial fibrillation. Am J Cardiovasc Drugs. 2001;1(2):127-39.

157. Frankel G, Kamrul R, Kosar L, Jensen B. Rate versus rhythm control in atrial fibrillation. Can Fam Physician. 2013;59(2):161-8.

158. Pariaut R. Atrial Fibrillation: Current Therapies. Vet Clin North Am Small Anim Pract. 2017;47(5):977-88.

159. Gasparova I, Kubatka P, Opatrilova R, Caprnda M, Filipova S, Rodrigo L, et al. Perspectives and challenges of antioxidant therapy for atrial fibrillation. Naunyn Schmiedebergs Arch Pharmacol. 2017;390(1):1-14.

160. Badiani S, van Zalen J, Treibel TA, Bhattacharyya S, Moon JC, Lloyd G. Aortic Stenosis, a Left Ventricular Disease: Insights from Advanced Imaging. Curr Cardiol Rep. 2016;18(8):80.

161. Spirito P, Bellone P, Harris KM, Bernabo P, Bruzzi P, Maron BJ. Magnitude of left ventricular hypertrophy and risk of sudden death in hypertrophic cardiomyopathy. N Engl J Med. 2000;342(24):1778-85.

162. Webb G, Gatzoulis MA. Atrial septal defects in the adult: recent progress and overview. Circulation. 2006;114(15):1645-53.

163. Iida K, el Sersi M, Fujieda K, Kawano S, Tabei F, Iwasaki Y, et al. Pathophysiologic significance of left ventricular hypertrophy in dilated cardiomyopathy. Clin Cardiol. 1996;19(9):704-8.

164. Nagata K, Hattori T. Cardioprotective mechanisms of lifestyle modifications and pharmacotherapies on cardiac remodeling and dysfunction in hypertensive heart disease: an overview. Nagoya J Med Sci. 2011;73(3-4):91-105.

165. Pfeffer MA, Shah AM, Borlaug BA. Heart Failure With Preserved Ejection Fraction In Perspective. Circ Res. 2019;124(11):1598-617.

166. Aurigemma GP, Gaasch WH. Clinical practice. Diastolic heart failure. N Engl J Med. 2004;351(11):1097-105.

167. Giudice R, Izzo R, Manzi MV, Pagnano G, Santoro M, Rao MA, et al. Lifestyle-related risk factors, smoking status and cardiovascular disease. High Blood Press Cardiovasc Prev. 2012;19(2):85-92.

168. Gerber Y, Weston SA, Redfield MM, Chamberlain AM, Manemann SM, Jiang R, et al. A contemporary appraisal of the heart failure epidemic in Olmsted County, Minnesota, 2000 to 2010. JAMA Intern Med. 2015;175(6):996-1004.

169. Brown DW, Haldeman GA, Croft JB, Giles WH, Mensah GA. Racial or ethnic differences in hospitalization for heart failure among elderly adults: Medicare, 1990 to 2000. Am Heart J. 2005;150(3):448-54.

170. Verdecchia P, Reboldi G, Gattobigio R, Bentivoglio M, Borgioni C, Angeli F, et al. Atrial fibrillation in hypertension: predictors and outcome. Hypertension. 2003;41(2):218-23.

171. Erkuner O, Dudink E, Nieuwlaat R, Rienstra M, Van Gelder IC, Camm AJ, et al. Effect of Systemic Hypertension With Versus Without Left Ventricular Hypertrophy on the Progression of Atrial Fibrillation (from the Euro Heart Survey). Am J Cardiol. 2018;122(4):578-83.

172. Hennersdorf MG, Schueller PO, Steiner S, Strauer BE. Prevalence of paroxysmal atrial fibrillation depending on the regression of left ventricular hypertrophy in arterial hypertension. Hypertens Res. 2007;30(6):535-40.

173. Yancy CW, Jessup M, Bozkurt B, Butler J, Casey DE, Jr., Drazner MH, et al. 2013 ACCF/AHA guideline for the management of heart failure: a report of the American College of Cardiology Foundation/American Heart Association Task Force on Practice Guidelines. J Am Coll Cardiol. 2013;62(16):e147-239.

174. Leopold JA. Aldosterone, mineralocorticoid receptor activation, and cardiovascular remodeling. Circulation. 2011;124(18):e466-8.

175. Cappuccio FP. Cardiovascular and other effects of salt consumption. Kidney Int Suppl (2011). 2013;3(4):312-5.

176. Wang JL, Yin WJ, Zhou LY, Wang YF, Zuo XC. Association Between Initiation, Intensity, and Cessation of Smoking and Mortality Risk in Patients With Cardiovascular Disease: A Cohort Study. Front Cardiovasc Med. 2021;8:728217.

177. Pina IL, Apstein CS, Balady GJ, Belardinelli R, Chaitman BR, Duscha BD, et al. Exercise and heart failure: A statement from the American Heart Association Committee on exercise, rehabilitation, and prevention. Circulation. 2003;107(8):1210-25.

178. Chung MK, Eckhardt LL, Chen LY, Ahmed HM, Gopinathannair R, Joglar JA, et al. Lifestyle and Risk Factor Modification for Reduction of Atrial Fibrillation: A Scientific Statement From the American Heart Association. Circulation. 2020;141(16):e750-e72.

179. Wright JW, Mizutani S, Harding JW. Pathways involved in the transition from hypertension to hypertrophy to heart failure. Treatment strategies. Heart Fail Rev. 2008;13(3):367-75.

180. Ponikowski P, Voors AA, Anker SD, Bueno H, Cleland JGF, Coats AJS, et al. 2016 ESC Guidelines for the Diagnosis and Treatment of Acute and Chronic Heart Failure. Rev Esp Cardiol (Engl Ed). 2016;69(12):1167.

181. Jessup M, Greenberg B, Mancini D, Cappola T, Pauly DF, Jaski B, et al. Calcium Upregulation by Percutaneous Administration of Gene Therapy in Cardiac Disease (CUPID): a phase 2 trial of intracoronary gene therapy of sarcoplasmic reticulum Ca2+-ATPase in patients with advanced heart failure. Circulation. 2011;124(3):304-13.

182. Jaski BE, Jessup ML, Mancini DM, Cappola TP, Pauly DF, Greenberg B, et al. Calcium upregulation by percutaneous administration of gene therapy in cardiac disease (CUPID Trial), a first-in-human phase 1/2 clinical trial. J Card Fail. 2009;15(3):171-81.

183. McMurray JJ, Packer M, Desai AS, Gong J, Lefkowitz MP, Rizkala AR, et al. Angiotensin-neprilysin inhibition versus enalapril in heart failure. N Engl J Med. 2014;371(11):993-1004.

184. Zhou LY, Liu JP, Wang K, Gao J, Ding SL, Jiao JQ, et al. Mitochondrial function in cardiac hypertrophy. Int J Cardiol. 2012.

185. Xiao H, Ma X, Feng W, Fu Y, Lu Z, Xu M, et al. Metformin attenuates cardiac fibrosis by inhibiting the TGFbeta1-Smad3 signalling pathway. Cardiovasc Res. 2010;87(3):504-13.

186. Nishida K, Michael G, Dobrev D, Nattel S. Animal models for atrial fibrillation: clinical insights and scientific opportunities. Europace. 2010;12(2):160-72.

187. Bukowska A, Felgendreher M, Scholz B, Wolke C, Schulte JS, Fehrmann E, et al. CREM-transgene mice: An animal model of atrial fibrillation and thrombogenesis. Thromb Res. 2018;163:172-9.

188. Etzion Y, Mor M, Shalev A, Dror S, Etzion O, Dagan A, et al. New insights into the atrial electrophysiology of rodents using a novel modality: the miniature-bipolar hook electrode. Am J Physiol Heart Circ Physiol. 2008;295(4):H1460-9.

189. Lee DI, Murninkas M, Elyagon S, Etzion Y, Anderson HD. Cannabinoid Receptor Agonist Inhibits Atrial Electrical Remodeling in a Tachypaced Ex Vivo Rat Model. Front Pharmacol. 2021;12:642398.

190. Soattin L, Lubberding AF, Bentzen BH, Christ T, Jespersen T. Inhibition of Adenosine Pathway Alters Atrial Electrophysiology and Prevents Atrial Fibrillation. Frontiers in Physiology. 2020;11.

191. Wu J. Cannabis, cannabinoid receptors, and endocannabinoid system: yesterday, today, and tomorrow. Acta Pharmacol Sin. 2019;40(3):297-9.

192. Stasiulewicz A, Znajdek K, Grudzien M, Pawinski T, Sulkowska AJI. A Guide to Targeting the Endocannabinoid System in Drug Design. Int J Mol Sci. 2020;21(8).

193. Moreno E, Cavic M, Krivokuca A, Casado V, Canela E. The Endocannabinoid System as a Target in Cancer Diseases: Are We There Yet? Front Pharmacol. 2019;10:339.

194. Matsuda LA, Lolait SJ, Brownstein MJ, Young AC, Bonner TI. Structure of a cannabinoid receptor and functional expression of the cloned cDNA. Nature. 1990;346(6284):561-4.

195. Bonz A, Laser M, Kullmer S, Kniesch S, Babin-Ebell J, Popp V, et al. Cannabinoids acting on CB1 receptors decrease contractile performance in human atrial muscle. J Cardiovasc Pharmacol. 2003;41(4):657-64.

196. Gebremedhin D, Lange AR, Campbell WB, Hillard CJ, Harder DR. Cannabinoid CB1 receptor of cat cerebral arterial muscle functions to inhibit L-type Ca2+ channel current. Am J Physiol. 1999;276(6 Pt 2):H2085-93.

197. Liu J, Gao B, Mirshahi F, Sanyal AJ, Khanolkar AD, Makriyannis A, et al. Functional CB1 cannabinoid receptors in human vascular endothelial cells. Biochem J. 2000;346 Pt 3:835-40.

198. Bouchard JF, Lepicier P, Lamontagne D. Contribution of endocannabinoids in the endothelial protection afforded by ischemic preconditioning in the isolated rat heart. Life Sci. 2003;72(16):1859-70.

199. Soderstrom K, Soliman E, Van Dross R. Cannabinoids Modulate Neuronal Activity and Cancer by CB1 and CB2 Receptor-Independent Mechanisms. Front Pharmacol. 2017;8:720.

200. Devane WA, Hanus L, Breuer A, Pertwee RG, Stevenson LA, Griffin G, et al. Isolation and structure of a brain constituent that binds to the cannabinoid receptor. Science. 1992;258(5090):1946-9.

201. Mechoulam R, Ben-Shabat S, Hanus L, Ligumsky M, Kaminski NE, Schatz AR, et al. Identification of an endogenous 2-monoglyceride, present in canine gut, that binds to cannabinoid receptors. Biochem Pharmacol. 1995;50(1):83-90.

202. Reggio PH. Endocannabinoid binding to the cannabinoid receptors: what is known and what remains unknown. Curr Med Chem. 2010;17(14):1468-86.

203. Le Boisselier R, Alexandre J, Lelong-Boulouard V, Debruyne D. Focus on cannabinoids and synthetic cannabinoids. Clin Pharmacol Ther. 2017;101(2):220-9.

204. Lu HC, Mackie K. An Introduction to the Endogenous Cannabinoid System. Biol Psychiatry. 2016;79(7):516-25.

205. Hillard CJ, Jarrahian A. The movement of N-arachidonoylethanolamine (anandamide) across cellular membranes. Chem Phys Lipids. 2000;108(1-2):123-34.

206. Maccarrone M, van der Stelt M, Rossi A, Veldink GA, Vliegenthart JF, Agro AF. Anandamide hydrolysis by human cells in culture and brain. J Biol Chem. 1998;273(48):32332-9.

207. Saario SM, Savinainen JR, Laitinen JT, Jarvinen T, Niemi R. Monoglyceride lipase-like enzymatic activity is responsible for hydrolysis of 2-arachidonoylglycerol in rat cerebellar membranes. Biochem Pharmacol. 2004;67(7):1381-7.

208. Di Marzo V, Bifulco M, De Petrocellis L. The endocannabinoid system and its therapeutic exploitation. Nat Rev Drug Discov. 2004;3(9):771-84.

209. Pertwee RG, Howlett AC, Abood ME, Alexander SP, Di Marzo V, Elphick MR, et al. International Union of Basic and Clinical Pharmacology. LXXIX. Cannabinoid receptors and their ligands: beyond CB(1) and CB(2). Pharmacol Rev. 2010;62(4):588-631.

210. Wouters E, Walraed J, Banister SD, Stove CP. Insights into biased signaling at cannabinoid receptors: synthetic cannabinoid receptor agonists. Biochem Pharmacol. 2019;169:113623.

211. Hurst DP, Grossfield A, Lynch DL, Feller S, Romo TD, Gawrisch K, et al. A lipid pathway for ligand binding is necessary for a cannabinoid G protein-coupled receptor. J Biol Chem. 2010;285(23):17954-64.

212. Puhl SL. Cannabinoid-sensitive receptors in cardiac physiology and ischaemia. Biochim Biophys Acta Mol Cell Res. 2020;1867(3):118462.

213. Munro S, Thomas KL, Abu-Shaar M. Molecular characterization of a peripheral receptor for cannabinoids. Nature. 1993;365(6441):61-5.

214. Maresz K, Carrier EJ, Ponomarev ED, Hillard CJ, Dittel BN. Modulation of the cannabinoid CB2 receptor in microglial cells in response to inflammatory stimuli. J Neurochem. 2005;95(2):437-45.

215. Galiegue S, Mary S, Marchand J, Dussossoy D, Carriere D, Carayon P, et al. Expression of central and peripheral cannabinoid receptors in human immune tissues and leukocyte subpopulations. Eur J Biochem. 1995;232(1):54-61.

216. Schmid PC, Schwartz KD, Smith CN, Krebsbach RJ, Berdyshev EV, Schmid HH. A sensitive endocannabinoid assay. The simultaneous analysis of N-acylethanolamines and 2-monoacylglycerols. Chem Phys Lipids. 2000;104(2):185-91.

217. Felder CC, Nielsen A, Briley EM, Palkovits M, Priller J, Axelrod J, et al. Isolation and measurement of the endogenous cannabinoid receptor agonist, anandamide, in brain and peripheral tissues of human and rat. FEBS Lett. 1996;393(2-3):231-5.

218. Bilfinger TV, Salzet M, Fimiani C, Deutsch DG, Tramu G, Stefano GB. Pharmacological evidence for anandamide amidase in human cardiac and vascular tissues. Int J Cardiol. 1998;64 Suppl 1:S15-22.

219. Ahn K, Johnson DS, Cravatt BF. Fatty acid amide hydrolase as a potential therapeutic target for the treatment of pain and CNS disorders. Expert Opin Drug Discov. 2009;4(7):763-84.

220. Hiley CR. Endocannabinoids and the heart. J Cardiovasc Pharmacol. 2009;53(4):267-76.

221. McManus DD, Shaikh AY, Abhishek F, Vasan RS. Atrial fibrillation and heart failure parallels: lessons for atrial fibrillation prevention. Crit Pathw Cardiol. 2011;10(1):46-51.

222. Krylatov AV, Ugdyzhekova DS, Bernatskaya NA, Maslov LN, Mekhoulam R, Pertwee RG, et al. Activation of type II cannabinoid receptors improves myocardial tolerance to arrhythmogenic effects of coronary occlusion and reperfusion. Bull Exp Biol Med. 2001;131(6):523-5.

223. Lagneux C, Lamontagne D. Involvement of cannabinoids in the cardioprotection induced by lipopolysaccharide. Br J Pharmacol. 2001;132(4):793-6.

224. Underdown NJ, Hiley CR, Ford WR. Anandamide reduces infarct size in rat isolated hearts subjected to ischaemia-reperfusion by a novel cannabinoid mechanism. Br J Pharmacol. 2005;146(6):809-16.

225. Lepicier P, Bouchard JF, Lagneux C, Lamontagne D. Endocannabinoids protect the rat isolated heart against ischaemia. Br J Pharmacol. 2003;139(4):805-15.

226. Di Filippo C, Rossi F, Rossi S, D'Amico M. Cannabinoid CB2 receptor activation reduces mouse myocardial ischemia-reperfusion injury: involvement of cytokine/chemokines and PMN. J Leukoc Biol. 2004;75(3):453-9.

227. Fulmer ML, Thewke DP. The Endocannabinoid System and Heart Disease: The Role of Cannabinoid Receptor Type 2. Cardiovasc Hematol Disord Drug Targets. 2018;18(1):34-51.

228. Alfulaij N, Meiners F, Michalek J, Small-Howard AL, Turner HC, Stokes AJ. Cannabinoids, the Heart of the Matter. J Am Heart Assoc. 2018;7(14).

229. Durst R, Danenberg H, Gallily R, Mechoulam R, Meir K, Grad E, et al. Cannabidiol, a nonpsychoactive Cannabis constituent, protects against myocardial ischemic reperfusion injury. Am J Physiol Heart Circ Physiol. 2007;293(6):H3602-7.

230. Wagner JA, Hu K, Bauersachs J, Karcher J, Wiesler M, Goparaju SK, et al. Endogenous cannabinoids mediate hypotension after experimental myocardial infarction. J Am Coll Cardiol. 2001;38(7):2048-54.

231. Wagner JA, Hu K, Karcher J, Bauersachs J, Schafer A, Laser M, et al. CB(1) cannabinoid receptor antagonism promotes remodeling and cannabinoid treatment prevents endothelial dysfunction and hypotension in rats with myocardial infarction. Br J Pharmacol. 2003;138(7):1251-8.

232. Barana A, Amoros I, Caballero R, Gomez R, Osuna L, Lillo MP, et al. Endocannabinoids and cannabinoid analogues block cardiac hKv1.5 channels in a cannabinoid receptor-independent manner. Cardiovasc Res. 2010;85(1):56-67.

233. Dziadulewicz EK, Bevan SJ, Brain CT, Coote PR, Culshaw AJ, Davis AJ, et al. Naphthalen-1-yl-(4-pentyloxynaphthalen-1-yl)methanone: a potent, orally bioavailable human CB1/CB2 dual agonist with antihyperalgesic properties and restricted central nervous system penetration. J Med Chem. 2007;50(16):3851-6.

234. Berrocoso E, Rey-Brea R, Fernandez-Arevalo M, Mico JA, Martin-Banderas L. Single oral dose of cannabinoid derivate loaded PLGA nanocarriers relieves neuropathic pain for eleven days. Nanomedicine. 2017;13(8):2623-32.

235. Hosking RD, Zajicek JP. Therapeutic potential of cannabis in pain medicine. Br J Anaesth. 2008;101(1):59-68.

236. Kunos G, Osei-Hyiaman D, Batkai S, Sharkey KA, Makriyannis A. Should peripheral CB(1) cannabinoid receptors be selectively targeted for therapeutic gain? Trends Pharmacol Sci. 2009;30(1):1-7.

237. Howlett AC, Barth F, Bonner TI, Cabral G, Casellas P, Devane WA, et al. International Union of Pharmacology. XXVII. Classification of cannabinoid receptors. Pharmacol Rev. 2002;54(2):161-202.

238. Cluny NL, Keenan CM, Duncan M, Fox A, Lutz B, Sharkey KA. Naphthalen-1-yl-(4-pentyloxynaphthalen-1-yl)methanone (SAB378), a peripherally restricted cannabinoid CB1/CB2 receptor agonist, inhibits gastrointestinal motility but has no effect on experimental colitis in mice. J Pharmacol Exp Ther. 2010;334(3):973-80.

239. Deutsch DG, Chin SA. Enzymatic synthesis and degradation of anandamide, a cannabinoid receptor agonist. Biochem Pharmacol. 1993;46(5):791-6.

240. Deutsch DG, Goligorsky MS, Schmid PC, Krebsbach RJ, Schmid HH, Das SK, et al. Production and physiological actions of anandamide in the vasculature of the rat kidney. J Clin Invest. 1997;100(6):1538-46.

241. Pacher P, Batkai S, Kunos G. The endocannabinoid system as an emerging target of pharmacotherapy. Pharmacol Rev. 2006;58(3):389-462.

242. Lopaschuk GD, Ussher JR, Folmes CD, Jaswal JS, Stanley WC. Myocardial fatty acid metabolism in health and disease. Physiol Rev. 2010;90(1):207-58.

243. Opie LH. Metabolism of the heart in health and disease. I. Am Heart J. 1968;76(5):685-98.

244. Ashrafian H, Frenneaux MP, Opie LH. Metabolic mechanisms in heart failure. Circulation. 2007;116(4):434-48.

245. Stanley WC. Myocardial energy metabolism during ischemia and the mechanisms of metabolic therapies. J Cardiovasc Pharmacol Ther. 2004;9 Suppl 1:S31-45.

246. Taylor D, Bhandari S, Seymour AM. Mitochondrial dysfunction in uremic cardiomyopathy. Am J Physiol Renal Physiol. 2015:ajprenal 00442 2014.

247. Doenst T, Pytel G, Schrepper A, Amorim P, Farber G, Shingu Y, et al. Decreased rates of substrate oxidation ex vivo predict the onset of heart failure and contractile dysfunction in rats with pressure overload. Cardiovasc Res. 2010;86(3):461-70.

248. Wu J, LaPointe MC, West BL, Gardner DG. Tissue-specific determinants of human atrial natriuretic factor gene expression in cardiac tissue. J Biol Chem. 1989;264(11):6472-9.

249. Alibin CP, Kopilas MA, Anderson HD. Suppression of cardiac myocyte hypertrophy by conjugated linoleic acid: role of peroxisome proliferator-activated receptors alpha and gamma. J Biol Chem. 2008;283(16):10707-15.

250. Zhang H, Shao Z, Alibin CP, Acosta C, Anderson HD. Liganded Peroxisome Proliferator-Activated Receptors (PPARs) Preserve Nuclear Histone Deacetylase 5 Levels in Endothelin-Treated Sprague-Dawley Rat Cardiac Myocytes. PLoS One. 2014;9(12):e115258.

251. Huang Y, Zhang H, Shao Z, O'Hara KA, Kopilas MA, Yu L, et al. Suppression of endothelin-1-induced cardiac myocyte hypertrophy by PPAR agonists: role of diacylglycerol kinase zeta. Cardiovasc Res. 2011;90(2):267-75.

252. Sun X, Kumar S, Sharma S, Aggarwal S, Lu Q, Gross C, et al. Endothelin-1 induces a glycolytic switch in pulmonary arterial endothelial cells via the mitochondrial translocation of endothelial nitric oxide synthase. Am J Respir Cell Mol Biol. 2014;50(6):1084-95.

253. Roy Chowdhury SK, Smith DR, Saleh A, Schapansky J, Marquez A, Gomes S, et al. Impaired adenosine monophosphate-activated protein kinase signalling in dorsal root ganglia neurons is linked to mitochondrial dysfunction and peripheral neuropathy in diabetes. Brain. 2012;135(Pt 6):1751-66.

254. Brand MD, Nicholls DG. Assessing mitochondrial dysfunction in cells. Biochem J. 2011;435(2):297-312.

255. Hill BG, Dranka BP, Zou L, Chatham JC, Darley-Usmar VM. Importance of the bioenergetic reserve capacity in response to cardiomyocyte stress induced by 4-hydroxynonenal. Biochem J. 2009;424(1):99-107.

256. Luiken JJ, Coort SL, Willems J, Coumans WA, Bonen A, van der Vusse GJ, et al. Contraction-induced fatty acid translocase/CD36 translocation in rat cardiac myocytes is mediated through AMP-activated protein kinase signaling. Diabetes. 2003;52(7):1627-34.

257. Makinde AO, Gamble J, Lopaschuk GD. Upregulation of 5'-AMP-activated protein kinase is responsible for the increase in myocardial fatty acid oxidation rates following birth in the newborn rabbit. Circ Res. 1997;80(4):482-9.

258. Witters LA, Kemp BE, Means AR. Chutes and Ladders: the search for protein kinases that act on AMPK. Trends Biochem Sci. 2006;31(1):13-6.

259. Beauloye C, Bertrand L, Horman S, Hue L. AMPK activation, a preventive therapeutic target in the transition from cardiac injury to heart failure. Cardiovasc Res. 2011;90(2):224-33.

260. Wu Z, Boss O. Targeting PGC-1 alpha to control energy homeostasis. Expert Opin Ther Targets. 2007;11(10):1329-38.

261. Kerner J, Hoppel C. Fatty acid import into mitochondria. Biochim Biophys Acta. 2000;1486(1):1-17.

262. Brown NF, Weis BC, Husti JE, Foster DW, McGarry JD. Mitochondrial carnitine palmitoyltransferase I isoform switching in the developing rat heart. J Biol Chem. 1995;270(15):8952-7.

263. Levy D, Garrison RJ, Savage DD, Kannel WB, Castelli WP. Prognostic implications of echocardiographically determined left ventricular mass in the Framingham Heart Study. N Engl J Med. 1990;322(22):1561-6.

264. Ho KK, Pinsky JL, Kannel WB, Levy D. The epidemiology of heart failure: the Framingham Study. J Am Coll Cardiol. 1993;22(4 Suppl A):6A-13A.

265. Berenji K, Drazner MH, Rothermel BA, Hill JA. Does load-induced ventricular hypertrophy progress to systolic heart failure? Am J Physiol Heart Circ Physiol. 2005;289(1):H8-H16.

266. Zhang Y, Yuan M, Bradley KM, Dong F, Anversa P, Ren J. Insulin-like growth factor 1 alleviates high-fat diet-induced myocardial contractile dysfunction: role of insulin signaling and mitochondrial function. Hypertension. 2012;59(3):680-93.

267. Luedde M, Flogel U, Knorr M, Grundt C, Hippe HJ, Brors B, et al. Decreased contractility due to energy deprivation in a transgenic rat model of hypertrophic cardiomyopathy. J Mol Med (Berl). 2009;87(4):411-22.

268. Afolayan AJ, Eis A, Alexander M, Michalkiewicz T, Teng RJ, Lakshminrusimha S, et al. Decreased Endothelial NOS Expression and Function Contributes to Impaired Mitochondrial Biogenesis and Oxidative Stress in Fetal Lambs with PPHN. Am J Physiol Lung Cell Mol Physiol. 2015:ajplung 00392 2014.

269. Zhang Y, Mi SL, Hu N, Doser TA, Sun A, Ge J, et al. Mitochondrial aldehyde dehydrogenase 2 accentuates aging-induced cardiac remodeling and contractile dysfunction: role of AMPK, Sirt1, and mitochondrial function. Free Radic Biol Med. 2014;71:208-20.

270. Salminen A, Kaarniranta K. AMP-activated protein kinase (AMPK) controls the aging process via an integrated signaling network. Ageing Res Rev. 2012;11(2):230-41.

271. Preston CC, Oberlin AS, Holmuhamedov EL, Gupta A, Sagar S, Syed RH, et al. Aging-induced alterations in gene transcripts and functional activity of mitochondrial oxidative phosphorylation complexes in the heart. Mech Ageing Dev. 2008;129(6):304-12.

272. Tang Y, Mi C, Liu J, Gao F, Long J. Compromised mitochondrial remodeling in compensatory hypertrophied myocardium of spontaneously hypertensive rat. Cardiovasc Pathol. 2014;23(2):101-6.

273. Garnier A, Zoll J, Fortin D, N'Guessan B, Lefebvre F, Geny B, et al. Control by circulating factors of mitochondrial function and transcription cascade in heart failure: a role for endothelin-1 and angiotensin II. Circ Heart Fail. 2009;2(4):342-50.

274. Garnier A, Fortin D, Delomenie C, Momken I, Veksler V, Ventura-Clapier R. Depressed mitochondrial transcription factors and oxidative capacity in rat failing cardiac and skeletal muscles. J Physiol. 2003;551(Pt 2):491-501.

275. Jager S, Handschin C, St-Pierre J, Spiegelman BM. AMP-activated protein kinase (AMPK) action in skeletal muscle via direct phosphorylation of PGC-1alpha. Proc Natl Acad Sci U S A. 2007;104(29):12017-22.

276. Rodgers JT, Lerin C, Haas W, Gygi SP, Spiegelman BM, Puigserver P. Nutrient control of glucose homeostasis through a complex of PGC-1alpha and SIRT1. Nature. 2005;434(7029):113-8.

277. Lu P, Kamboj A, Gibson SB, Anderson CM. Poly(ADP-ribose) polymerase-1 causes mitochondrial damage and neuron death mediated by Bnip3. J Neurosci. 2014;34(48):15975-87.

278. Lan F, Cacicedo JM, Ruderman N, Ido Y. SIRT1 modulation of the acetylation status, cytosolic localization, and activity of LKB1. Possible role in AMP-activated protein kinase activation. J Biol Chem. 2008;283(41):27628-35.

279. Jiang S, Wang W, Miner J, Fromm M. Cross regulation of sirtuin 1, AMPK, and PPARgamma in conjugated linoleic acid treated adipocytes. PLoS One. 2012;7(11):e48874.

280. Ventura-Clapier R, Garnier A, Veksler V. Transcriptional control of mitochondrial biogenesis: the central role of PGC-1alpha. Cardiovasc Res. 2008;79(2):208-17.

281. St-Pierre J, Drori S, Uldry M, Silvaggi JM, Rhee J, Jager S, et al. Suppression of reactive oxygen species and neurodegeneration by the PGC-1 transcriptional coactivators. Cell. 2006;127(2):397-408.

282. Lehman JJ, Kelly DP. Transcriptional activation of energy metabolic switches in the developing and hypertrophied heart. Clin Exp Pharmacol Physiol. 2002;29(4):339-45.

283. Planavila A, Iglesias R, Giralt M, Villarroya F. Sirt1 acts in association with PPARalpha to protect the heart from hypertrophy, metabolic dysregulation, and inflammation. Cardiovasc Res. 2011;90(2):276-84.

284. Li L, Wu L, Wang C, Liu L, Zhao Y. Adiponectin modulates carnitine palmitoyltransferase-1 through AMPK signaling cascade in rat cardiomyocytes. Regul Pept. 2007;139(1-3):72-9.

285. Zheng X, Sun T, Wang X. Activation of type 2 cannabinoid receptors (CB2R) promotes fatty acid oxidation through the SIRT1/PGC-1alpha pathway. Biochem Biophys Res Commun. 2013;436(3):377-81.

286. Felder CC, Joyce KE, Briley EM, Mansouri J, Mackie K, Blond O, et al. Comparison of the pharmacology and signal transduction of the human cannabinoid CB1 and CB2 receptors. Mol Pharmacol. 1995;48(3):443-50.

287. Tedesco L, Valerio A, Dossena M, Cardile A, Ragni M, Pagano C, et al. Cannabinoid receptor stimulation impairs mitochondrial biogenesis in mouse white adipose tissue, muscle, and liver: the role of eNOS, p38 MAPK, and AMPK pathways. Diabetes. 2010;59(11):2826-36.

288. Perwitz N, Wenzel J, Wagner I, Buning J, Drenckhan M, Zarse K, et al. Cannabinoid type 1 receptor blockade induces transdifferentiation towards a brown fat phenotype in white adipocytes. Diabetes Obes Metab. 2010;12(2):158-66.

289. Li Q, Guo HC, Maslov LN, Qiao XW, Zhou JJ, Zhang Y. Mitochondrial permeability transition pore plays a role in the cardioprotection of CB2 receptor against ischemia-reperfusion injury. Can J Physiol Pharmacol. 2014;92(3):205-14.

290. Li Q, Wang F, Zhang YM, Zhou JJ, Zhang Y. Activation of cannabinoid type 2 receptor by JWH133 protects heart against ischemia/reperfusion-induced apoptosis. Cell Physiol Biochem. 2013;31(4-5):693-702.

291. Fisar Z, Singh N, Hroudova J. Cannabinoid-induced changes in respiration of brain mitochondria. Toxicol Lett. 2014;231(1):62-71.

292. Tomaselli GF. Ventricularization of atrial gene expression in the fibrillating heart? Circ Res. 2005;96(9):923-4.

293. Lippi G, Sanchis-Gomar F, Cervellin G. Global epidemiology of atrial fibrillation: An increasing epidemic and public health challenge. Int J Stroke. 2020:1747493019897870.

294. Ramirez FD, Reddy VY, Viswanathan R, Hocini M, Jaïs P. Emerging Technologies for Pulmonary Vein Isolation. Circ Res. 2020;127(1):170-83.

295. Dobrev D, Nattel S. New antiarrhythmic drugs for treatment of atrial fibrillation. Lancet. 2010;375(9721):1212-23.

296. Li N, Brundel B. Inflammasomes and Proteostasis Novel Molecular Mechanisms Associated With Atrial Fibrillation. Circ Res. 2020;127(1):73-90.

297. Nattel S, Heijman J, Zhou L, Dobrev D. Molecular Basis of Atrial Fibrillation Pathophysiology and Therapy: A Translational Perspective. Circ Res. 2020;127(1):51-72.

298. Lee TW, Lee TI, Lin YK, Chen YC, Kao YH, Chen YJ. Effect of antidiabetic drugs on the risk of atrial fibrillation: mechanistic insights from clinical evidence and translational studies. Cell Mol Life Sci. 2020.

299. Harada M, Nattel SN, Nattel S. AMP-activated protein kinase: potential role in cardiac electrophysiology and arrhythmias. Circ Arrhythm Electrophysiol. 2012;5(4):860-7.

300. Qiu J, Zhou S, Liu Q. Energy metabolic alterations in the progression of atrial fibrillation: Potential role of AMP-activated protein kinase as a critical regulator. Int J Cardiol. 2016;212:14-5.

301. Montecucco F, Di Marzo V. At the heart of the matter: the endocannabinoid system in cardiovascular function and dysfunction. Trends Pharmacol Sci. 2012;33(6):331-40.

302. Lu Y, Lee DI, Roy Chowdhury S, Lu P, Kamboj A, Anderson CM, et al. Activation of Cannabinoid Receptors Attenuates Endothelin-1-Induced Mitochondrial Dysfunction in Rat Ventricular Myocytes. J Cardiovasc Pharmacol. 2020;75(1):54-63.

303. Mor M, Shalev A, Dror S, Pikovsky O, Beharier O, Moran A, et al. INO-8875, a highly selective A1 adenosine receptor agonist: evaluation of chronotropic, dromotropic, and hemodynamic effects in rats. J Pharmacol Exp Ther. 2013;344(1):59-67.

304. Murninkas M, Gillis R, Lee DI, Elyagon S, Bhandarkar NS, Levi O, et al. A new implantable tool for repeated assessment of supraventricular electrophysiology and atrial fibrillation susceptibility in freely moving rats. Am J Physiol Heart Circ Physiol. 2020;AiPS(10.1152/ajpheart.00676.2020).

305. Weresa J, Pędzińska-Betiuk A, Kossakowski R, Malinowska B. Cannabinoid CB(1) and CB(2) receptors antagonists AM251 and AM630 differentially modulate the chronotropic and inotropic effects of isoprenaline in isolated rat atria. Pharmacol Rep. 2019;71(1):82-9.

306. Krylatov AV, Maslov LN, Lasukova OV, Pertwee RG. Cannabinoid receptor antagonists SR141716 and SR144528 exhibit properties of partial agonists in experiments on isolated perfused rat heart. Bull Exp Biol Med. 2005;139(5):558-61.

307. Gorbunov AS, Maslov LN, Tsibulnikov SY, Khaliulin IG, Tsepokina AV, Khutornaya MV, et al. CB-Receptor Agonist HU-210 Mimics the Postconditioning Phenomenon of Isolated Heart. Bull Exp Biol Med. 2016;162(1):27-9.

308. Sterin-Borda L, Del Zar CF, Borda E. Differential CB1 and CB2 cannabinoid receptor-inotropic response of rat isolated atria: endogenous signal transduction pathways. Biochem Pharmacol. 2005;69(12):1705-13.

309. Tiyerili V, Zimmer S, Jung S, Wassmann K, Naehle CP, Lutjohann D, et al. CB1 receptor inhibition leads to decreased vascular AT1 receptor expression, inhibition of oxidative stress and improved endothelial function. Basic Res Cardiol. 2010;105(4):465-77.

310. Molica F, Burger F, Thomas A, Staub C, Tailleux A, Staels B, et al. Endogenous cannabinoid receptor CB1 activation promotes vascular smooth-muscle cell proliferation and neointima formation. J Lipid Res. 2013;54(5):1360-8.

311. Sugamura K, Sugiyama S, Nozaki T, Matsuzawa Y, Izumiya Y, Miyata K, et al. Activated endocannabinoid system in coronary artery disease and antiinflammatory effects of cannabinoid 1 receptor blockade on macrophages. Circulation. 2009;119(1):28-36.

312. Dol-Gleizes F, Paumelle R, Visentin V, Mares AM, Desitter P, Hennuyer N, et al. Rimonabant, a selective cannabinoid CB1 receptor antagonist, inhibits atherosclerosis in LDL receptor-deficient mice. Arterioscler Thromb Vasc Biol. 2009;29(1):12-8.

313. Rajesh M, Mukhopadhyay P, Hasko G, Liaudet L, Mackie K, Pacher P. Cannabinoid-1 receptor activation induces reactive oxygen species-dependent and -independent mitogen-activated protein kinase activation and cell death in human coronary artery endothelial cells. Br J Pharmacol. 2010;160(3):688-700.

314. Rajesh M, Batkai S, Kechrid M, Mukhopadhyay P, Lee WS, Horvath B, et al. Cannabinoid 1 receptor promotes cardiac dysfunction, oxidative stress, inflammation, and fibrosis in diabetic cardiomyopathy. Diabetes. 2012;61(3):716-27.

315. Mukhopadhyay P, Batkai S, Rajesh M, Czifra N, Harvey-White J, Hasko G, et al. Pharmacological inhibition of CB1 cannabinoid receptor protects against doxorubicin-induced cardiotoxicity. J Am Coll Cardiol. 2007;50(6):528-36.

316. Mukhopadhyay P, Rajesh M, Batkai S, Patel V, Kashiwaya Y, Liaudet L, et al. CB1 cannabinoid receptors promote oxidative stress and cell death in murine models of doxorubicin-induced cardiomyopathy and in human cardiomyocytes. Cardiovasc Res. 2010;85(4):773-84.

317. Mulla W, Hajaj B, Elyagon S, Mor M, Gillis R, Murninkas M, et al. Rapid Atrial Pacing Promotes Atrial Fibrillation Substrate in Unanesthetized Instrumented Rats. Front Physiol. 2019;10:1218.

318. Wiersma M, Meijering RAM, Qi XY, Zhang D, Liu T, Hoogstra-Berends F, et al. Endoplasmic Reticulum Stress Is Associated With Autophagy and Cardiomyocyte Remodeling in Experimental and Human Atrial Fibrillation. J Am Heart Assoc. 2017;6(10):e006458.

319. Zhang D, Hu X, Li J, Liu J, Baks-Te Bulte L, Wiersma M, et al. DNA damage-induced PARP1 activation confers cardiomyocyte dysfunction through NAD(+) depletion in experimental atrial fibrillation. Nat Commun. 2019;10(1):1307.

320. Klapper-Goldstein H, Murninkas M, Gillis R, Mulla W, Levanon E, Elyagon S, et al. An implantable system for long-term assessment of atrial fibrillation substrate in unanesthetized rats exposed to underlying pathological conditions. Sci Rep. 2020;10(1):553.

321. Dolinsky VW, Dyck JR. Role of AMP-activated protein kinase in healthy and diseased hearts. Am J Physiol Heart Circ Physiol. 2006;291(6):H2557-69.

322. Korantzopoulos P, Kolettis TM, Galaris D, Goudevenos JA. The role of oxidative stress in the pathogenesis and perpetuation of atrial fibrillation. Int J Cardiol. 2007;115(2):135-43.

323. Yoshizawa T, Niwano S, Niwano H, Tamaki H, Nakamura H, Igarashi T, et al. Antiremodeling Effect of Xanthine Oxidase Inhibition in a Canine Model of Atrial Fibrillation. Int Heart J. 2018;59(5):1077-85.

324. Ozgen N, Dun W, Sosunov EA, Anyukhovsky EP, Hirose M, Duffy HS, et al. Early electrical remodeling in rabbit pulmonary vein results from trafficking of intracellular SK2 channels to membrane sites. Cardiovasc Res. 2007;75(4):758-69.

325. Kim J, Yang G, Kim Y, Kim J, Ha J. AMPK activators: mechanisms of action and physiological activities. Exp Mol Med. 2016;48:e224.

326. Woods A, Vertommen D, Neumann D, Turk R, Bayliss J, Schlattner U, et al. Identification of phosphorylation sites in AMP-activated protein kinase (AMPK) for upstream AMPK kinases and study of their roles by site-directed mutagenesis. J Biol Chem. 2003;278(31):28434-42.

327. Hurley RL, Anderson KA, Franzone JM, Kemp BE, Means AR, Witters LA. The Ca2+/calmodulin-dependent protein kinase kinases are AMP-activated protein kinase kinases. J Biol Chem. 2005;280(32):29060-6.

328. Hawley SA, Pan DA, Mustard KJ, Ross L, Bain J, Edelman AM, et al. Calmodulin-dependent protein kinase kinase-beta is an alternative upstream kinase for AMP-activated protein kinase. Cell Metab. 2005;2(1):9-19.

329. Vara D, Salazar M, Olea-Herrero N, Guzman M, Velasco G, Diaz-Laviada I. Anti-tumoral action of cannabinoids on hepatocellular carcinoma: role of AMPK-dependent activation of autophagy. Cell Death Differ. 2011;18(7):1099-111.

330. Zhou LY, Liu JP, Wang K, Gao J, Ding SL, Jiao JQ, et al. Mitochondrial function in cardiac hypertrophy. Int J Cardiol. 2013;167(4):1118-25.

331. Alesutan I, Voelkl J, Stockigt F, Mia S, Feger M, Primessnig U, et al. AMP-activated protein kinase alpha1 regulates cardiac gap junction protein connexin 43 and electrical remodeling following pressure overload. Cell Physiol Biochem. 2015;35(1):406-18.

332. Luo B, Yan Y, Zeng Z, Zhang Z, Liu H, Liu H, et al. Connexin 43 reduces susceptibility to sympathetic atrial fibrillation. Int J Mol Med. 2018;42(2):1125-33.

333. Boengler K, Schulz R. Connexin 43 and Mitochondria in Cardiovascular Health and Disease. Adv Exp Med Biol. 2017;982:227-46.

334. Nattel S, Shiroshita-Takeshita A, Brundel BJ, Rivard L. Mechanisms of atrial fibrillation: lessons from animal models. Prog Cardiovasc Dis. 2005;48(1):9-28.

335. Wiersma M, van Marion DMS, Wust RCI, Houtkooper RH, Zhang D, Groot NMS, et al. Mitochondrial Dysfunction Underlies Cardiomyocyte Remodeling in Experimental and Clinical Atrial Fibrillation. Cells. 2019;8(10):1202.

336. Gao S, Yuan K, Shah A, Kim JS, Park WH, Kim SH. Suppression of high pacing-induced ANP secretion by antioxidants in isolated rat atria. Peptides. 2011;32(12):2467-73.

337. Kim M, Shen M, Ngoy S, Karamanlidis G, Liao R, Tian R. AMPK isoform expression in the normal and failing hearts. J Mol Cell Cardiol. 2012;52(5):1066-73.

338. Go AS, Hylek EM, Phillips KA, Chang Y, Henault LE, Selby JV, et al. Prevalence of diagnosed atrial fibrillation in adults: national implications for rhythm management and stroke prevention: the AnTicoagulation and Risk Factors in Atrial Fibrillation (ATRIA) Study. JAMA. 2001;285(18):2370-5.

339. Colilla S, Crow A, Petkun W, Singer DE, Simon T, Liu X. Estimates of current and future incidence and prevalence of atrial fibrillation in the U.S. adult population. Am J Cardiol. 2013;112(8):1142-7.

340. Chiang CE, Naditch-Brule L, Murin J, Goethals M, Inoue H, O'Neill J, et al. Distribution and risk profile of paroxysmal, persistent, and permanent atrial fibrillation in routine clinical practice: insight from the real-life global survey evaluating patients with atrial fibrillation international registry. Circ Arrhythm Electrophysiol. 2012;5(4):632-9.

341. Forrester SJ, Booz GW, Sigmund CD, Coffman TM, Kawai T, Rizzo V, et al. Angiotensin II Signal Transduction: An Update on Mechanisms of Physiology and Pathophysiology. Physiol Rev. 2018;98(3):1627-738.

342. Jansen HJ, Bohne LJ, Gillis AM, Rose RA. Atrial remodeling and atrial fibrillation in acquired forms of cardiovascular disease. Heart Rhythm O2. 2020;1(2):147-59.

343. Schotten U, Verheule S, Kirchhof P, Goette A. Pathophysiological mechanisms of atrial fibrillation: a translational appraisal. Physiol Rev. 2011;91(1):265-325.

344. Kim N, Jung Y, Nam M, Sun Kang M, Lee MK, Cho Y, et al. Angiotensin II affects inflammation mechanisms via AMPK-related signalling pathways in HL-1 atrial myocytes. Sci Rep. 2017;7(1):10328.

345. Kim GE, Young LH. AMPK and the Atrial Response to Metabolic Inhibition. J Am Coll Cardiol. 2015;66(1):59-61.

346. Arad M, Seidman CE, Seidman JG. AMP-activated protein kinase in the heart: role during health and disease. Circ Res. 2007;100(4):474-88.

347. Mihm MJ, Yu F, Carnes CA, Reiser PJ, McCarthy PM, Van Wagoner DR, et al. Impaired myofibrillar energetics and oxidative injury during human atrial fibrillation. Circulation. 2001;104(2):174-80.

348. Jansen HJ, Mackasey M, Moghtadaei M, Belke DD, Egom EE, Tuomi JM, et al. Distinct patterns of atrial electrical and structural remodeling in angiotensin II mediated atrial fibrillation. J Mol Cell Cardiol. 2018;124:12-25.

349. Chen Y, Qiao X, Zhang L, Li X, Liu Q. Apelin-13 regulates angiotensin ii-induced Cx43 downregulation and autophagy via the AMPK/mTOR signaling pathway in HL-1 cells. Physiol Res. 2020;69(5):813-22.

350. Anderson HD, Wang F, Gardner DG. Role of the epidermal growth factor receptor in signaling strain-dependent activation of the brain natriuretic peptide gene. J Biol Chem. 2004;279(10):9287-97.

351. Harada M, Melka J, Sobue Y, Nattel S. Metabolic Considerations in Atrial Fibrillation-Mechanistic Insights and Therapeutic Opportunities. Circ J. 2017;81(12):1749-57.

352. Ahmad Waza A, Andrabi K, Ul Hussain M. Adenosine-triphosphate-sensitive K+ channel (Kir6.1): a novel phosphospecific interaction partner of connexin 43 (Cx43). Exp Cell Res. 2012;318(20):2559-66.

353. Ikeda Y, Sato K, Pimentel DR, Sam F, Shaw RJ, Dyck JR, et al. Cardiac-specific deletion of LKB1 leads to hypertrophy and dysfunction. J Biol Chem. 2009;284(51):35839-49.

354. Lenski M, Schleider G, Kohlhaas M, Adrian L, Adam O, Tian Q, et al. Arrhythmia causes lipid accumulation and reduced glucose uptake. Basic Res Cardiol. 2015;110(4):40.

355. Hausenloy DJ, Maddock HL, Baxter GF, Yellon DM. Inhibiting mitochondrial permeability transition pore opening: a new paradigm for myocardial preconditioning? Cardiovasc Res. 2002;55(3):534-43.

356. Minners J, van den Bos EJ, Yellon DM, Schwalb H, Opie LH, Sack MN. Dinitrophenol, cyclosporin A, and trimetazidine modulate preconditioning in the isolated rat heart: support for a mitochondrial role in cardioprotection. Cardiovasc Res. 2000;47(1):68-73.

357. Argaud L, Gateau-Roesch O, Chalabreysse L, Gomez L, Loufouat J, Thivolet-Bejui F, et al. Preconditioning delays Ca2+-induced mitochondrial permeability transition. Cardiovasc Res. 2004;61(1):115-22.

358. Argaud L, Gateau-Roesch O, Muntean D, Chalabreysse L, Loufouat J, Robert D, et al. Specific inhibition of the mitochondrial permeability transition prevents lethal reperfusion injury. J Mol Cell Cardiol. 2005;38(2):367-74.

359. Hausenloy DJ, Yellon DM, Mani-Babu S, Duchen MR. Preconditioning protects by inhibiting the mitochondrial permeability transition. Am J Physiol Heart Circ Physiol. 2004;287(2):H841-9.

360. Oka N, Wang L, Mi W, Caldarone CA. Inhibition of mitochondrial remodeling by cyclosporine A preserves myocardial performance in a neonatal rabbit model of cardioplegic arrest. J Thorac Cardiovasc Surg. 2008;135(3):585-93.

361. Clarke SJ, McStay GP, Halestrap AP. Sanglifehrin A acts as a potent inhibitor of the mitochondrial permeability transition and reperfusion injury of the heart by binding to cyclophilin-D at a different site from cyclosporin A. J Biol Chem. 2002;277(38):34793-9.

362. Romashko DN, Marban E, O'Rourke B. Subcellular metabolic transients and mitochondrial redox waves in heart cells. Proc Natl Acad Sci U S A. 1998;95(4):1618-23.

363. Aon MA, Cortassa S, Marban E, O'Rourke B. Synchronized whole cell oscillations in mitochondrial metabolism triggered by a local release of reactive oxygen species in cardiac myocytes. J Biol Chem. 2003;278(45):44735-44.

364. Zorov DB, Filburn CR, Klotz LO, Zweier JL, Sollott SJ. Reactive oxygen species (ROS)-induced ROS release: a new phenomenon accompanying induction of the mitochondrial permeability transition in cardiac myocytes. J Exp Med. 2000;192(7):1001-14.

365. Huser J, Blatter LA. Fluctuations in mitochondrial membrane potential caused by repetitive gating of the permeability transition pore. Biochem J. 1999;343 Pt 2:311-7.

366. Akar FG, Aon MA, Tomaselli GF, O'Rourke B. The mitochondrial origin of postischemic arrhythmias. J Clin Invest. 2005;115(12):3527-35.

367. Brown DA, Aon MA, Akar FG, Liu T, Sorarrain N, O'Rourke B. Effects of 4'-chlorodiazepam on cellular excitation-contraction coupling and ischaemia-reperfusion injury in rabbit heart. Cardiovasc Res. 2008;79(1):141-9.

368. Billman GE, Englert HC, Scholkens BA. HMR 1883, a novel cardioselective inhibitor of the ATP-sensitive potassium channel. Part II: effects on susceptibility to ventricular fibrillation induced by myocardial ischemia in conscious dogs. J Pharmacol Exp Ther. 1998;286(3):1465-73.

369. Glukhov AV, Fedorov VV, Kalish PW, Ravikumar VK, Lou Q, Janks D, et al. Conduction remodeling in human end-stage nonischemic left ventricular cardiomyopathy. Circulation. 2012;125(15):1835-47.

370. Duerr GD, Feisst A, Halbach K, Verfuerth L, Gestrich C, Wenzel D, et al. CB2-deficiency is associated with a stronger hypertrophy and remodeling of the right ventricle in a murine model of left pulmonary artery occlusion. Life Sci. 2018;215:96-105.

371. Duerr GD, Heinemann JC, Dunkel S, Zimmer A, Lutz B, Lerner R, et al. Myocardial hypertrophy is associated with inflammation and activation of endocannabinoid system in patients with aortic valve stenosis. Life Sci. 2013;92(20-21):976-83.

372. Liao Y, Bin J, Asakura M, Xuan W, Chen B, Huang Q, et al. Deficiency of type 1 cannabinoid receptors worsens acute heart failure induced by pressure overload in mice. Eur Heart J. 2012;33(24):3124-33.

373. Batkai S, Mukhopadhyay P, Harvey-White J, Kechrid R, Pacher P, Kunos G. Endocannabinoids acting at CB1 receptors mediate the cardiac contractile dysfunction in vivo in cirrhotic rats. Am J Physiol Heart Circ Physiol. 2007;293(3):H1689-95.

374. Buckley CL, Stokes AJ. Mice lacking functional TRPV1 are protected from pressure overload cardiac hypertrophy. Channels (Austin). 2011;5(4):367-74.

375. Horton JS, Buckley CL, Stokes AJ. Successful TRPV1 antagonist treatment for cardiac hypertrophy and heart failure in mice. Channels (Austin). 2013;7(1):17-22.

376. Patwardhan AM, Jeske NA, Price TJ, Gamper N, Akopian AN, Hargreaves KM. The cannabinoid WIN 55,212-2 inhibits transient receptor potential vanilloid 1 (TRPV1) and evokes peripheral antihyperalgesia via calcineurin. Proc Natl Acad Sci U S A. 2006;103(30):11393-8.

377. Slivicki RA, Yi J, Brings VE, Huynh PN, Gereau RWt. The cannabinoid agonist CB-13 produces peripherally mediated analgesia in mice but elicits tolerance and signs of central nervous system activity with repeated dosing. Pain. 2021.

378. Levine A, Liktor-Busa E, Lipinski AA, Couture S, Balasubramanian S, Aicher SA, et al. Sex differences in the expression of the endocannabinoid system within V1M cortex and PAG of Sprague Dawley rats. Biol Sex Differ. 2021;12(1):60.

379. Rubino T, Parolaro D. Sexually dimorphic effects of cannabinoid compounds on emotion and cognition. Front Behav Neurosci. 2011;5:64.

380. Riebe CJ, Hill MN, Lee TT, Hillard CJ, Gorzalka BB. Estrogenic regulation of limbic cannabinoid receptor binding. Psychoneuroendocrinology. 2010;35(8):1265-9.

381. D'Angelo DD, Sakata Y, Lorenz JN, Boivin GP, Walsh RA, Liggett SB, et al. Transgenic Galphaq overexpression induces cardiac contractile failure in mice. Proc Natl Acad Sci U S A. 1997;94(15):8121-6.

382. Bosier B, Doyen PJ, Brolet A, Muccioli GG, Ahmed E, Desmet N, et al. Inhibition of the regulator of G protein signalling RGS4 in the spinal cord decreases neuropathic hyperalgesia and restores cannabinoid CB1 receptor signalling. Br J Pharmacol. 2015;172(22):5333-46.

383. Shibata R, Ouchi N, Ito M, Kihara S, Shiojima I, Pimentel DR, et al. Adiponectin-mediated modulation of hypertrophic signals in the heart. Nat Med. 2004;10(12):1384-9.

384. Zarrinpashneh E, Beauloye C, Ginion A, Pouleur AC, Havaux X, Hue L, et al. AMPKalpha2 counteracts the development of cardiac hypertrophy induced by isoproterenol. Biochem Biophys Res Commun. 2008;376(4):677-81.

385. Sukhodub A, Jovanovic S, Du Q, Budas G, Clelland AK, Shen M, et al. AMP-activated protein kinase mediates preconditioning in cardiomyocytes by regulating activity and trafficking of sarcolemmal ATP-sensitive K(+) channels. J Cell Physiol. 2007;210(1):224-36.

386. Ghezelbash S, Molina CE, Dobrev D. Altered atrial metabolism: an underappreciated contributor to the initiation and progression of atrial fibrillation. J Am Heart Assoc. 2015;4(3):e001808.

387. Lipina C, Irving AJ, Hundal HS. Mitochondria: a possible nexus for the regulation of energy homeostasis by the endocannabinoid system? Am J Physiol Endocrinol Metab. 2014;307(1):E1-13.

388. Turdi S, Fan X, Li J, Zhao J, Huff AF, Du M, et al. AMP-activated protein kinase deficiency exacerbates aging-induced myocardial contractile dysfunction. Aging Cell. 2010;9(4):592-606.

389. Eid BG. Cannabinoids for Treating Cardiovascular Disorders: Putting Together a Complex Puzzle. J Microsc Ultrastruct. 2018;6(4):171-6.

390. King A. Prevention: Neuropsychiatric adverse effects signal the end of the line for rimonabant. Nat Rev Cardiol. 2010;7(11):602.

391. Verty AN, Stefanidis A, McAinch AJ, Hryciw DH, Oldfield B. Anti-Obesity Effect of the CB2 Receptor Agonist JWH-015 in Diet-Induced Obese Mice. PLoS One. 2015;10(11):e0140592.

392. Narimatsu S, Watanabe K, Yamamoto I, Yoshimura H. Sex difference in the oxidative metabolism of delta 9-tetrahydrocannabinol in the rat. Biochem Pharmacol. 1991;41(8):1187-94.

393. Adegbala O, Adejumo AC, Olakanmi O, Akinjero A, Akintoye E, Alliu S, et al. Relation of Cannabis Use and Atrial Fibrillation Among Patients Hospitalized for Heart Failure. Am J Cardiol. 2018;122(1):129-34.

394. Joyeux M, Arnaud C, Godin-Ribuot D, Demenge P, Lamontagne D, Ribuot C. Endocannabinoids are implicated in the infarct size-reducing effect conferred by heat stress preconditioning in isolated rat hearts. Cardiovasc Res. 2002;55(3):619-25.

395. Hajrasouliha AR, Tavakoli S, Ghasemi M, Jabehdar-Maralani P, Sadeghipour H, Ebrahimi F, et al. Endogenous cannabinoids contribute to remote ischemic preconditioning via cannabinoid CB2 receptors in the rat heart. Eur J Pharmacol. 2008;579(1-3):246-52.

396. Motobe T, Hashiguchi T, Uchimura T, Yamakuchi M, Taniguchi N, Komiya S, et al. Endogenous cannabinoids are candidates for lipid mediators of bone cement implantation syndrome. Shock. 2004;21(1):8-12.

397. Weijs B, Pisters R, Haest RJ, Kragten JA, Joosen IA, Versteylen M, et al. Patients originally diagnosed with idiopathic atrial fibrillation more often suffer from insidious coronary artery disease compared to healthy sinus rhythm controls. Heart Rhythm. 2012;9(12):1923-9.

398. Murninkas M, Gillis R, Lee DI, Elyagon S, Bhandarkar NS, Levi O, et al. A new implantable tool for repeated assessment of supraventricular electrophysiology and atrial fibrillation susceptibility in freely moving rats. American Journal of Physiology-Heart and Circulatory Physiology. 2020.

399. Kariyanna PT, Wengrofsky P, Jayarangaiah A, Haseeb S, Salciccioli L, Hegde S, et al. Marijuana and Cardiac Arrhythmias: A Scoping Study. Int J Clin Res Trials. 2019;4(1).

400. Fisher BA, Ghuran A, Vadamalai V, Antonios TF. Cardiovascular complications induced by cannabis smoking: a case report and review of the literature. Emerg Med J. 2005;22(9):679-80.

401. Abe Y, Sakairi T, Kajiyama H, Shrivastav S, Beeson C, Kopp JB. Bioenergetic characterization of mouse podocytes. Am J Physiol Cell Physiol. 2010;299(2):C464-76.

402. Liu J, Cao L, Chen J, Song S, Lee IH, Quijano C, et al. Bmi1 regulates mitochondrial function and the DNA damage response pathway. Nature. 2009;459(7245):387-92.

403. Choi SW, Gerencser AA, Nicholls DG. Bioenergetic analysis of isolated cerebrocortical nerve terminals on a microgram scale: spare respiratory capacity and stochastic mitochondrial failure. J Neurochem. 2009;109(4):1179-91.